NASA CR-168072
BAC ER 15049

National Aeronautics and
Space Administration

PRELIMINARY DESIGN OF FLIGHT HARDWARE FOR TWO-PHASE FLUID RESEARCH

by D. C. Hustvedt and R. L. Oonk

BEECH AIRCRAFT CORPORATION

prepared for

NATIONAL AERONAUTICS AND SPACE ADMINISTRATION

NASA Lewis Research Center
Contract NAS 3-23160

1. Report No.	2. Government Accession No.	3. Recipient's Catalog No.
CR 168072		

4. Title and Subtitle	5. Report Date
Preliminary Design of Flight Hardware for Two-Phase Fluid Research	February 1982
	6. Performing Organization Code
7. Author(s)	8. Performing Organization Report No.
D. C. Hustvedt, R. L. Oonk	BAC-ER-15049
	10. Work Unit No.
9. Performing Organization Name and Address	
Beech Aircraft Corporation P. O. Box 9631 Boulder, Colorado 80301	11. Contract or Grant No. NAS3-23160
	13. Type of Report and Period Covered
12. Sponsoring Agency Name and Address	Contractor Report
NASA Lewis Research Center Cleveland, Ohio 44135	14. Sponsoring Agency Code

15. Supplementary Notes

Project Manager Liam Sarsfield
NASA Lewis Research Center
Cleveland, Ohio 44135

16. Abstract

This study defined the preliminary designs of flight hardware for the Space Shuttle Orbiter for three two-phase fluid research experiments: (1) liquid reorientation--to study the motion of liquid in tanks subjected to small accelerations; (2) pool boiling--to study low-gravity boiling from horizontal cylinders; and (3) flow boiling--to study low-gravity forced flow boiling heat transfer and flow phenomena in a heated horizontal tube.

The study consisted of eight major tasks: reassessment of the existing experiment designs, assessment of the Spacelab facility approach, assessment of the individual carry-on approach, selection of the preferred approach, preliminary design of flight hardware, safety analysis, preparation of a development plan, estimates of detailed design, fabrication and ground testing costs.

The most cost effective design approach for the experiments is individual carry-ons in the Orbiter middeck. The experiments were designed to fit into one or two middeck lockers. Development schedules for the detailed design, fabrication and ground testing ranged from 15½ to 18 months. Minimum costs (in 1981 dollars) ranged from $463K for the liquid reorientation experiment to $998K for the pool boiling experiment.

17. Key Words (Suggested by Author(s))	18. Distribution Statement
Liquid Reorientation, Pool Boiling, Flow Boiling, Low Gravity, Orbiter Middeck, Heat Transfer, Fluid Mechanics	Unclassified - Unlimited

19. Security Classif. (of this report)	20. Security Classif. (of this page)	21. No. of Pages	22. Price*
	Unclassified	206	

* For sale by the National Technical Information Service, Springfield, Virginia 22161

NASA-C-168 (Rev. 10-75)

N83-25766 #

FOREWORD

This Final Report summarizes the technical effort conducted by Beech Aircraft Corporation under Contract No. NAS3-23160. The National Aeronautics and Space Administration, Lewis Research Center, administered the contract.

NASA/LeRC Program Manager	L. P. Sarsfield
Beech Study Director	D. C. Hustvedt
Lead Engineer	R. L. Oonk
Design	J. D. Breuel
Cost Analysis	B. L. Sperry

In addition, Dr. J. H. Lienhard of the University of Houston, provided a technical review of the pool boiling experiment test matrix and heater and cell design analyses, and Ms. P. J. Giarratano of the National Bureau of Standards assisted in the development of the revised test matrix for the flow boiling experiment.

All data is presented in the International Systems of Units as primary units with English units as the secondary system.

TABLE OF CONTENTS

LIST OF FIGURES

LIST OF FIGURES (Concluded)

LIST OF TABLES

LIST OF TABLES (Concluded)

SUMMARY

This study defined preliminary designs of flight hardware for the Space Shuttle Orbiter for three two-phase fluid research experiments:

- Liquid reorientation - to study the motion of liquid in tanks subjected to small accelerations.
- Pool boiling - to study low-gravity boiling from horizontal cylinders.
- Flow boiling - to study low-gravity heat transfer and flow phenomena in heated horizontal tubes.

The study consisted of eight major tasks:

1. Reassessment of the experiment designs given in NASA CR-159810.

2. Assessment of the feasibility of conducting the experiments in a dedicated Spacelab Facility.

3. Assessment of the feasibility of conducting the three experiments as individual carry-ons.

4. Selection of the preferred approach.

5. Preliminary design of flight hardware for the preferred approach.

6. Preparation of documentation for a Phase Zero safety review of the flight hardware.

7. Establishment of a development plan.

8. Estimation of program costs to develop and fabricate flight hardware.

It was found that the most cost effective location for the experiments was the Orbiter middeck. The experiments were designed to fit into one or two middeck stowage lockers.

The liquid reorientation and pool boiling experiments are completely self-contained and do not interface with Orbiter power, data or fluid systems. The flow boiling experiment requires a middeck water cooling system available on Orbiters 099 and 102.

The design definition for each experiment consists of flow and electrical schematics, assembly drawings, safety matrix (NASA JSC Form 542) and hazard lists (NASA JSC Form 542A).

The effort required to develop the three experiments includes detailed design, hardware procurement, fabrication, and ground testing. The development program span times were estimated to be:

Liquid Reorientation - 14½ months
Pool Boiling - 18½ months
Flow Boiling - 18 months

The minimum costs for experiment development were estimated to be (in 1981 dollars)

Liquid Reorientation - $463K
Pool Boiling - $998K
Flow Boiling - $803K

1.0 INTRODUCTION

Two-phase heat transfer and fluid dynamics data in reduced gravity are essential for the design of advanced space systems such as Orbital Transfer Vehicles and Space Operation Centers. Existing empirical correlations have been developed in normal earth gravity and are not in good agreement with the limited low-gravity experimental data that are available. The Shuttle/Spacelab System provides the opportunity to conduct experiments in a sustained low-gravity environment and develop reliable heat transfer/fluid dynamic correlations.

Recognizing the need for low-gravity heat transfer and fluid dynamics data, NASA commissioned an effort to develop a conceptual design of two-phase flow experiments for Spacelab. The two experiments included in this design were a two-phase flow pattern and pressure drop experiment, and a two-phase flow boiling experiment. The results of this study are summarized in NASA CR-135327.

NASA sponsored a parallel effort to develop a conceptual design for a pool boiling experiment to be incorporated with the two-phase flow experiments in Spacelab. This design effort is reported in NASA CR-135378.

Subsequently, NASA funded the conceptual design of a two-phase fluid mechanics and heat transfer facility for Spacelab. This facility consisted of five experiments: (1) two-phase isothermal flow pattern and pressure drop, (2) two-phase flow boiling, (3) pool boiling, (4) liquid reorientation, and (5) bubble dynamics. The results of this effort are summarized in NASA CR-159810.

Recognizing that a Spacelab facility might not be the most cost effective approach for obtaining low-gravity data, NASA initiated the current study. The basic objectives of this study were to provide a preliminary design of flight hardware for only three experiments--liquid reorientation, pool boiling, and flow boiling, and to determine the optimum location for each experiment--either Spacelab or elsewhere in the Orbiter. The scope of the current study was to:

1. Reassess the experiment designs given in NASA CR-159810.

2. Assess the feasibility of conducting the three experiments in a dedicated Spacelab facility.

3. Assess the feasibility of conducting the three experiments as individual carry-ons.

4. Compare the two approaches and select the preferred approach.

5. Develop preliminary designs of flight hardware for the three experiments.

6. Conduct safety analyses.

7. Create a development plan and cost estimate for detailed design, fabrication and ground testing of the flight hardware.

2.0 ESTABLISHMENT OF EXPERIMENT CONCEPTUAL DESIGN

A conceptual design of a Two-Phase Fluid Mechanics and Heat Transfer Facility for Spacelab was presented in NASA CR-159810 (Reference 1). The facility included five experiments:

- Two-phase flow boiling
- Isothermal flow pattern and pressure drop
- Pool boiling
- Liquid reorientation
- Bubble dynamics

The facility was designed to fit into a Spacelab double rack and to take advantage of the services available in Spacelab such as venting, power and data acquisition.

The objective of the current study was to modify the facility design presented in Reference 1 as necessary to include only three experiments--liquid reorientation, pool boiling and flow boiling. In addition, the feasibility of conducting the three experiments in Spacelab versus individual carry-on experiments in other parts of the Orbiter was to be evaluated. The general approach adopted during the initial feasibility evaluation was to review in detail the designs presented in Reference 1 to identify experiment objectives, test matrices and design deficiencies. Conceptual designs were then developed for each experiment that were: (1) suitable for either the carry-on or Spacelab facility approach; (2) consistent with Orbiter limitations; (3) met experiment objectives; and (4) eliminated design deficiencies identified during the review of Reference 1.

2.1 Experiment Baseline Designs. Each of the applicable experiment designs presented in Reference 1 was reviewed to identify the following:

- Experiment objectives
- Test matrix
- Flow schematic
- Design deficiencies and development requirements

2.1.1 Liquid Reorientation Experiment. A major problem for space vehicles using liquid propellants is positioning the propellant over the tank outlet in low-gravity. One

technique that avoids the use of screen devices is to reorient the liquid propellant by means of propulsive settling. This is accomplished by the use of auxiliary thrusters to provide a small acceleration along the axis of the tank. To minimize the fuel requirements of the auxiliary thrusters it is necessary to determine the minimum vehicle velocity increment required to settle the propellants without excessive geysering, vapor entrainment or sloshing. Reorientation experiments have been performed in drop towers; however, data from these experiments are of limited value since they span less than ten seconds and do not include the complete reorientation process. The sustained low-gravity environment of the Space Shuttle Orbiter provides an opportunity to study liquid reorientation without the limitations inherent in drop tower testing.

Objectives. The liquid reorientation experiment is designed to study the effects of tank geometry, liquid quantity, fluid properties, and acceleration on liquid motion during reorientation.

Test Matrix. The test matrix is shown in Table I. The fineness ratio is defined as the ratio of tank length to tank diameter.

TABLE I TEST MATRIX, LIQUID REORIENTATION EXPERIMENT

Fineness Ratio	No. of Runs	Fill Ratio	Acceleration
2	5	0.20-0.70	$1.8\text{-}2.6 \times 10^{-4} g_o$ constant
4	5	0.20-0.70	$5.5\text{-}7.8 \times 10^{-4} g_o$ constant
2	5	0.20-0.70	$0.01\ g_o$ 0.3 second impulse
4	5	0.20-0.70	$0.005\ g_o$ 1.2 second impulse

Flow Schematic. The flow schematic is shown in Figure 1. The experiment consists of two clear plastic tanks (in which the liquid reorientation occurs), a Freon 113 supply tank with a screen device to provide liquid to the reorientation tanks, and a liquid/vapor separator to deliver vapor to the Spacelab vent system and liquid to the fill lines.

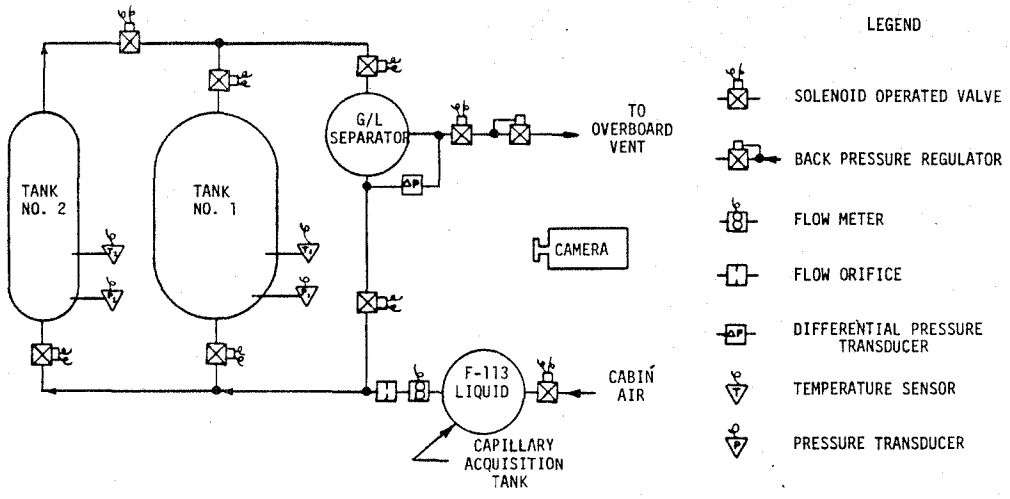

Figure 1 FLOW SCHEMATIC, LIQUID REORIENTATION EXPERIMENT

Settling acceleration impulses are provided by the Orbiter Reaction Control System (RCS); data is in the form of high speed films of the reorientation process.

Design Deficiencies and Development Requirements. The design presented in Reference 1 has four serious deficiencies:

- Freon is not compatible with the Spacelab vent system.
- The acceleration levels proposed in the test matrix are not attainable with the RCS.
- Accurate control of the liquid level in the reorientation tanks is very difficult--liquid may accumulate in the liquid/vapor separator.
- Two different reorientation tank sizes do not provide an adequate determination of the effect of size on reorientation (three points should be considered to be a minimum).

2.1.2 Pool Boiling Experiment. Low-gravity boiling heat transfer data is useful for two reasons: (1) designing high performance heat transfer devices for spacecraft; and (2) understanding the fundamental processes involved in convection and boiling. All previous low-gravity boiling experiments have been carried out in drop tower experiments which last at most three seconds and in aircraft where the low-gravity may last up to 30 seconds but is quite unsteady. Horizontal cylinder boiling experiments carried out by

Bakhru and Lienhard (Reference 2) in normal earth gravity showed that the peak heat flux was a function of both gravity level and cylinder diameter, and suggested that the hydrodynamically determined peak and minimum heat fluxes would cease to exist at sufficiently low-gravity levels. Low-gravity testing is needed to identify the effects of heater diameter and gravity level and determine whether or not small diameter heaters at high gravity are equivalent to large diameter heaters at low-gravity as Bakhru and Lienhard suggest.

In Reference 3 Lienhard showed that the peak heat flux of heated horizontal cylinders could be correlated with a dimensionless heater radius, R':

$$R' = R \sqrt{g (\rho_f - \rho_g) / \sigma} \qquad \text{(Equation 1)}$$

The correlation developed by Sun and Lienhard (Reference 4) is shown in Figure 2.

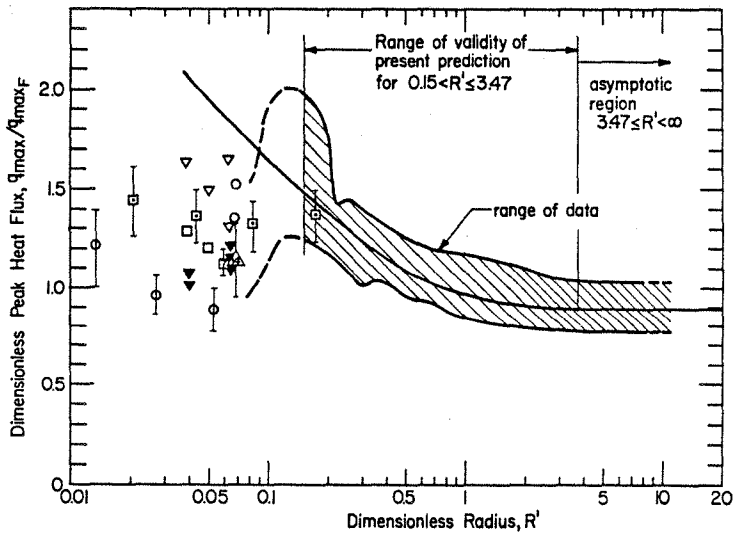

Figure 2 PEAK HEAT FLUX VERSUS R'

Objectives. There are three objectives for the pool boiling experiment:

- Verify peak heat flux prediction for cylinders with $R' > 0.1$.
- Observe low-gravity boiling for $R' < 0.01$ and $0.01 < R' < 0.1$ to generate curves of heat flux versus temperature difference.
- Observe vapor formation on heater for $R' < 0.01$ (unsteady vapor formation associated with film boiling--flickering).

Test Matrix. The experiment test matrix is shown in Table II.

TABLE II TEST MATRIX, POOL BOILING EXPERIMENT

Test No.	Fluid	Temperature °C(°F)	Pressure kN/m^2 (psia)	Cell Size	Volts	Amps	g/g_o
1	H_2O	37 (134.6)	17.2 (2.3)	Small	0.843	15.3	1.0×10^{-4}
2	H_2O	37 (134.6)	17.2 (2.3)	Small	1.04	19.1	3.3×10^{-3}
3	H_2O	37 (134.6)	17.2 (2.3)	Small	1.37	4.0	1.0×10^{-4}
4	H_2O	37 (134.6)	17.2 (2.3)	Small	1.87	4.76	3.3×10^{-3}
5	CH_3OH	39 (102.2)	33.4 (4.85)	Large	3.33	35.4	3.3×10^{-3}
6	CH_3OH	39 (102.2)	33.4 (4.85)	Large	2.74	29.1	1.0×10^{-4}
7	CH_3OH	39 (102.2)	33.4 (4.85)	Small	0.87	17.8	1.0×10^{-4}
8	CH_3OH	39 (102.2)	33.4 (4.85)	Small	1.1	12.9	3.3×10^{-3}
9	F-113	36 (96.8)	67.9 (9.85)	Small	0.687	4.8	1.0×10^{-4}
10	F-113	36 (96.8)	67.9 (9.85)	Small	0.837	5.35	3.3×10^{-3}
11	F-113	36 (96.8)	67.9 (9.85)	Large	1.774	18.1	1.0×10^{-4}
12	F-113	36 (96.8)	67.9 (9.85)	Large	2.155	22.0	3.3×10^{-3}

Schematic. The general arrangement of the experiment hardware is shown in Figure 3. The experiment consists of 12 sealed test cells containing test fluid and cylindrical heaters, as shown in Figure 4.

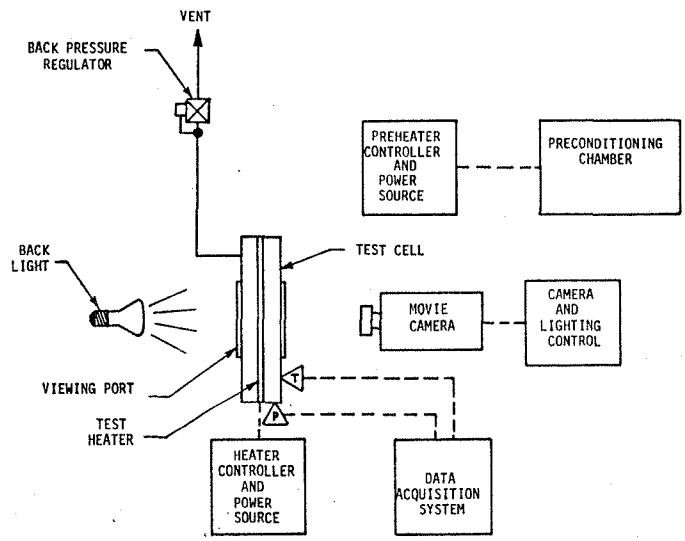

Figure 3 SCHEMATIC, POOL BOILING EXPERIMENT

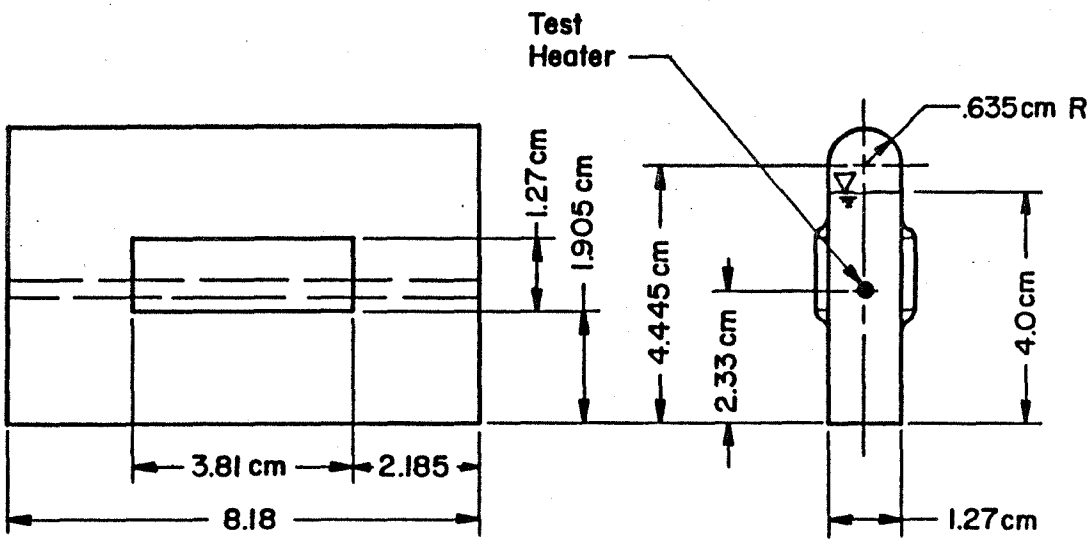

Figure 4 SCHEMATIC, TEST CELLS AND HEATERS

Design Deficiencies and Development Requirements. Major problems with the proposed experiment design include the following:

- The acceleration levels proposed in the test matrix are not attainable with the RCS.
- As shown in the schematic, cell pressure regulation is accomplished by venting vapor through a regulator; this is undesirable because Freon vapor is not compatible with the Spacelab vent system and pressure regulation will be poor at the low flow rates produced by boiling in the cell.
- The test cells are operated above ambient temperature and require pre-heating to reach saturated conditions at the start of testing. Non-equilibrium conditions such as stratification may therefore exist at the start of the test.

The temperature instrumentation for the heater wires is a major development item. The design presented in Reference 1 suggested the use of thermocouples inside the heater wires. This poses serious problems:

- Heat conduction down the relatively massive thermocouple wires may interfere with the temperature measurement.
- The use of very thin thermocouple wires to minimize conduction will make fabrication exceedingly difficult.

- Achieving a good metallurgical bond between the thermocouple and the heater sheath may be difficult; a poor bond would result in unreliable temperature measurements.
- The thermal mass of the heating element must be very small in order for the heater to achieve thermal equilibrium during the experiment operation; the additional mass of the thermocouples would probably lead to unacceptably large heater time constants.

2.1.3 Flow Boiling Experiment. The purpose of the flow boiling experiment is to provide data for the development of empirical correlations for flow boiling in reduced gravity and to provide insights into the flow boiling process. The flow boiling process depends on the contributions of both nucleate boiling and forced convection. The relative magnitude of these contributions in reduced gravity must be determined by experiment. Since boiling heat transfer is regime dependent, it is necessary to determine the effect of reduced gravity in each flow regime.

The effect of gravity on flow regime boundaries is difficult to accurately determine, since there are few low-gravity flow regime test data available. Test data obtained from low gravity parabolic aircraft flights examining the effect of gravity on flow regime boundaries was presented in NASA CR-135327. Due to the short duration and unsteady nature of the low gravity, only qualitative results were obtained. These data showed a downward shift (on G versus x plot) of the flow regime boundaries as gravity was reduced.

The best available flow regime boundary prediction algorithm which accounts for the above mentioned gravity shift is that developed by Dukler and Taitel (Reference 5). Until verified or modified by low-gravity test data, the model should be considered approximate and used only to indicate trends. A flow regime boundary map generated for Freon 11 at normal gravity using Dukler and Taitel's equations is shown in Figure 5.

Objectives. The specific objectives of the flow boiling experiment consist of the following:

- Determine two-phase flow regime boundaries in low-gravity and evaluate the effects of the two-phase flow type on flow boiling heat transfer.
- Determine heat transfer as a function of flow regime.

- Collect flow boiling pressure drop data.
- Verify quality meter performance in low-gravity.

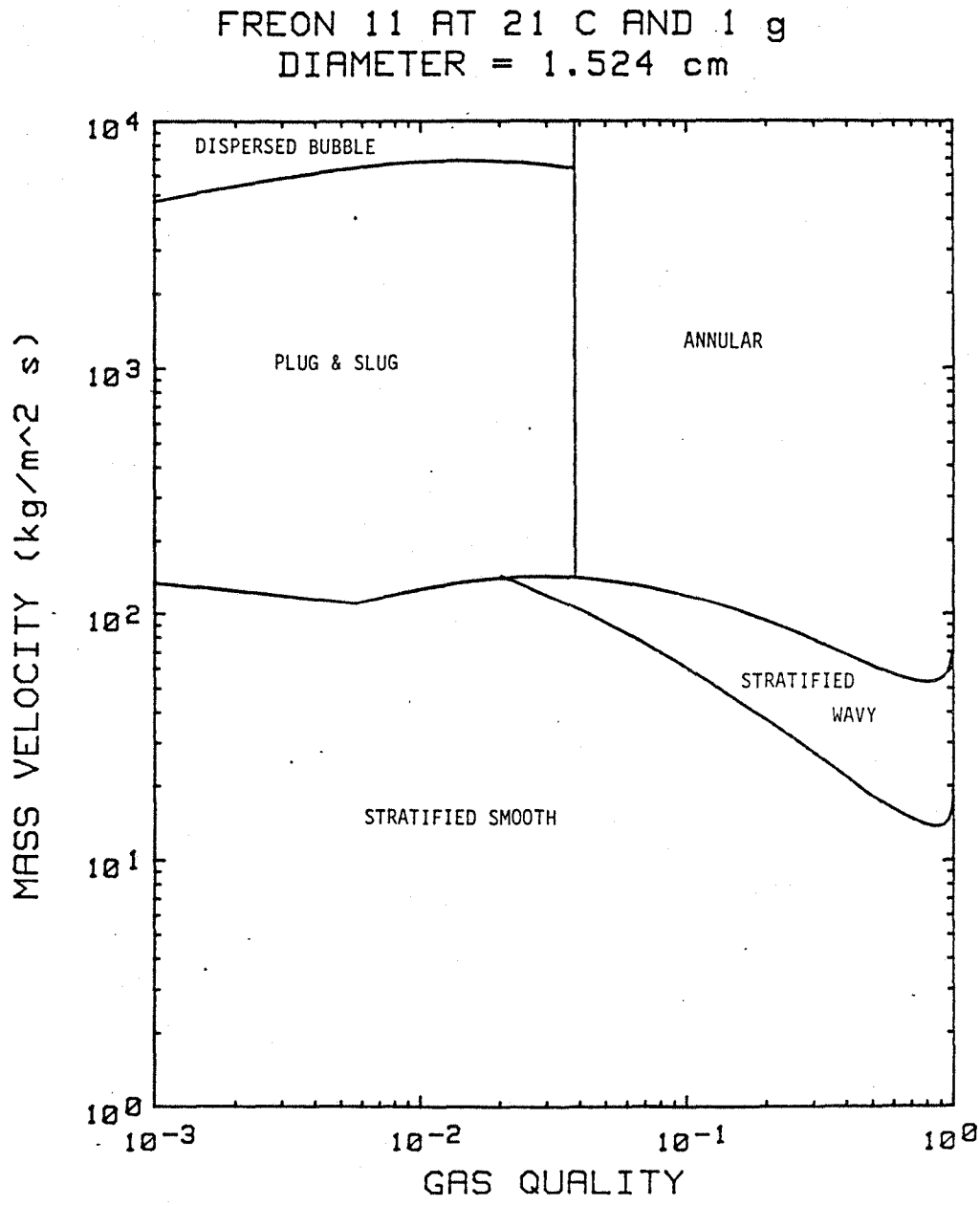

Figure 5 FLOW REGIME BOUNDARY MAP

Test Matrix. The test matrix for the experiment is shown in Figure 6, in which the data points to be taken are shown overlaid on a flow regime boundary map. Problems with the proposed test matrix include:

- There are too many test points; RCS fuel limitations limit the time available for testing.
- Ten of the test points proposed in Reference 1 are undefined.
- The proposed accelerations during the test are not attainable with the RCS.

Flow Schematic. The schematic of the flow boiling experiment is shown in Figure 7. As proposed, the experiment is an open loop system that boils Freon 11 in a clear quartz test section. Vapor is vented overboard through a liquid/vapor separator and the Spacelab vent system. Make-up liquid is supplied from a supply tank with a capillary acquisition device.

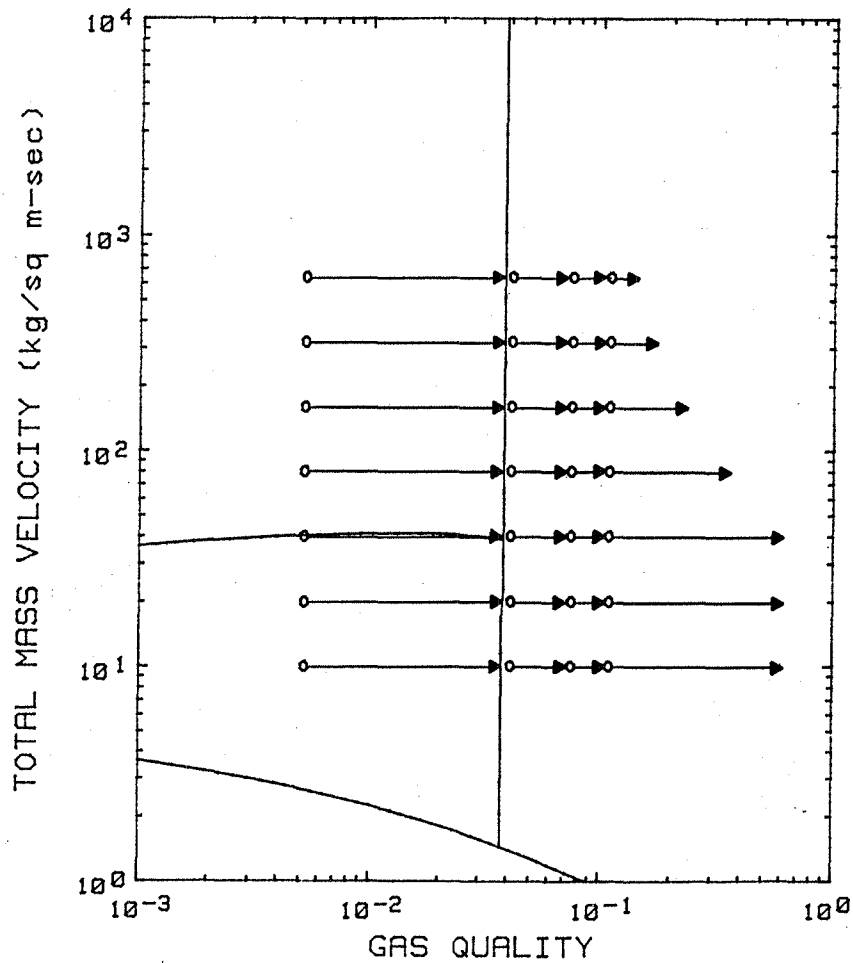

Figure 6 ORIGINAL TEST MATRIX FOR FLOW BOILING EXPERIMENT

The flow rate in the test loop is controlled by a variable capacity pump. Fluid quality at the inlet to the test section is controlled by a pressure regulator which isenthalpically expands the liquid before it enters the test section. The inlet and outlet qualities are measured; temperature and pressure are measured along the test section.

Design Deficiencies and Development Requirements. Major design deficiencies include:

- Freon 11 venting is not compatible with the Spacelab vent system.
- Control of the experiment may be difficult since three regulators control liquid and vapor flow in the loop and liquid may accumulate in the liquid vapor separator.
- Control of inlet quality to the test section is dependent on measurements from a quality meter which is, as yet, undeveloped.

In addition, the proposed experiment design requires development of the following major items:

- Quality meter to monitor and control the inlet quality
- Liquid/vapor separator
- Liquid acquisition system for the supply tank

2.2 Review of Baseline Design. The individual experiment baseline designs were reviewed to identify design changes which would reduce experiment complexity, reduce

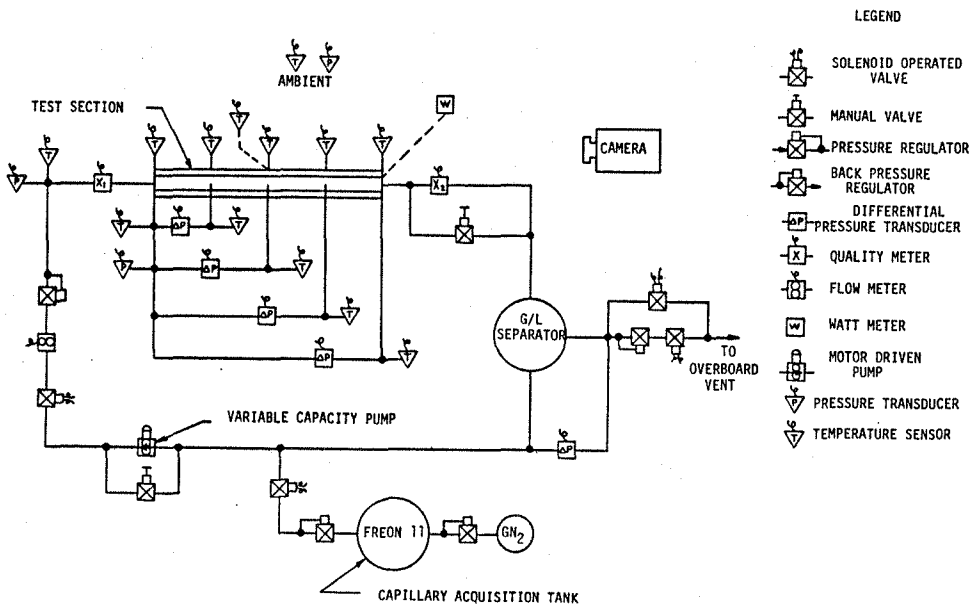

Figure 7 ORIGINAL FLOW BOILING EXPERIMENT SCHEMATIC

Orbiter interface requirements, minimize power consumption and heat dissipation and minimize hardware development risk and cost. Specific design changes which were implemented to achieve these goals were:

- Elimination of Fluid Venting. All three experiments required venting of test fluid. The Freons used in the flow boiling and liquid reorientation experiments are incompatible with the Orbiter vent system. Further, no venting by any experiment is allowed in most of the potential carry-on locations. Eliminating venting of test fluid by the experiments not only reduces Orbiter interfacing problems but further reduces experiment complexity and simplifies experiment control.

- Ambient Temperature Operation. To reduce the power and heat dissipation of the pool boiling experiment, test cell preheating was replaced by ambient temperature operation at subatmospheric pressure. This change eliminates the potential for fluid stratification which may result from preheating.

- Elimination of Unnecessary Development Hardware. High-risk development hardware which was not necessary to achieve the experiment objectives was replaced by off-the-shelf components or low-risk development hardware. Thus, the capillary liquid acquisition devices, liquid vapor separator and inlet fluid quality measurement device (for flow boiling) that were required in the baseline designs were eliminated.

- Elimination of Hazardous Fluids. Fluids which were considered particularly hazardous (methanol, Freon 113) were replaced by less toxic alternates (ethanol, FC-77). It was not possible, however, to completely eliminate all toxic fluids and still achieve the experimental objectives.

- Separation of Fluid Flow Systems. Independent flow systems were developed for each experiment. This change simplified the designs and the control requirements of each experiment. It also satisfied the requirements of independent systems needed for the individual carry-on approach.

- Reduction of Test Matrix Size. The test matrices of the liquid reorientation and flow boiling experiments were reduced in size. Benefits from this change included reduced power consumption and heat dissipation and reduced total test time. Reducing the time at an induced acceleration is

extremely important since analysis showed that the RCS jets were the only acceptable "active" acceleration producing system, and total RCS firing time available to experiments is extremely limited.

2.2.1 Establishment of On-Orbit Acceleration Capabilities of Orbiter. As part of the review of the baseline design of the experiments, the ability to produce the on-orbit accelerations for each experiment was assessed. The baseline test matrices require accelerations ranging from $10^{-2}g_o$ to $10^{-4}g_o$. Four methods of producing the accelerations were considered: (1) Orbiter drag -g, (2) Orbiter RCS translation, (3) acceleration by rotation of the experiment, and (4) acceleration by independent translation of the experiment.

Orbiter Drag -g. One method of producing a uniform acceleration field is simply to operate the experiments with the Orbiter crew in a "quiet" mode and all station keeping RCS firings temporarily discontinued. This has the advantage of requiring no RCS fuel for experiment operation. The acceleration field produced by this method is of the order of $10^{-5}g_o$ to $10^{-6}g_o$ and would therefore require a change in the baseline experiment test matrices. In addition, this acceleration method could not be used for the liquid reorientation experiment, since it is too low to reorient the liquid in the test tanks.

Orbiter RCS Translations. The ability of the Orbiter RCS to produce accelerations for the experiments was evaluated by means of a Beech computer program which calculates the accelerations (in the Orbiter dynamic coordinate system) at any point in the Orbiter for any specified RCS jet group combination.

The Beech program is based on a program obtained from NASA/Johnson Space Center ("JETACC") which calculates the axial and rotational accelerations at the Orbiter center of gravity. The accelerations calculated by JETACC are based on flight data from STS-1 and STS-2.

Beech has modified JETACC to include the following general expression for the absolute acceleration of a point in a moving reference frame:

$$\vec{a} = \ddot{\vec{R}} + \dot{\vec{\omega}} \times \vec{\rho} + \vec{\omega} \times (\vec{\omega} \times \vec{\rho}) + \ddot{\vec{\rho}} + 2\,\vec{\omega} \times \dot{\vec{\rho}} \qquad \text{(Equation 2)}$$

Table III summarizes the normal jet groups used to produce any of the six nominal axial accelerations of the Orbiter. Figure 8 shows RCS jet location and orientations. Table III also shows the nominal RCS propellant usage for a 60 second firing; a +X firing uses the least amount of propellant and a -Z the largest amount.

Figures 9 and 10 show the RCS accelerations versus time for nominal $\pm$X, $\pm$Y, $\pm$Z translations for the Spacelab location and for a typical carry-on location in the middeck. These figures show the +X RCS firing as the most desirable since it is very uniform over the 60 second firing duration and uses the least amount of propellant. The acceleration level produced by the RCS +X is 0.008 g_o and would require changes in the baseline test matrices.

TABLE III RCS JET GROUPS AND PROPELLANT USAGE

Translation Maneuver	Thrusters Fired	Propellant Usage* - Normal (kg)
+X	R3A, L3A	178
-X	F1F, F2F	210
+Y	F3L, L1L	202
-Y	F4R, R3R	204
+Z	F3U, L1U, R1U	235
-Z	F4D, F3D, L3D, L2D, R3D, R2D	488

* 60-Second Firing

Acceleration by Rotation. As an alternative to using the Orbiter RCS, use of the centripetal acceleration produced by experiment rotation was considered. The experiment could be rotated by performing a yaw or pitchover maneuver with the Orbiter or by mounting the experiment on a turntable. The potential advantages of this approach are that the acceleration produced is not restricted to the Orbiter RCS or drag -g acceleration levels, and that use of RCS propellant is reduced (no RCS propellant is needed for the turntable approach).

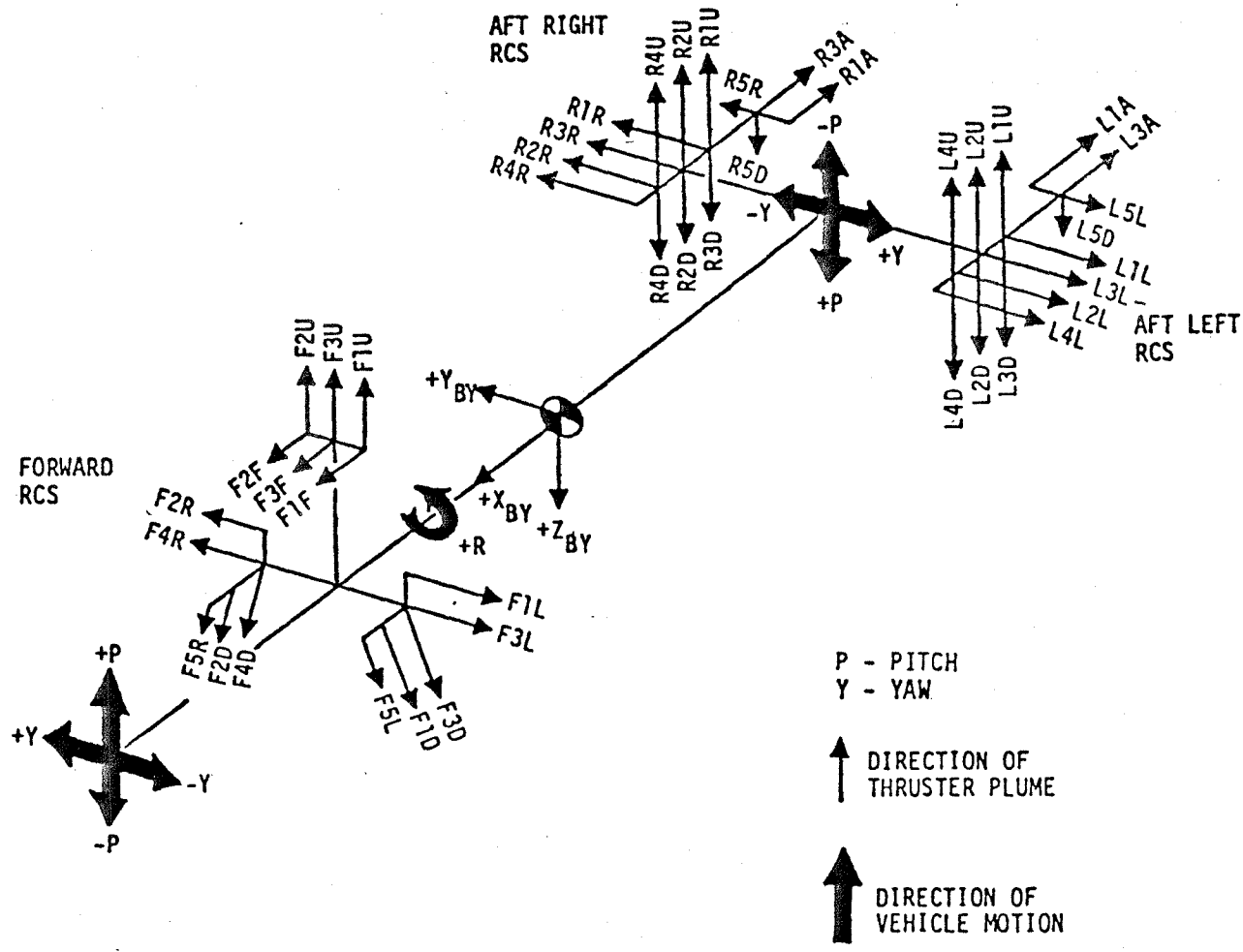

Figure 8 RCS THRUSTER LOCATIONS AND ORIENTATIONS

Figure 11 gives the required radius arm versus rotational speed for centripetal acceleration levels from $10^{-1}g_o$ to $10^{-4}g_o$. The centripetal acceleration was determined from:

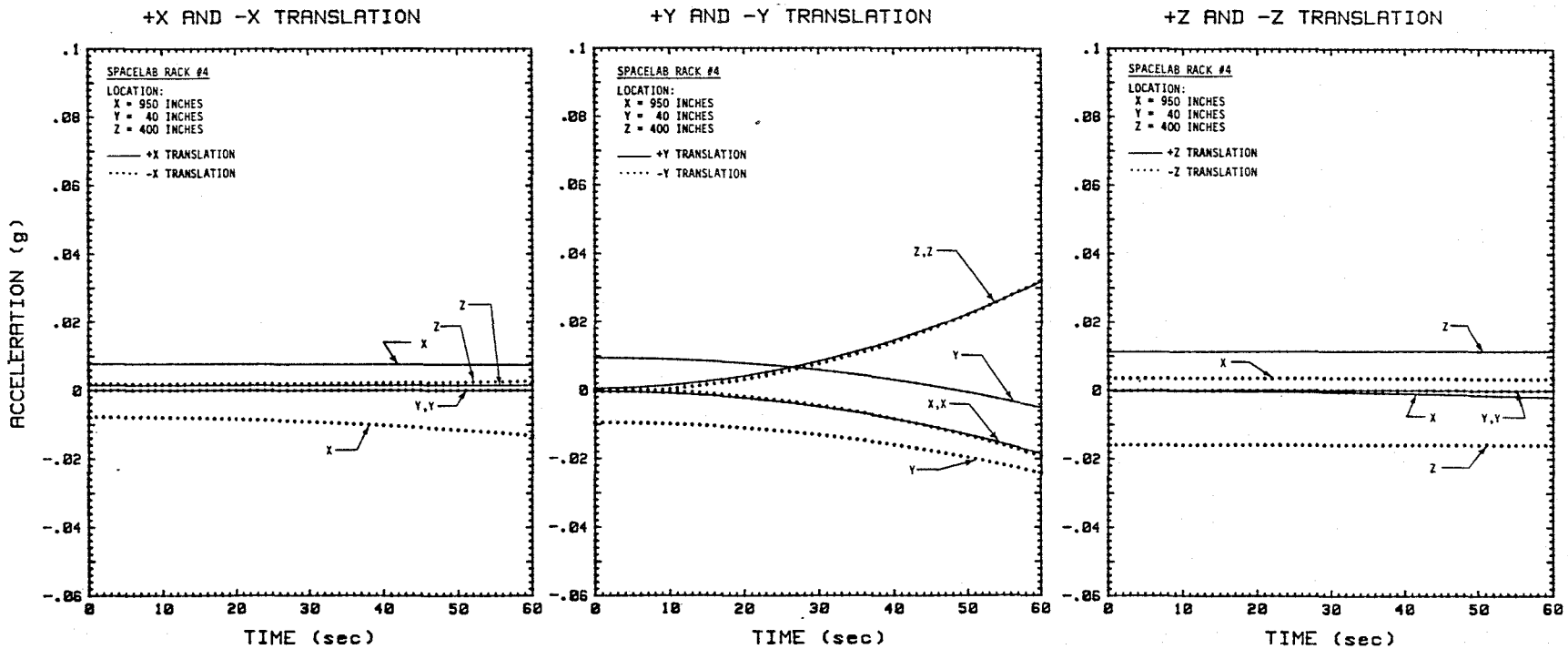

Figure 9 RCS ACCELERATIONS FOR SPACELAB

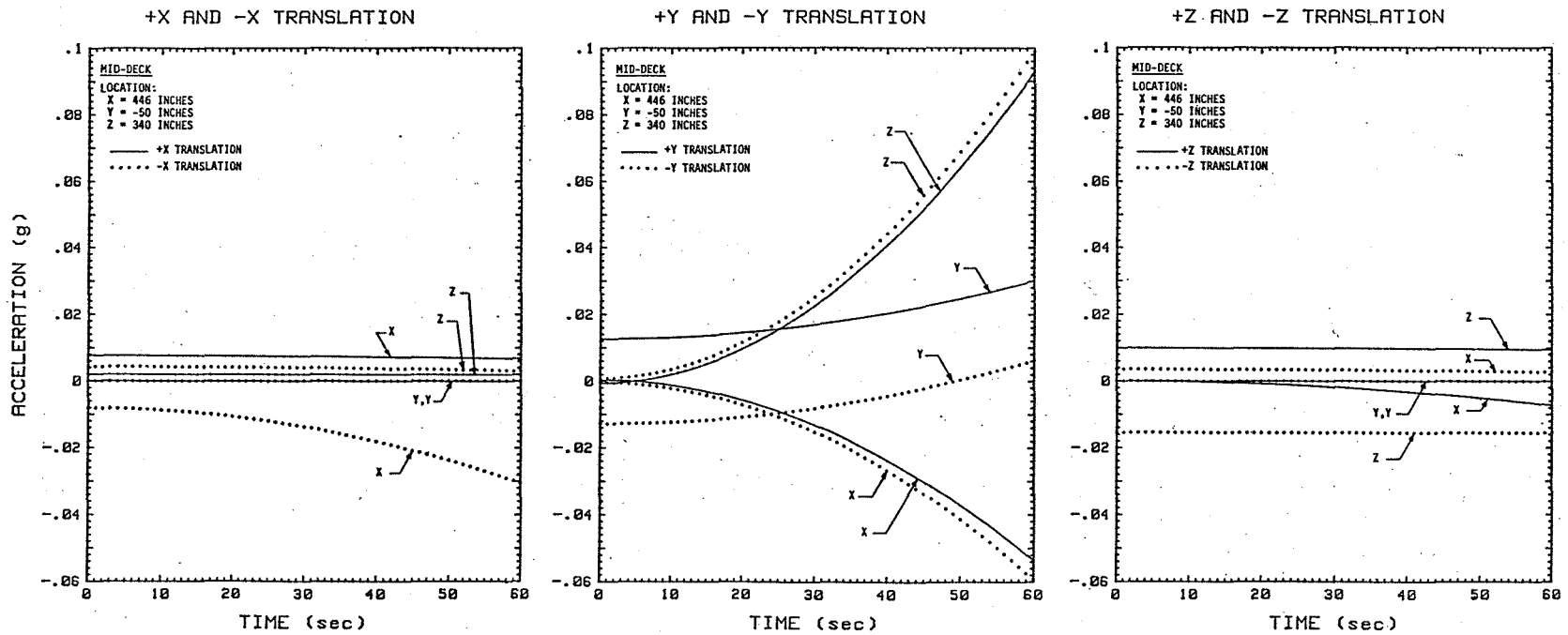

Figure 10 RCS ACCELERATIONS FOR THE MIDDECK

$$a_{cent} = \vec{\omega} \times \vec{\omega} \times \vec{\rho} \qquad \text{(Equation 3)}$$

Also shown in Figure 11 is the "ACCEPTABLE RANGE," where Coriolis accelerations are less than ten percent of the centripetal acceleration.

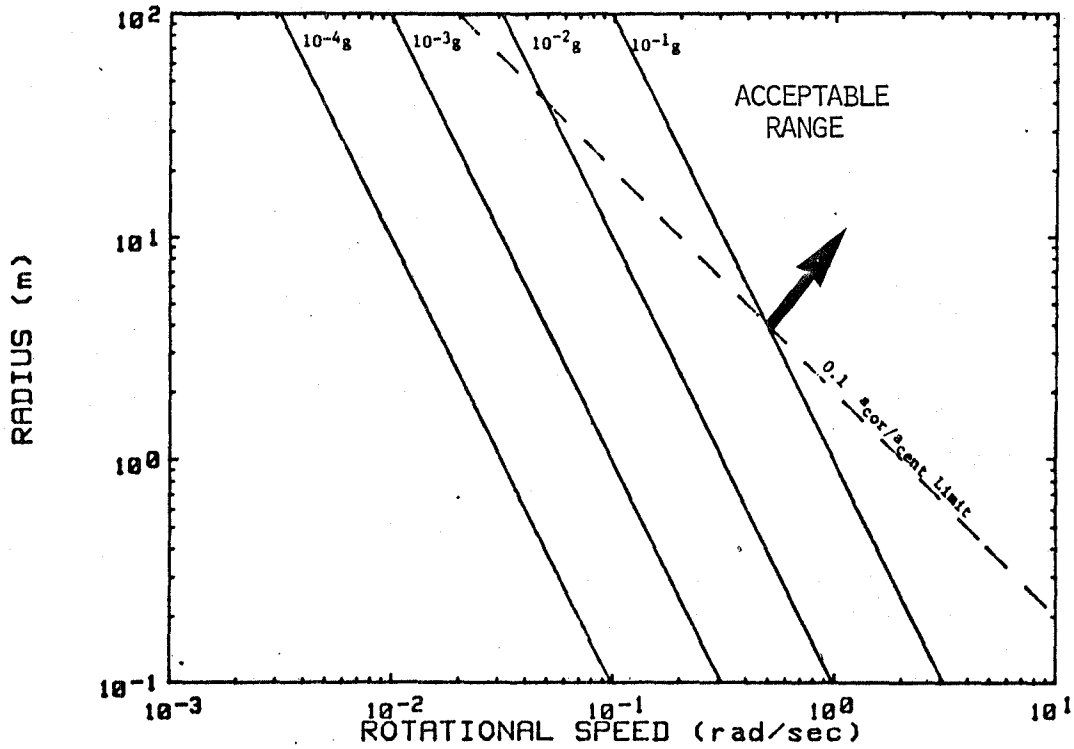

Figure 11 REQUIRED RADIUS ARM VERSUS ROTATIONAL SPEED FOR ACCELERATIONS PRODUCED BY ROTATION

Coriolis accelerations were determined from

$$a_{cor} = 2\,\vec{\omega} \times \dot{\vec{\rho}} \qquad \text{(Equation 4)}$$

where the velocity of the test fluid, $\dot{\vec{\rho}}$, was conservatively assumed equal to 1 m/s.

Figure 11 shows that to operate in the acceptable range of a_{cor}/a_{cent} and produce accelerations of $10^{-2}g_o$ to $10^{-4}g_o$, unacceptably long radius arms are required. Acceleration by rotation was rejected as a method of producing the required acceleration levels for this reason.

Acceleration by Independent Translation. The final method of producing accelerations considered was translation of the experiments independent of the Orbiter. Translation could be accomplished by towing the experiment or using gas jets. The advantages of this approach are the same as with experiment rotation in that acceleration level is not restricted to Orbiter RCS or drag -g levels and no RCS propellant is used. The disadvantages of this approach are the maximum acceleration level that can be achieved for 45 seconds in the middeck or Spacelab is $2.4 \times 10^{-4} g_o$ (assuming the maximum available travel distance is approximately 2 m). In addition, the kinetic energy of the experiment at the end of the translation is a potential hazard. Also, changes in the experiment center of mass would change the acceleration level during the translation. For these reasons, independent translation was rejected as a method of producing the required acceleration levels.

Acceleration Summary. From the analyses of the acceleration methods, we selected Orbiter RCS +X and Orbiter drag -g as the only practical means of producing the acceleration levels required by the experiment test objectives. Therefore, the test matrices had to be modified to meet the experimental objectives at the available acceleration levels.

2.3 Revised Experiment Designs. The revised test matrices and designs of the individual experiments that were developed are summarized below.

2.3.1 Liquid Reorientation Experiment. The revised test matrix for the liquid reorientation experiment is summarized in Table IV, where the acceleration level is 0.008 g_o (RCS +X), time for reorientation is 60 seconds, and the test fluid is FC-77. Tank fineness ratio is defined as the ratio of the tank length to diameter. The Weber numbers associated with this test matrix range from 2 to 15 and should cover reorientation without any geysering through most of the geysering range, based on data from Reference 6.

As shown in Figure 12, the experiment consists of three clear reorientation tanks and a clear cylindrical supply tank with an O-ring sealed piston for liquid expulsion. Initially all three reorientation tanks are evacuated. The supply tank and the piping between the supply tank and the valves isolating each tank are filled with FC-77 liquid. The air contained in the supply tank permits the piston to move as the liquid expands due to environmental temperature changes. If the piston jams, or for some reason the air pressure exceeds maximum design pressure, a relief valve will open and allow liquid to enter one of the reorientation tanks.

TABLE IV LIQUID REORIENTATION EXPERIMENT TEST MATRIX

Tank Diameter (cm)	Tank Fineness Ratio	Bond Number	Tank Fill Ratios (%)
8.33	1.50	65	20, 50, 70
5.10	2.45	24	20, 50, 70
3.13	4.00	9	20, 50, 70

The experiment is operated in flight by opening the supply tank piston air-side vent and then opening one of the reorientation tank valves to allow liquid to enter the tank. The piston is driven by the pressure differential across the piston which is the difference between the saturation pressure of FC-77 at ambient temperature 5.5-6.2 kPa (0.80-0.90 psia) and ambient pressure 94-110 kPa (13.6-16 psia). Metering of the liquid volume entering each tank is accomplished by monitoring the position of the piston.

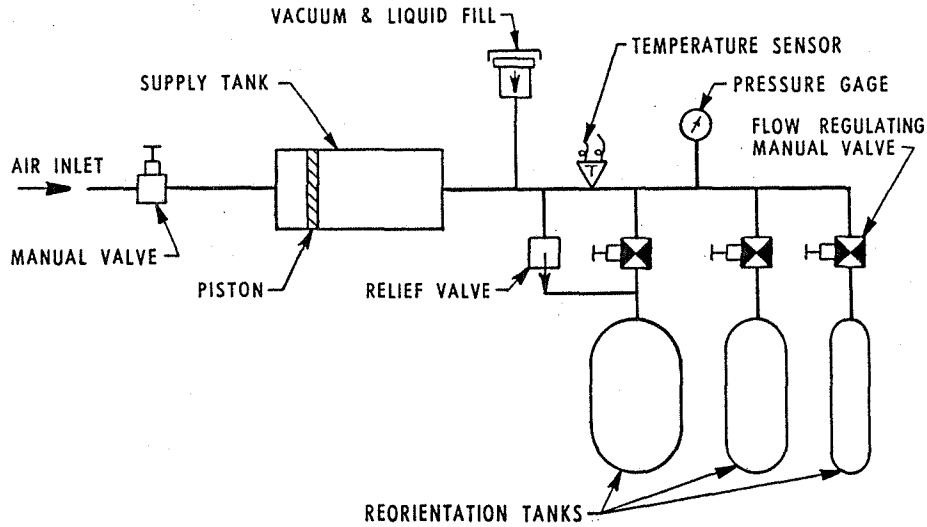

Figure 12 LIQUID REORIENTATION EXPERIMENT FLOW SCHEMATIC

The capillary acquisition device in the supply tank and the overboard vent required in the baseline design have been eliminated.

Pool Boiling Experiment. The revised test matrix for the pool boiling experiment is given in Table V. The parameter R' is given for the RCS +X acceleration level and the Orbiter drag acceleration level. Total time required at each test point is 45 seconds. The heater wire diameters shown in Table V are larger than those given in the baseline test matrix so

that temperature measurement along the length of the heaters can more readily be accomplished. Also, the hazardous test fluid methanol was replaced by ethanol.

Figure 13 gives the flow schematic for the pool boiling experiment. Prior to launch, each test cell and associated plumbing is evacuated through the charging valve. The appropriate test fluid is then loaded into each cell, while the overflow tank remains evacuated, with the manual valve closed. After each cell is filled, the manual valves are opened slightly to allow test fluid vapor to fill the overflow tank and to allow the pressure to equalize, after which they are closed again. By following this procedure, the test cells remain full of liquid with virtually no entrained vapor, assuring vapor bubbles are not present at the start of the test. The relief valve prevents overpressurization of the test cells, by allowing test fluid to flow from the cell to the overflow tank.

Just prior to the start of a test, the manual valves of the cells to be tested are opened, allowing pressure equilization and allowing the cells to operate in the presence of a test fluid vapor volume of approximately 10 per cent. This assures that an almost constant pressure is maintained during the test, and that saturated conditions exist at the start of the test. After the first test on a cell is complete (using RCS thrust firings), the manual valve is closed to prevent liquid from escaping into the overflow tank. The valve is opened again just prior to the start of the second test of a cell (using drag-g acceleration). The revised design avoids the overboard venting and the preheating requirements of the baseline design.

Proof-of-Concept Testing. In order to verify that the pressure rise in a pool boiling cell is small during a test, proof-of-concept testing of the pool boiling experiment was performed. Boiling tests were made with the acrylic test cell shown in Figure 14. This cell was filled with water and then pumped down to the saturation pressure at 26°C of 3.46 Pa. Table VI gives tabular test results of two 300-second boiling runs. In the first test, the heater power was set at 234 watts and in the second test 169 watts. Also in the second test, the cell initial pressure was 5.07 kPa. These tests clearly show that the pressure rise in the cell over the length of the test was very small, indicating that the cell operated at or near thermodynamic equilibrium during the entire test run. The testing also confirmed that only small amounts of vapor were actually generated during a run, indicating that no special method of vapor removal would be required for the pool boiling experiment between the high-g (RCS +X) and low-g (drag) runs. Figure 15 shows the boiling taking place during the first run.

TABLE V POOL BOILING EXPERIMENT TEST MATRIX

Cell	Test Fluid	Heater Diameter, cm	R' @ 10^{-6}g	R' @ 0.008g	Heater Power, W
1	Water	0.800	0.0016	0.14	20
2	Water	0.318	0.00062	0.056	15
3	Water	0.051	0.00010	0.0089	10
4	Ethanol	0.800	0.0025	0.22	124
5	Ethanol	0.318	0.00099	0.089	96
6	Ethanol	0.051	0.00016	0.014	62
7	Freon 113	0.800	0.0039	0.35	34
8	Freon 113	0.318	0.0016	0.14	26
9	Freon 113	0.051	0.00025	0.22	17

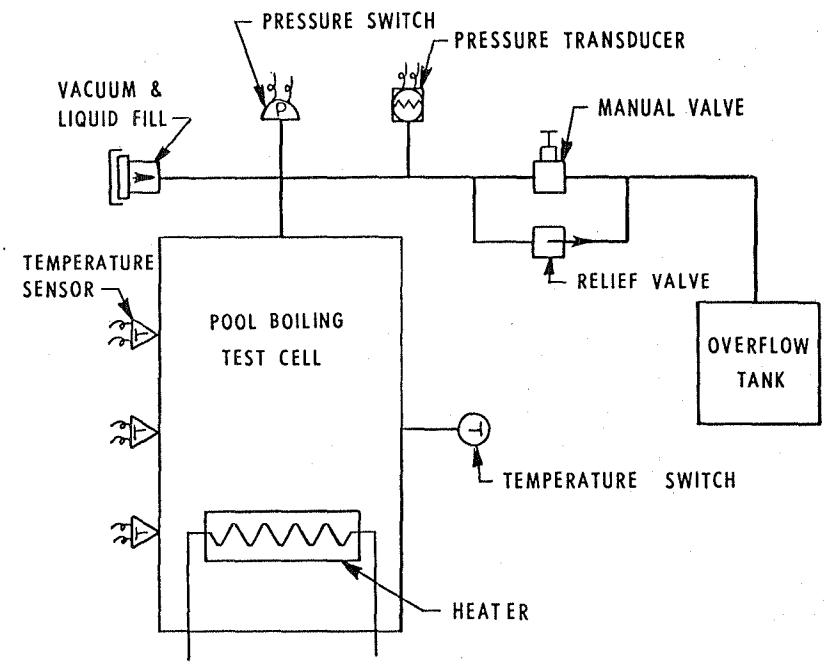

Figure 13 POOL BOILING EXPERIMENT FLOW SCHEMATIC

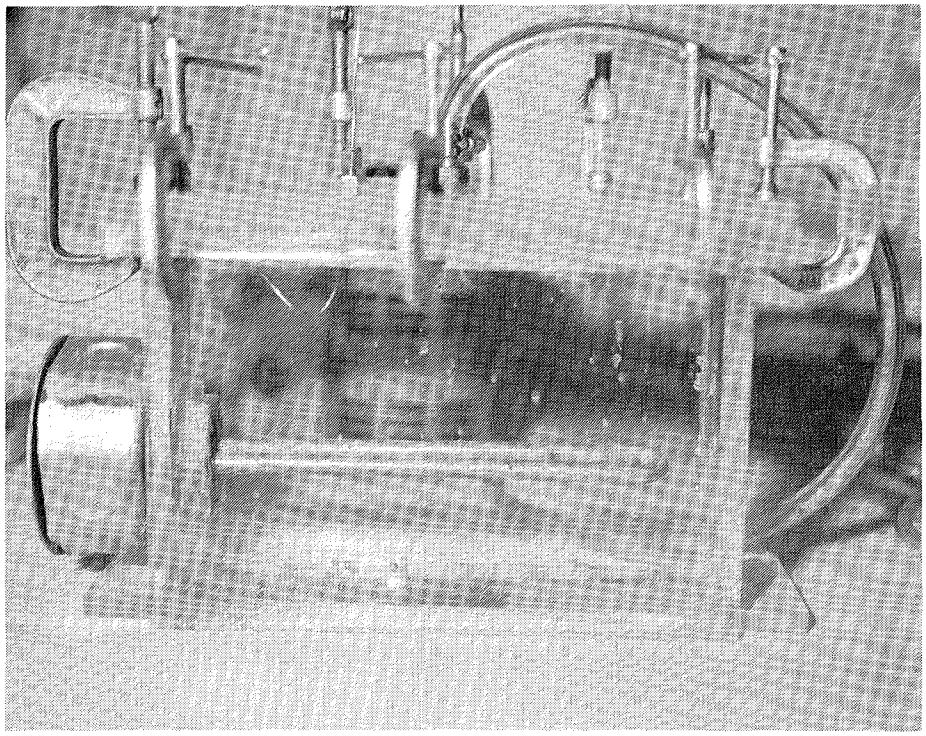

Figure 14 POOL BOILING PROOF-OF-CONCEPT TEST CELL

Figure 15 POOL BOILING AT Q = 234 W

TABLE VI POOL BOILING TEST PRESSURE RISE

Time (sec)	Q = 234 W Cell Pressure (kPa)	Q = 169 W Cell Pressure (kPa)
0	3.46	5.07
30	3.63	5.16
60	3.74	5.45
90	3.85	5.61
120	3.93	5.78
150	4.01	5.98
180	4.08	6.16
210	4.16	6.30
240	4.36	6.41
270	4.54	6.44
300	4.72	6.49

Flow Boiling Experiment. The revised test matrix for the flow boiling experiment is given in Table VII. Figure 16 shows these test points on the mass velocity versus quality plot with flow regime boundaries estimated using Reference 5 for 0.008 g_o and $10^{-6}g_o$. The 38 test points given in the baseline design have been reduced to 15, with 9 at 0.008 g_o and 6 at $10^{-6}g_o$. Also, all inlet conditions are the same (slightly subcooled), eliminating the need for inlet quality measurement and simplifying the experiment control requirements.

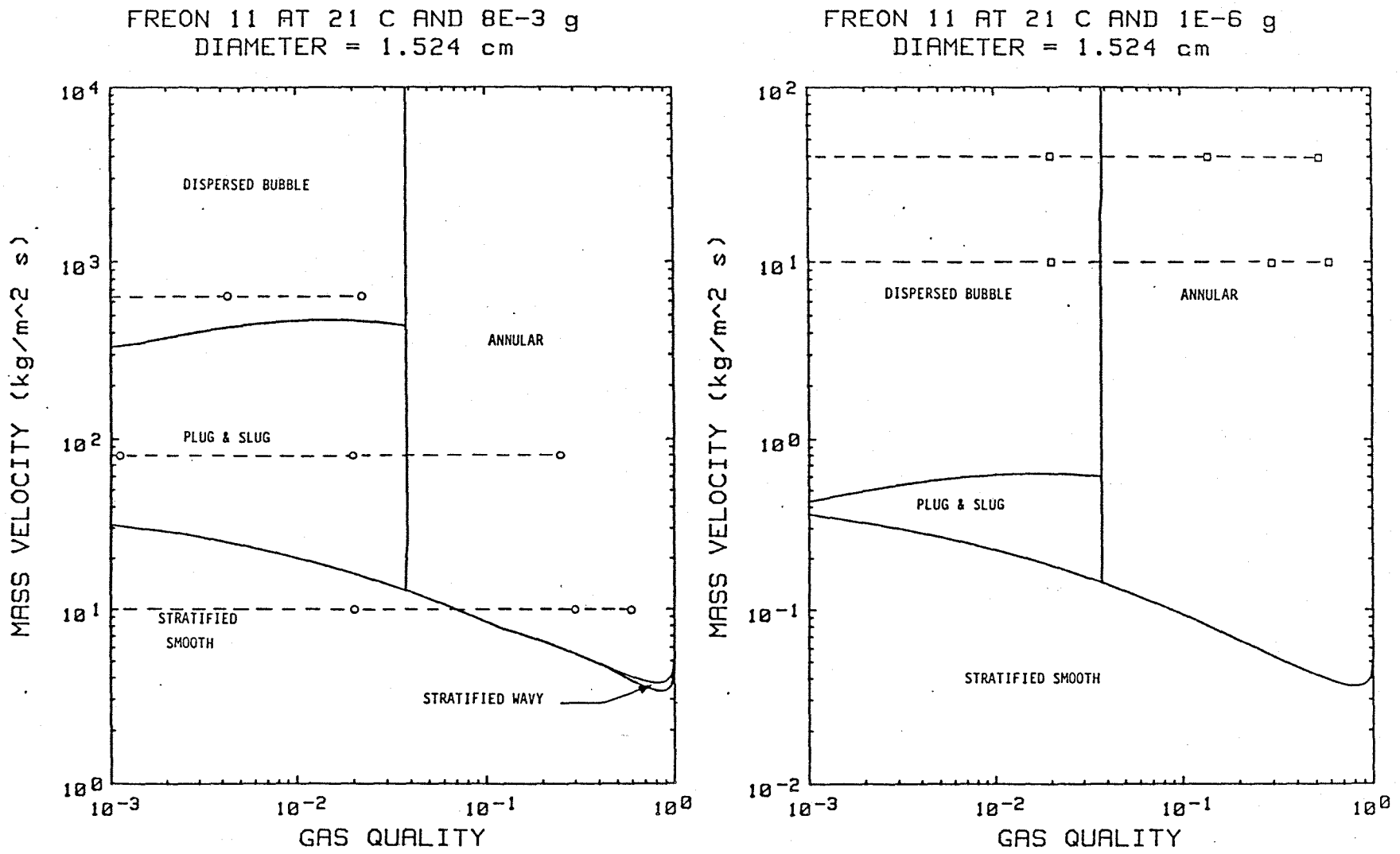

Figure 16 FLOW BOILING EXPERIMENT TEST MATRIX

TABLE VII FLOW BOILING TEST MATRIX

Mass Velocity (kg/m^2s)	Gravity Level (g)	Heater Power (W)	Inlet Quality	Outlet Quality
10	8×10^{-3}	10	-0.011	0.020
10	8×10^{-3}	100	-0.011	0.302
10	8×10^{-3}	195	-0.011	0.598
80	8×10^{-3}	32	-0.011	0.001
80	8×10^{-3}	80	-0.011	0.020
80	8×10^{-3}	679	-0.011	0.250
640	8×10^{-3}	128	-0.011	-0.005
640	8×10^{-3}	320	-0.011	0.004
640	8×10^{-3}	679	-0.011	0.022
10	10^{-6}	10	-0.011	0.020
10	10^{-6}	100	-0.011	0.302
10	10^{-6}	195	-0.011	0.598
40	10^{-6}	40	-0.011	0.020
40	10^{-6}	200	-0.011	0.145
40	10^{-6}	679	-0.011	0.520

The revised flow schematic for the flow boiling experiment is given in Figure 17. The major revisions made to the experiment design are elimination of the inlet quality measurement and replacement, by a condenser and accumulator, of the liquid vapor separator and capillary acquisition tank. Orbiter cooling water is used as the cooling source. The design thus eliminates the need to vent test fluid overboard, and furthermore, eliminates the need to develop a high risk capillary acquisition supply tank. Flow, temperature and pressure switches prevent over-temperature or over-pressurization of the experiment by shutting down the test section heater and the preheater.

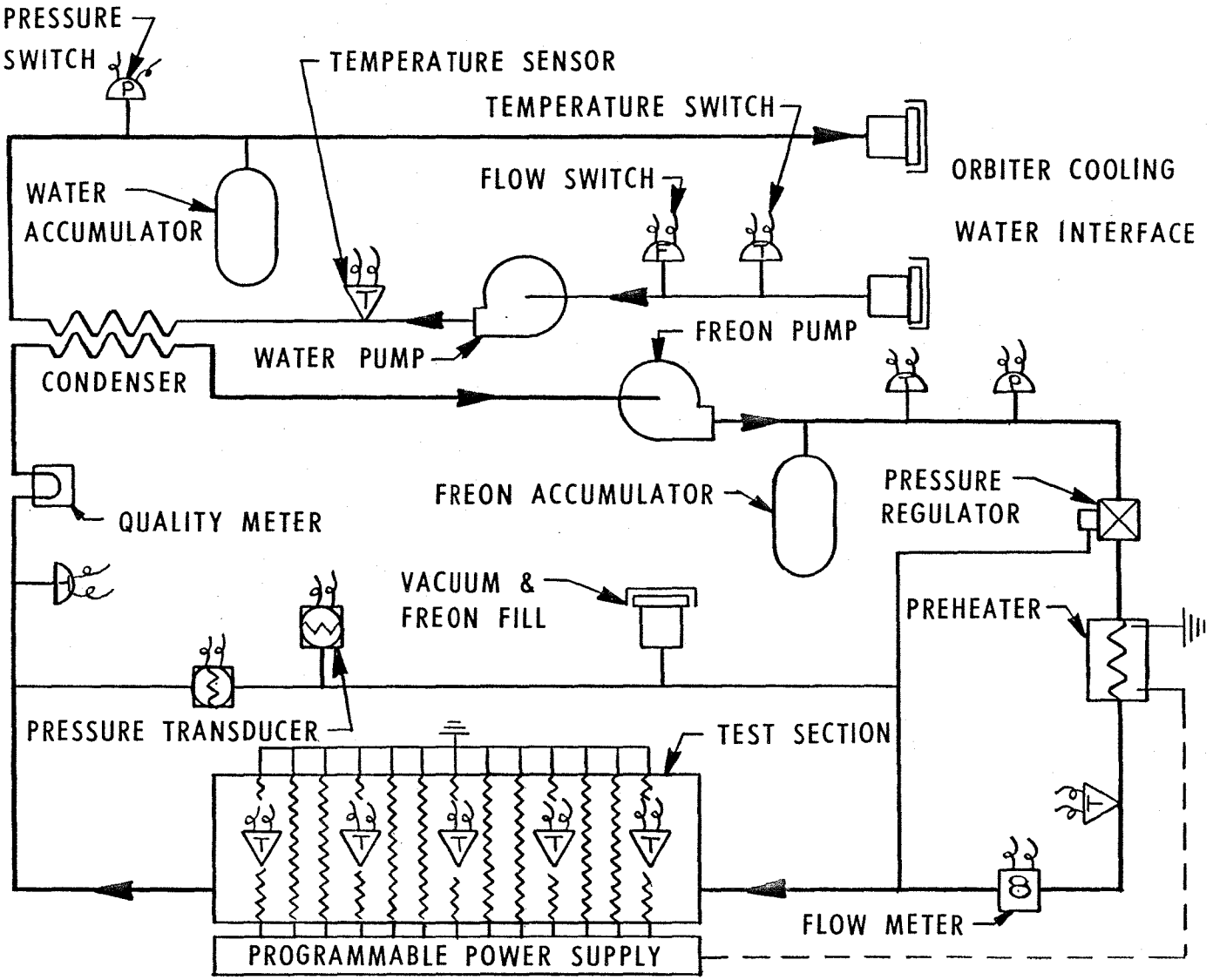

Figure 17 FLOW BOILING EXPERIMENT FLOW SCHEMATIC

3.0 EVALUATION OF DESIGN APPROACHES

Selection of the preferred experiment design approach--that is, the facility approach or carry-on approach--was based on a comparison of the weight, volume, power, development costs and flight costs of conceptual designs based on the revised schematics described in Section 2.3. The selection of the preferred approach is discussed in detail in Section 3.4. The general method for developing the estimates consists of the following:

- A conceptual design for a Spacelab fluid research facility was developed for both a rack and the center aisle.
- The optimum carry-on location was selected from a number of possibilities based on a comparison of the capabilities, cost, availability and limitations of each possible location.
- Conceptual designs for each experiment were developed for the selected carry-on location.
- The preferred approach for each experiment was selected.

3.1 Conceptual Facility Design. A layout of the two-phase fluid research facility in Spacelab Rack 4 is shown in Figure 18. Rack 4 is used because it contains the Experiment Heat Exchanger (EHX) which serves as the heat sink for the flow boiling experiment condenser. An alternate location for the facility in Spacelab is in the center aisle at the aft end of the habitable module. The center aisle has provisions for air cooling, power and access to the subfloor for routing of water cooling lines to the EHX in Rack 4. (Use of this location presupposes that the EHX is available.) The facility layout in the center aisle is shown in Figure 19.

Power and cooling requirements are identical for either the rack mounted or center aisle versions of the facility. Table VIII summarizes the power requirements. Table IX summarizes the cooling requirements. Table X summarizes the weights of the facility. If all three experiments were operated simultaneously, the total power consumption (and cooling load) would be 1887 watts, which is within the Spacelab limit for a double rack or the center aisle.

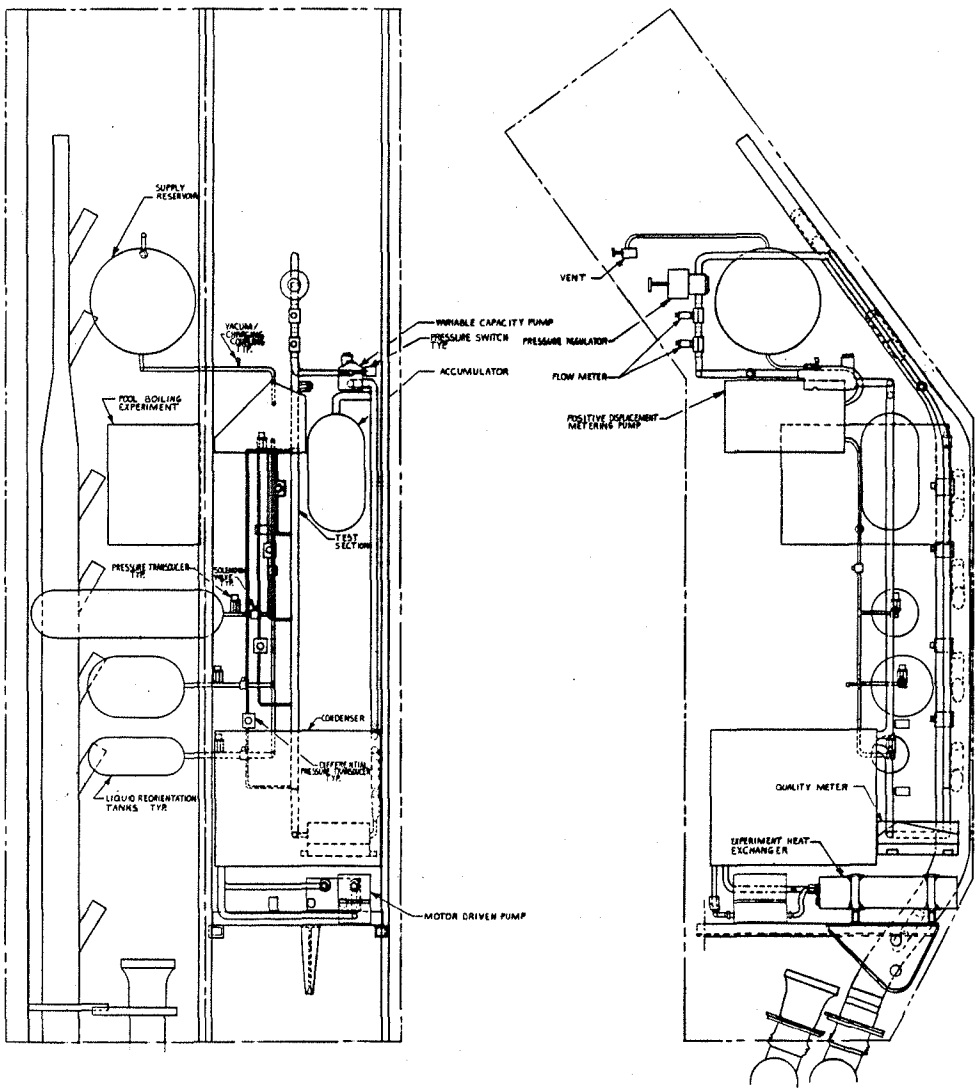

Figure 18 RACK MOUNTED VERSION OF TWO-PHASE FLUID RESEARCH FACILITY

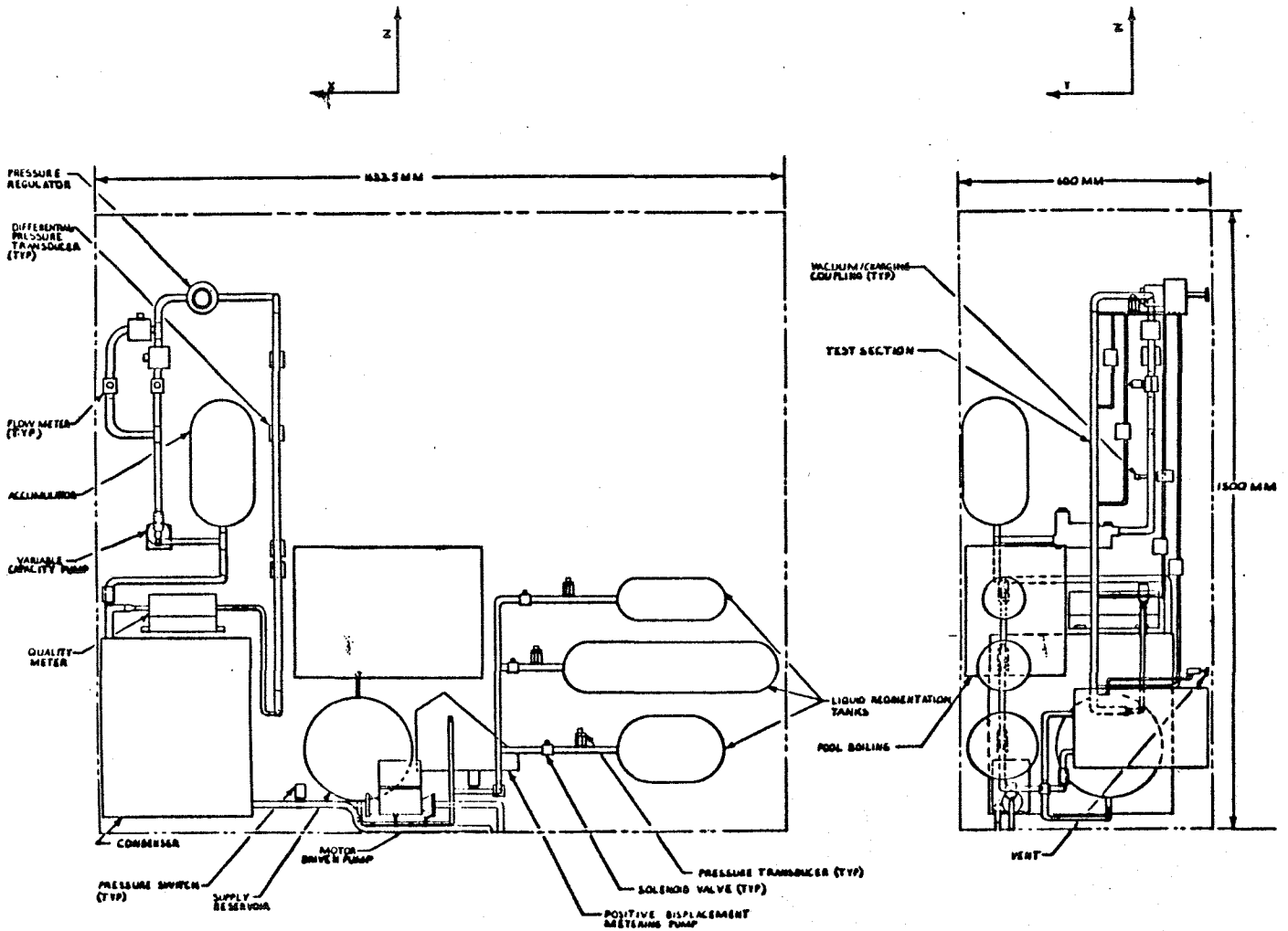

Figure 19 TWO-PHASE FLUID RESEARCH FACILITY - SPACELAB CENTER AISLE

TABLE VIII SPACELAB FACILITY - POWER REQUIREMENTS

Component	Flow Boiling Experiment Power Required (watts)	Liquid Reorientation Experiment Power Required (watts)	Pool Boiling Experiment Power Required (watts)
Camera	56.0	56.0	56.0
Lighting	100.0	100.0	60.0
Data Acquisition Computer	67.0	67.0	67.0
Accelerometers	5.0	5.0	5.0
Pressure Transducers	1.0	1.5	0.5
Temperature Sensors	6.0	1.5	3.0
Differential Pressure Transducers	2.0	--	--
Solenoid Valves	--	14.0	--
Metering Pump	--	75.0	--
Heater	680.0	--	117.0*
Preheater	50.0	--	--
Variable Speed Pump	200.0	--	--
Condenser Circulation Pump	75.0	--	--
Flow Meter	1.0	--	--
Quality Meter	15.0	--	--
Totals	1,258.0	320.0	308.5

*Maximum

TABLE IX SPACELAB FACILITY - COOLING REQUIREMENTS

Component	Flow Boiling Experiment Heat Dissipation (watts)		Liquid Reorientation Experiment Heat Dissipation (watts)	Pool Boiling Experiment Heat Dissipation (watts)
	To Avionics or Cabin Air Loop	To Exper. Heat Exchanger	To Avionics or Cabin Air Loop	To Avionics or Cabin Air Loop
Camera	56.0		56.0	56.0
Lighting	100.0		100.0	60.0
Data Acquisition Computer	67.0		67.0	67.0
Accelerometers	5.0		5.0	5.0
Pressure Transducers	1.0		1.5	0.5
Temperature Sensors	6.0		1.5	3.0
Differential Pressure Transducers	2.0			
Solenoid Valves			14.0	
Metering Pump			75.0	
Heater		680.0		117.0 *
Preheater		50.0		
Variable Speed Pump		200.0		
Condenser Circulation Pump		75.0		
Flowmeter	1.0			
Quality Meter	15.0			
Totals	253.0	1005.0	320.0	308.5
	1258.0			

*Maximum

TABLE X SPACELAB FACILITY - WEIGHTS

Experiment	Dry Weight (kg)	Fluid Weight (kg)	Total (kg)
Flow Boiling	81.6	14.8	96.4
Pool Boiling	18.1	10.0	28.1
Liquid Reorientation	30.2	23.5	53.7
Total	129.9	48.3	178.2

Table XI summarizes the RCS propellant requirements for the three experiments. If the experiments were run serially, the propellant requirements would exceed the allowance of 1811 kg provided for experiments. In fact, to stay within the experiment propellant allowance, all three experiments must be run simultaneously.

TABLE XI RCS FUEL REQUIREMENTS
SPACELAB FACILITY

Experiment	Number of Burns	Duration (sec)	Propellant Used (kg)
Flow Boiling	9	60	1604
Pool Boiling	9	45	1203
Liquid Reorientation	3	60	535
Total	21	-	3342

Development costs for the facility were estimated using Beech's experience with similar hardware. The ROM development costs are summarized in Table XII. The costs shown in the table are for the development items only and do not include the basic costs of fabricating, testing or qualifying the overall experiment package. It was assumed for the purposes of comparison between the facility and the carry-ons that hardware fabrication and qualification costs (exclusive of development items) would be approximately equal. No vendor estimates were included in Table XII. (Actual estimates of experiment costs are given in Section 5.0.)

TABLE XII SPACELAB FACILITY - DEVELOPMENT COST

(Costs are in Thousands of 1982 Dollars)

Item	Design	Test	Fabrication	Total
Flow Boiling:				
- Test Section	20	25	25	70
- Condenser	20	25	16	61
Pool Boiling:				
- Test Cell (Includes Heaters)	5	10	6	21
Liquid Reorientation				
- Test Tanks	10	30	6	46
Data Acquisition and Control System	45	10	50	105
Total	100	100	103	303

3.2 Carry-on Location Assessment. Various areas in the Orbiter were evaluated to determine their suitability for carry-on versions of the three experiments. The incentives for considering the carry-on option are potentially lower flight costs than for an equivalent experiment in a Spacelab facility and more flight opportunities.

Areas in the Orbiter considered were:

- Middeck
- Spacelab overhead storage lockers
- Materials experiment assembly
- Aft flight deck
- Getaway special container.

Each area was evaluated with respect to experimental capabilities (power, heat dissipation, etc.), flight cost, availability and limitations.

3.2.1 Middeck. The middeck includes the crew living accommodations such as the galley, head, and stowage lockers below the flight deck. There were actually two areas in the middeck considered during this evaluation: the middeck stowage lockers and a rack mounted in place of the galley.

The general arrangement of the middeck lockers is shown in Figure 20.

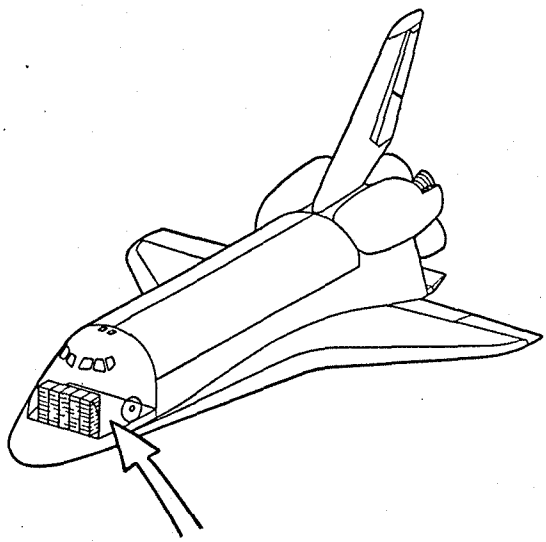

Figure 20 MIDDECK LOCKER LOCATIONS

The locker itself is shown in Figure 21.

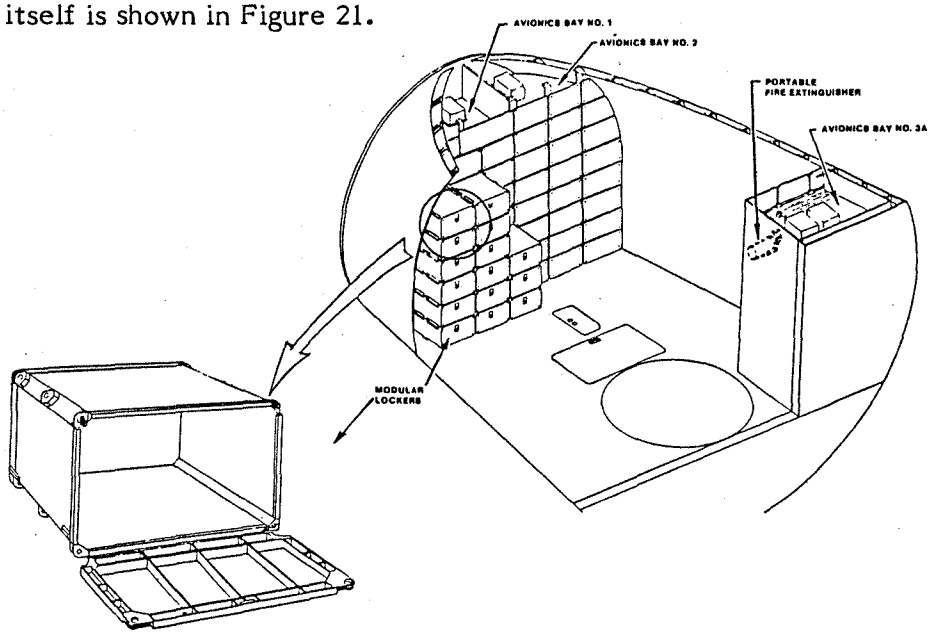

Figure 21 MIDDECK STOWAGE LOCKER

The available services of the middeck lockers include:

- Volume: 0.057 m^3
- Weight: 27 kg
- Energy: A 10 amp 28 volt DC utility outlet, potentially
- Dissipation: 10 watt-hour, maximum per locker
- Crew involvement: 15 minutes of crew time; 15 minutes of Orbiter control

These capabilities are based on the draft version of the middeck experiment policy (Reference 7).

Limitations of the middeck locker are the uncertainty of utility power availability and the very limited power dissipation. In effect, any middeck locker experiment will be battery powered with self-contained data acquisition and control systems.

Another possible configuration of a middeck experiment is shown in Figure 22.

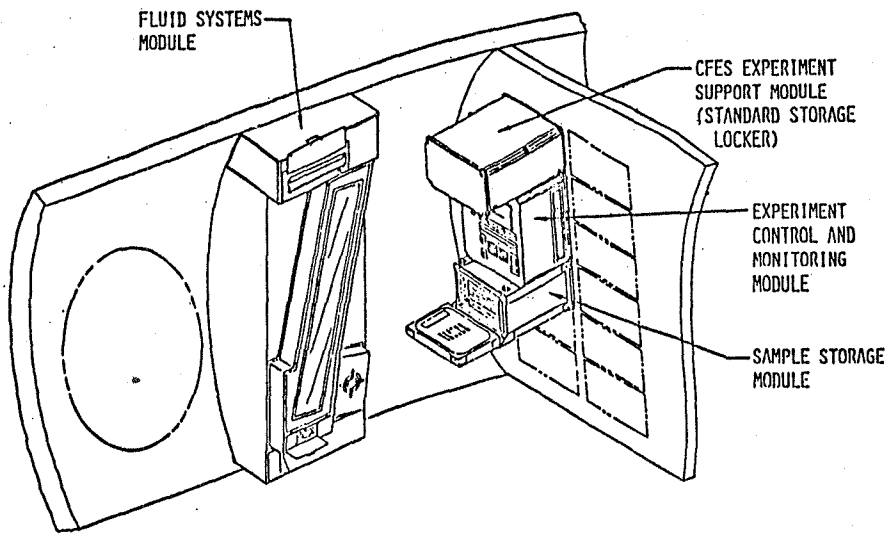

Figure 22 MIDDECK GALLEY RACK

As shown in the Figure, a fluid systems module (the Galley Rack) is mounted in the galley location and takes advantage of the power and water cooling normally available to the galley. Data acquisition and control modules are mounted in nearby middeck lockers.

Such an experiment configuration has been flown on Orbiter 099--an electrophoresis experiment designed by McDonnell Douglas (Reference 8). The services available in the galley rack include:

- Volume: 0.57 m^3
- Weight: 227 kg
- Power: 500 watts
- Dissipation: 1000 watts

There are two major limitations associated with the galley rack:

- Availability and pricing are completely undefined
- The active cooling capability is available only on Orbiters 099 and 102, and is not available on these Orbiters when the galley is required.

3.2.2 Spacelab Overhead Storage Lockers. A limited number of overhead storage lockers are provided in Spacelab for the stowage of miscellaneous experiment hardware. The locker configuration is shown in Figure 23.

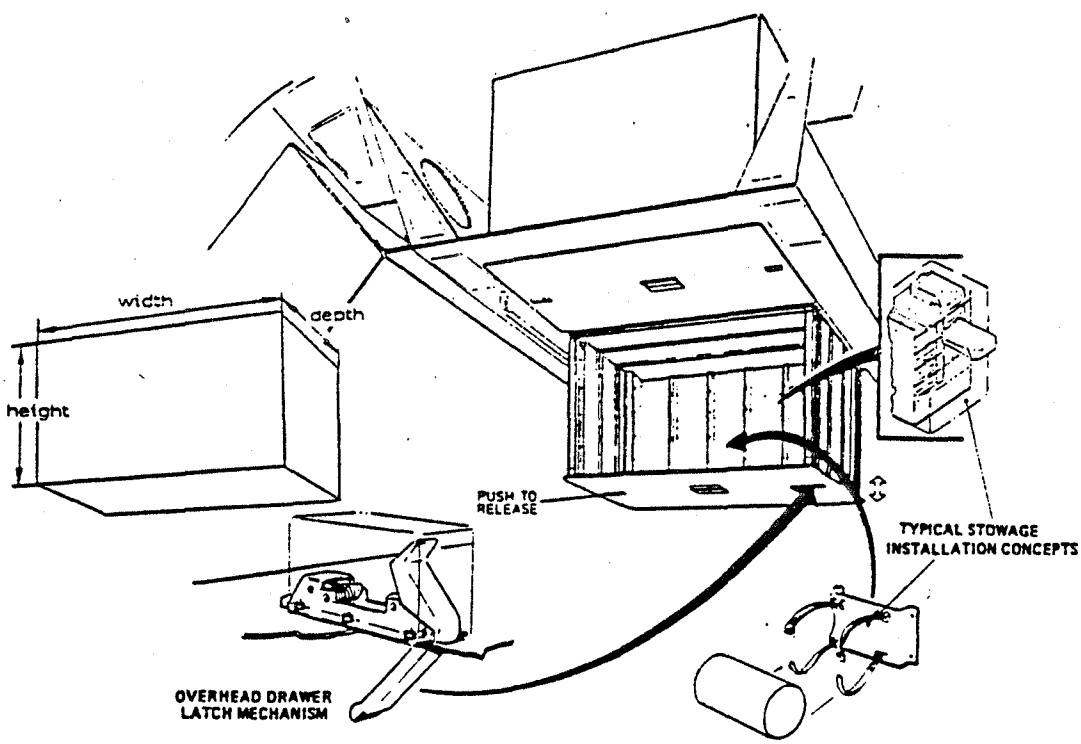

Figure 23 SPACELAB OVERHEAD STORAGE LOCKER

The services available from the overhead locker include:

- Volume: 0.0813 m^3
- Weight: 33.5 kg
- Power: none (plug into Spacelab utility outlets)

Costs for the overhead locker, listed in Reference 9, are $450K (1982 dollars)--the minimum Spacelab flight costs. Limitations include:

- Limited availability: eight lockers per module; only available on Spacelab missions.
- Limited space available in Spacelab for experiment activities.

3.2.3 Materials Experiment Assembly. The Materials Experiment Assembly (MEA) was developed to provide a relatively inexpensive platform for materials processing research in the Orbiter. As can be seen in Figure 24, the MEA consists of four cylinders mounted in a small power, control and thermal protection module.

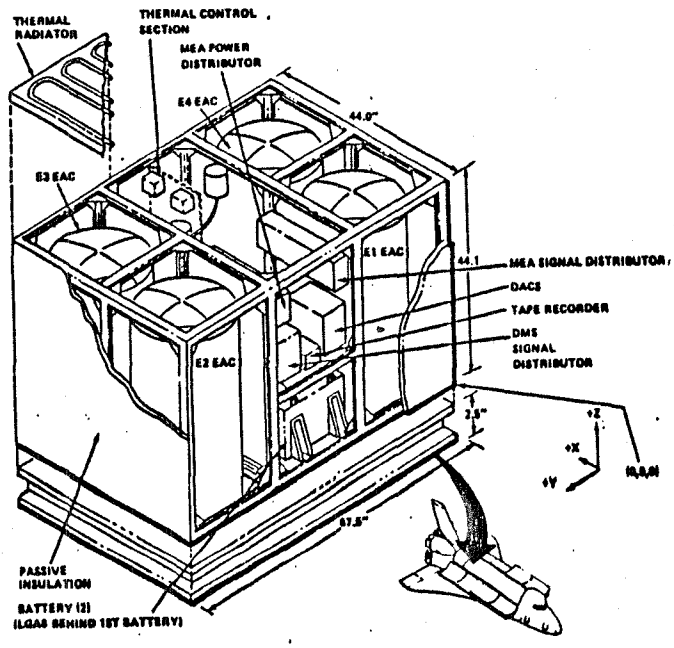

Figure 24 MATERIALS EXPERIMENT ASSEMBLY

The basic available services of the MEA are:

- Volume: Four cylinders of 0.13 m^3 each
- Weight: 36 kg per cylinder
- Power: 500 amp-hour at 36 volts total

The major limitation of the MEA is complete absence of astronaut interaction with the experiment. This is a serious drawback for experiments where the primary data is a visual record of the phenomenon being studied. In addition, the MEA is subject to design temperature extremes of 0-52°C, which complicates the design of the experiment compared to a middeck or Spacelab version of the experiment. Finally, the size and shape of the experiment cylinders is not compatible with the liquid reorientation experiment.

3.2.4 Aft Flight Deck. The aft flight deck (AFD) is located immediately behind the Orbiter flight crew stations and is intended primarily for the avionics required to control or service payloads mounted in the payload bay or in Spacelab. The general arrangement of the AFD is shown in Figure 25.

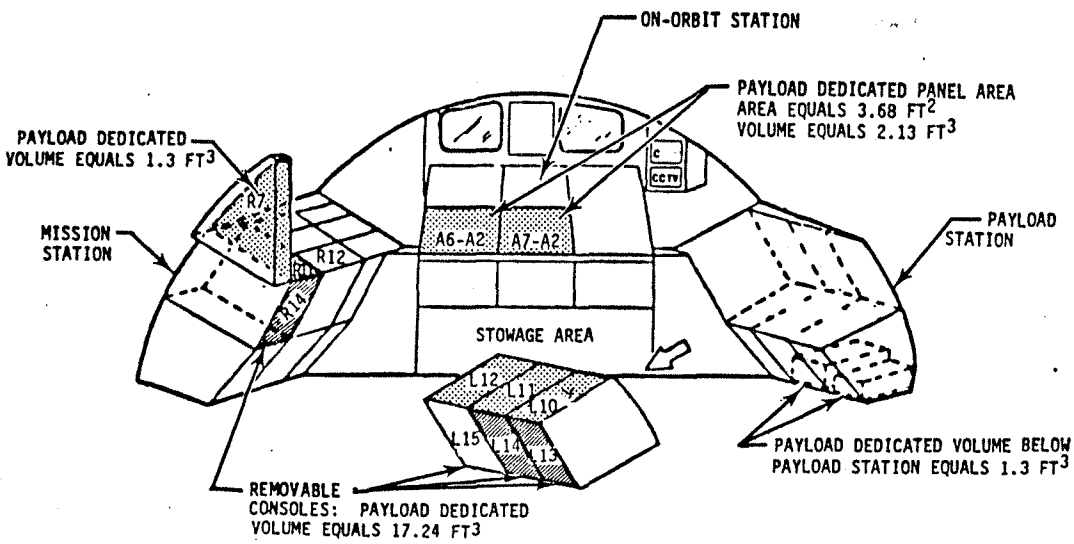

Figure 25 AFT FLIGHT DECK INSTALLATION PROVISIONS

The available services of the AFD include:

- Volume: 0.49 m^3
- Power: 750 watt (continuous); 1000 watt (peak)

The major limitation of the AFD is that it is reserved for support hardware for payload bay experiments and is not intended for the storage of individual experiments. In addition, no water or Freon cooling is available for the flow boiling experiment.

3.2.5 Getaway Special Container. The getaway special container was developed to provide a low cost opportunity for individuals or corporations to fly experiments in the Orbiter payload bay. The package is designed to minimize the impact of the payload on the normal operations of the Shuttle and consequently has very limited experiment support capabilities. The arrangement of the getaway special container is shown in Figure 26.

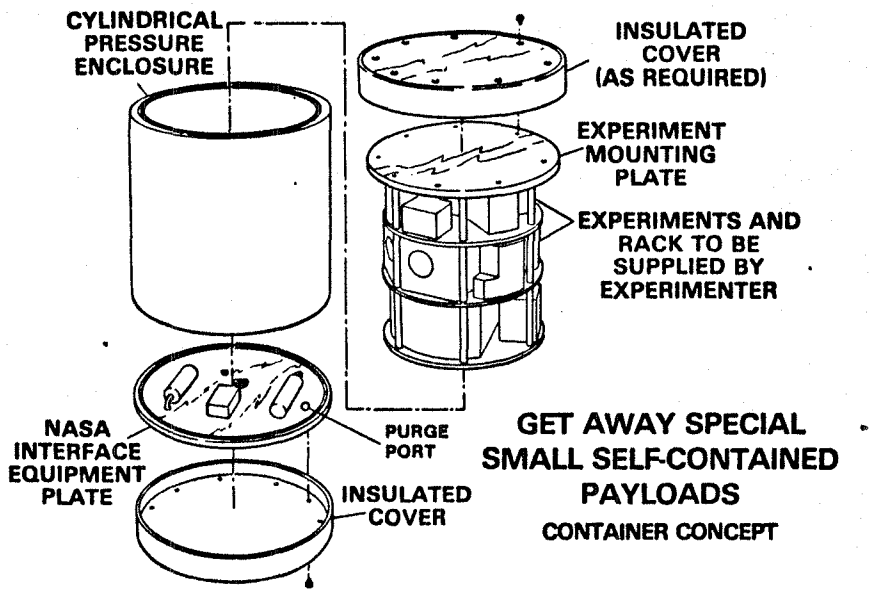

Figure 26 GETAWAY SPECIAL CONTAINER

Services include:

- Volume: 0.14 m^3
- Weight: 91 kg

The getaway special has some serious limitations:

- No access to RCS for required accelerations
- No cooling or power available
- Thermal control system required to maintain payload temperature.

3.3 Middeck Carry-on Designs. The only practical location for carry-on versions of these experiments is the middeck. Figures 27, 28, and 29 are conceptual designs of each of the three experiments in the middeck. Tables XIII, XIV, and XV give the power and heat rejection for each experiment. Both the pool boiling and liquid reorientation experiments fall within the allowable heat rejection for middeck experiments of 10 watt-hours per locker. The 10 watt-hour minimum allowable heat rejection was obtained from Reference 7.

TABLE XIII POWER AND HEAT REJECTION REQUIREMENTS FOR THE CARRY-ON FLOW BOILING EXPERIMENT

Component	Power Required (watts)	Heat Rejection	
		To Cabin Air (watts)	To Coolant Loop (watts)
Camera	56.0	56.0	--
Lighting	50.0	50.0	--
Data Acquisition Computer	67.0	67.0	--
Accelerometers	5.0	5.0	-
Pressure Transducers	1.0	1.0	-
Temperature Sensors	6.0	6.0	-
Differential Pressure Transducers	2.0	2.0	-
Heater	123.0	-	123.0
Preheater	10.0	-	10.0
Variable Speed Pump	100.0	-	100.0
Condenser Circulation Pump	50.0	-	50.0
Flowmeter	1.0	1.0	-
Quality Meter	15.0	15.0	-
Totals	486.0	203.0	283.0

Total power dissipated during fifteen 120-second runs is 102 watt-hours.

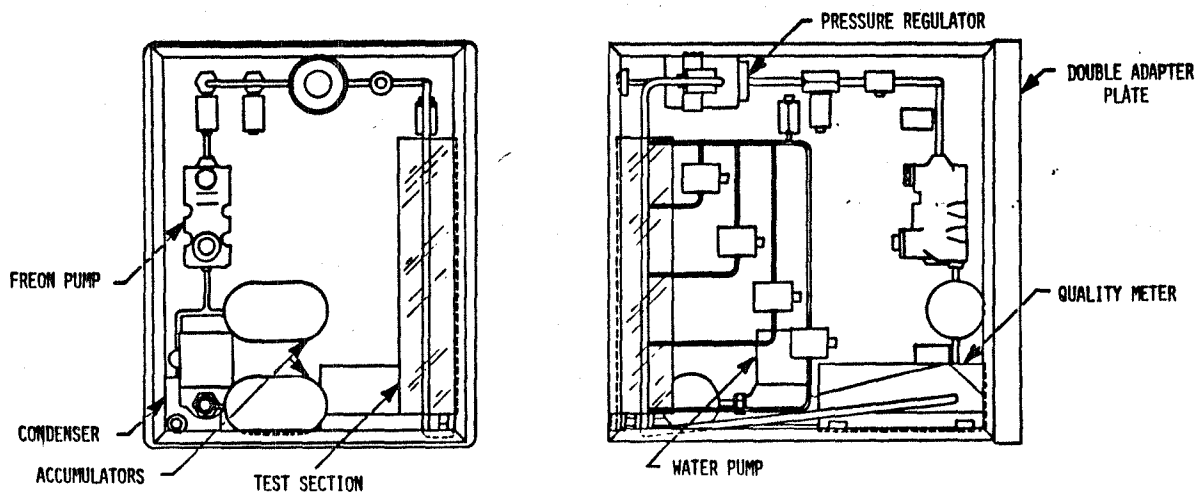

Figure 27 CARRY-ON FLOW BOILING EXPERIMENT CONCEPTUAL DESIGN

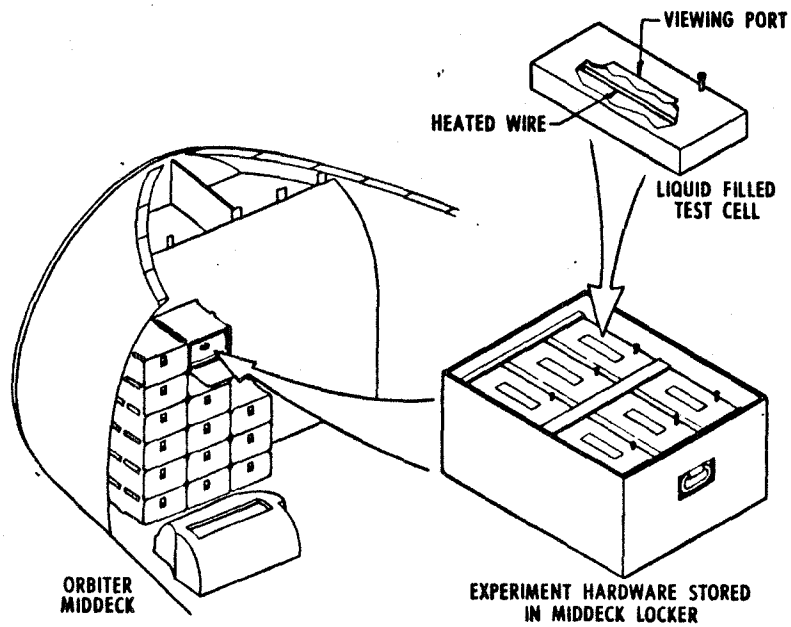

Figure 28 CARRY-ON POOL BOILING EXPERIMENT CONCEPTUAL DESIGN

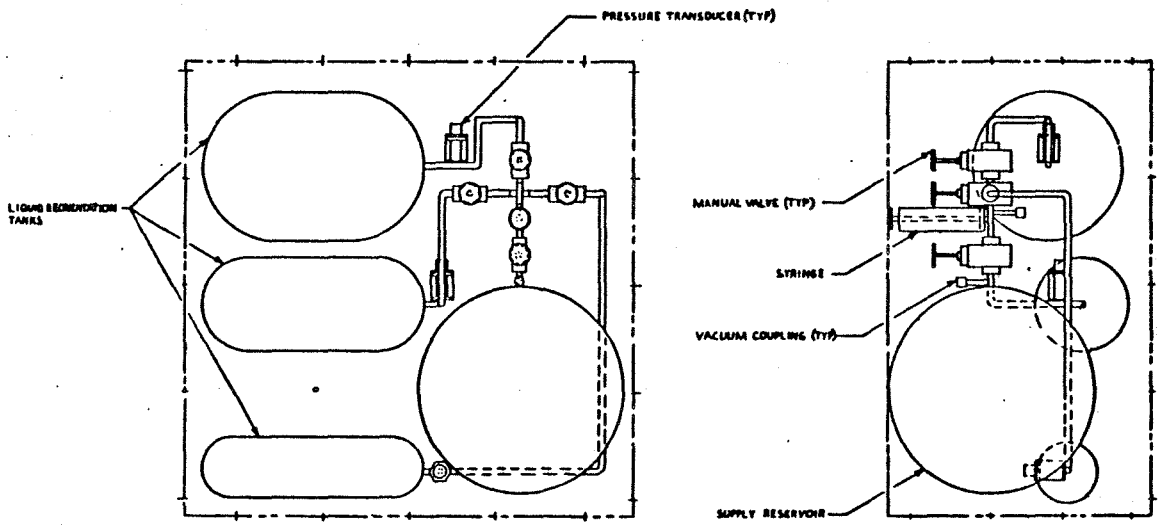

Figure 29 CARRY-ON LIQUID REORIENTATION EXPERIMENT CONCEPTUAL DESIGN

TABLE XIV POWER AND HEAT REJECTION REQUIREMENTS FOR THE CARRY-ON POOL BOILING EXPERIMENT

Component	Power Required (watts)
Camera	56.0
Lights	100.0
Accelerometer	5.0
Pressure/Temperature Switches	0.5
Total	161.5

Total Power Dissipated During Three 60-second Runs is 8.1 watt-hours

TABLE XV POWER AND HEAT REJECTION REQUIREMENTS FOR THE CARRY-ON LIQUID REORIENTATION EXPERIMENT

Component	Power Required (watts)
Camera	56.0
Lights	50.0
Data Acquisition Computer	67.0
Accelerometers	5.0
Pressure Transducers	0.5
Temperature Sensors	3.0
Heater	66.0
Totals	244.0

Total Power Dissipated During Three 60-second Runs is 8.1 watt-hours

Table XVI gives the RCS propellant requirements for each of the individual carry-on experiments. These data show that the flow boiling experiment cannot be flown on the same mission as the other two experiments, because the total RCS propellant used would exceed the 1811 kg available for experiments.

TABLE XVI RCS PROPELLANT REQUIREMENTS FOR THE CARRY-ON EXPERIMENT

Experiment	Number of Burns	Duration (sec)	Propellant Used (kg)
Flow Boiling	9	60	1604
Pool Boiling	3	45	401
Liquid Reorientation	3	60	535
Total	15	-	2540

The weight of each of the carry-on experiments is given in Table XVII. The flow boiling and pool boiling experiments fall under the 27.3 kg maximum weight per locker while the liquid reorientation experiment exceeds this value by 2.3 kg.

TABLE XVII CARRY-ON EXPERIMENT - WEIGHTS

Experiment	Dry Weight (kg)	Fluid Weight (kg)	Total (kg)
Flow Boiling	54.1	1.0	55.1
Pool Boiling	15.5	11.4	26.9
Liquid Reorientation	15.9	13.7	29.6

The development items and their ROM costs for the three carry-on experiments are given in Table XVIII. The flow boiling and pool boiling experiments each require a DACS and subsequently, higher development costs than the two-phase facility, which requires only one DACS.

TABLE XVIII CARRY-ON EXPERIMENTS ROM DEVELOPMENT COSTS
(Costs are in Thousands of 1982 Dollars)

Item	Design	Test	Fabrication	Total
Flow Boiling:				
- Test Section	20	25	25	70
- Condenser	20	25	16	61
- DACS	30	10	50	90
Total	70	60	91	221
Pool Boiling:				
- Test Cell (Includes Heaters)	5	10	6	21
- DACS	15	10	50	75
Total	20	20	56	96
Liquid Reorientation				
- Test Tanks	10	30	6	46
Grand Total				363

3.4 Comparison of Approaches. The two-phase facility conceptual design was compared to the individual middeck carry-on conceptual designs to determine the preferred approach for the preliminary design of flight hardware. The evaluation criteria included:

- Potential for meeting experimental objectives
- Safety and shuttle compatibility
- Development risks
- Astronaut/mission specialist involvement
- Flight opportunities
- Weight, volume and power requirements
- Flight and development costs.

The potential for meeting the experimental objectives is equivalent for either approach for pool boiling and liquid reorientation. For flow boiling, the facility design uses a larger

diameter test section, allowing a better view of the flow boiling process. Tests were carried out at Beech with two-phase (water-nitrogen) flow in a 1.524 cm tube and a 0.635 cm tube to evaluate the difference. The results of the test are shown in Figure 30. The flow testing demonstrates that there is no compelling reason to select the facility design, since the small test section used in the carry-on approach allows an adequate view of the two-phase flow process.

Shuttle integration requirements for the experiments containing potentially hazardous fluids such as Freon may be more complex for the middeck than for Spacelab; initial conversations with safety personnel at NASA/Johnson Space Center indicate that use of hazardous fluid in middeck experiments would not be impossible, however.

The development risks and the astronaut/mission specialist involvement are equivalent for either approach.

The carry-on approach offers a significant advantage over the facility approach in terms of flight opportunities. The middeck area will be available nearly every flight whereas the facility can only be flown on Spacelab flights (8 of the first 61 flights are Spacelab flights).

The weight, volume and power requirements for both approaches are summarized in Table XIX. The values presented in Table XIX fall under the allowable values for each location with exception of the weight of the liquid reorientation carry-on which slightly exceeds 27.3 kg maximum per locker and the carry-on flow boiling heat rejection, which exceeds the minimum allowable heat rejection for three middeck lockers of 30 watt-hours.

Table XX gives the hardware development and flight costs for both approaches. Development costs were taken directly from Tables XVII and XVIII. Flight costs for the Spacelab Center Aisle and Double Rack No. 4 were calculated from equations given in Reference 9. Middeck flight costs were calculated from Reference 7.

The cost data in Table XX demonstrate the significant cost advantages of developing carry-on experiments. The total cost savings for the carry-on approach over the facility approach ranges from $4M to $5.5M, due to the large difference in flight costs.

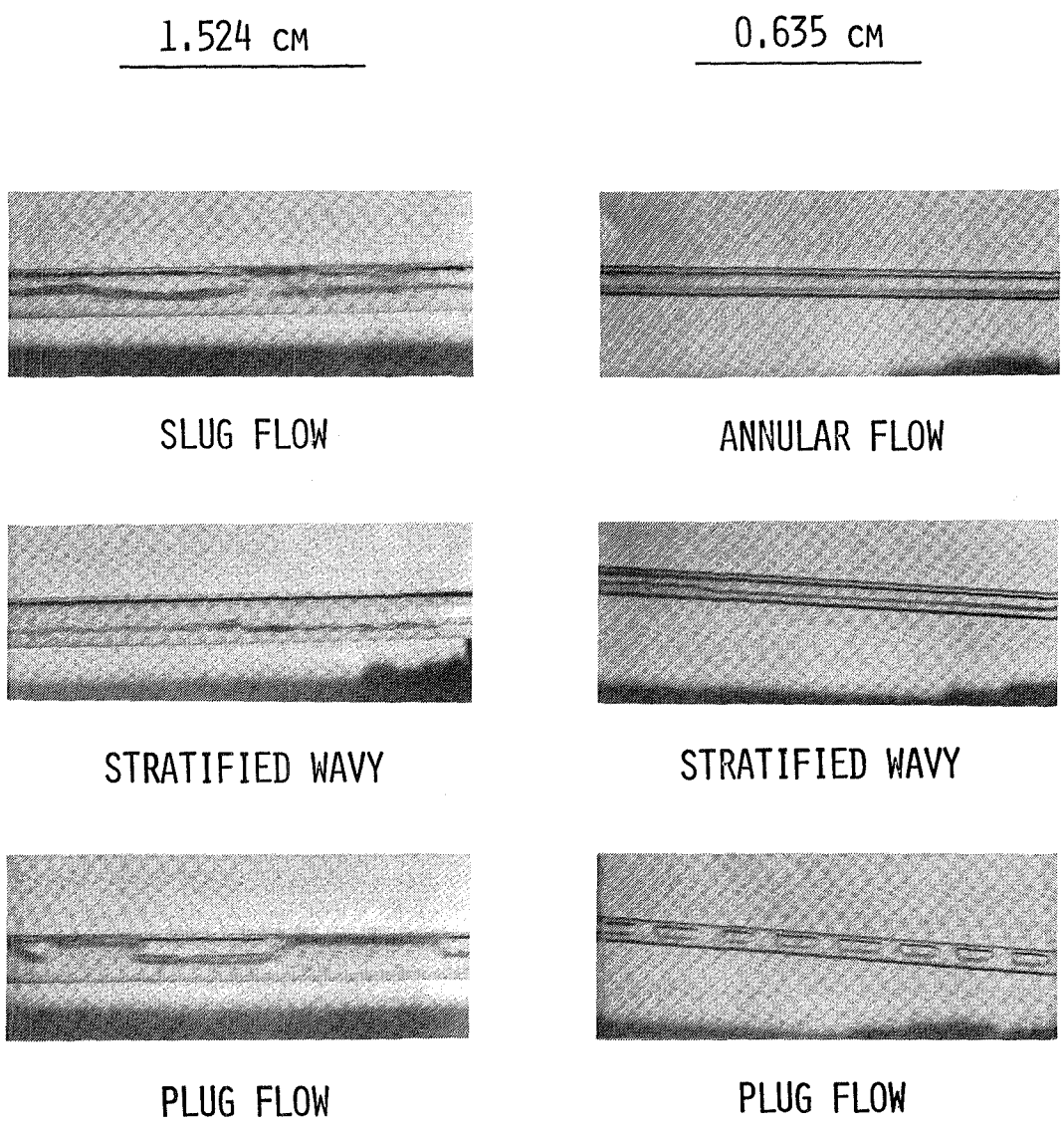

Figure 30 COMPARISON OF THE 1.524 cm AND 0.635 cm DIAMETER TEST SECTIONS

TABLE XIX WEIGHT, VOLUME AND POWER REQUIREMENTS FOR BOTH APPROACHES

	Spacelab Facility Double Rack or Center Aisle		Middeck Carry-ons		
	Weight (kg)	Power (watts)	Number Lockers	Weight (kg)	Power (watts)
Flow Boiling	96.4	1258	3	55.1	486 (102 W-h)
Pool Boiling	28.1	320	2	26.9	244 (18.3 W-h)
Liquid Reorientation	53.7	309	1	29.6	162 (8.1 W-h)
Total	178.2	1887	6	111.6	892

Volumes:

Double Rack = 1.34 m^3

Center Aisle = 1.15 m^3

Middeck Locker = 0.057 m^3

TABLE XX DEVELOPMENT AND FLIGHT COSTS FOR BOTH APPROACHES

Costs are in 1982 Dollars
Spacelab Costs Assume Long Module

	Spacelab Facility		
	Development Costs	Flight Costs	Total Costs
Double Rack	$ 0.303M	$ 6.68M	$ 6.983M
Center Aisle	$ 0.303M	$ 5.03M	$ 5.333M
	Middeck Carry-ons		
	Development Costs	Flight Costs	Total Costs
Flow Boiling	$ 0.221M	$ 0.560M	$ 0.781M
Pool Boiling	$ 0.096M	$ 0.374M	$ 0.470M
Liquid Reorientation	$ 0.046M	$ 0.187M	$ 0.233M
Total	$ 0.363M	$ 1.120M	$ 1.484M

3.5 Preferred Approach. Since the middeck also offers significantly more flight opportunities and no compelling technical disadvantages, it was recommended as the preferred approach. Beech received approval from NASA/Lewis Research Center to proceed with the preliminary design of the three experiments as middeck carry-ons.

4.0 PRELIMINARY DESIGN OF FLIGHT HARDWARE

The basic objective of the preliminary design effort was to generate a design with sufficient detail to permit accurate estimation of hardware costs and fabrication schedules. The design to be described later in this section is therefore not a mature design; significant areas for development, testing and analysis remain.

Design Approach. The general approach during the preliminary design effort included the following:

- Wherever possible existing Shuttle qualified hardware (such as valves or transducers) were incorporated in the design.
- The experiments were designed to be independent of Orbiter power, fluid or data systems. It was felt that this was a conservative approach that reduced integration requirements and costs; as middeck payload facilities become better defined, it may be possible to take advantage of Orbiter facilities without significant redesign of the experiments.
- In order to reduce hazards to the crew, the experiments were designed to operate at subatmospheric pressure and ambient temperature. The experiments are therefore largely fail-safe - if experiment pressure vessel leak, the pressure rises at most to ambient pressure.
- It was assumed that experiment hardware inside the lockers could be adequately supported by impact absorbing foam. This eliminated the need for the extensive design of support structures.

Design Constraints. During the preliminary design, the constraints on the design of a middeck payload were assumed to be the following:

- The center of gravity allowances are shown in Table XXI (Reference 10) for payloads mounted on an adapter plate.

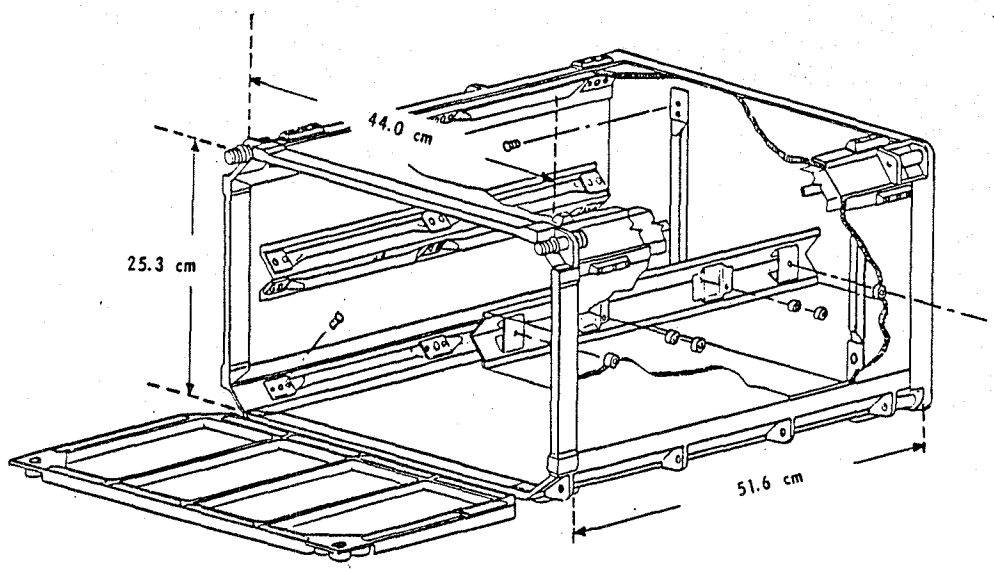

Figure 31 LOCKER DIMENSIONS

TABLE XXI PAYLOAD CG/WEIGHT LIMITATIONS

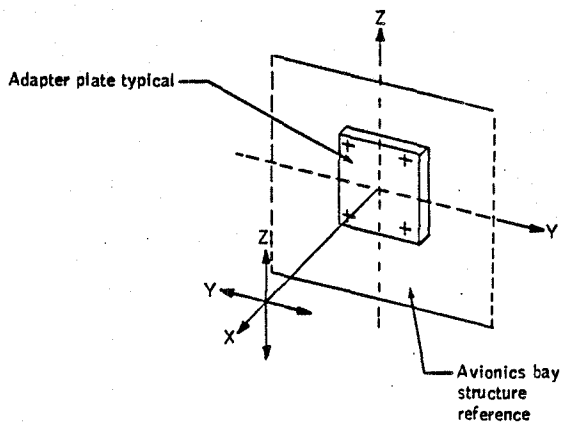

Center of plate		± 3 inch Y		± 3 inch Z	
CG (in) X	Wt. (lb)	CG (in) X	Wt. (lb)	CG (in) X	Wt. (lb)
14	51	14	37	14	31
13	55	13	40	13	34
12	59	12	44	12	37
11	65	11	48	11	40
10	69	10	52	10	44

- Power from middeck utility outlets was assumed to not be available for experiment use. It is worth noting however, that 28 VDC and 115 VAC power may be available for middeck payloads if Orbiter operations permit. Outlet configurations are described in Reference 10.

- The payload storage provisions available include:

  - Large stowage tray (0.05 m^3)
  - Small stowage tray (half locker) (0.02 m^3)
  - Locker (.057 m^3)
  - Single adapter plate. NASA Drawing Number V733-660310
  - Double adapter plate, NASA Drawing Number V733-660311.
  - Maximum locker weight 27 kg

- The maximum power dissipation allowed without special provision was assumed to be 10 watt-hours (Reference 11).

- For the purposes of preliminary design it was assumed that the experiment hardware would be subjected to a maximum of 5 g's in any direction during normal flight operation and 20 g's in the x-axis during a crash landing. Design criteria were that the experiment hardware would not be adversely affected by the normal flight loads and would not create hazards (e.g., fragments or leakage) during a crash landing.

- Pressure vessels were designed in accordance with the requirements of Reference 12. The basic technical design requirements were supplied by References 13 and 14.

- The flammability, odor and offgassing characteristics of experiment materials were constrained by Reference 15.

- Ambient conditions in the middeck were assumed to be the following from Reference 16:

  - Pressure: 0.20 MPa. Nominal pressure 0.1 MPa
  - Temperature: 18 - 49°C (65 - 120°F)

- Safety analyses were conducted in accordance with References 12, 17 and 18.

4.1 Liquid Reorientation Experiment. The preliminary design of the liquid reorientation experiment is described in the following paragraphs. Paragraph 4.1.1 shows the design, including flow and electrical schematics. Paragraph 4.1.2 gives the details of the analyses supporting the experiment design and includes analyses of the supply and reorientation tanks. The mission analyses, including the experiment operating procedures and mission timelines, are given in Paragraph 4.1.3. The safety analysis of the liquid reorientation experiment is given in Paragraph 4.1.4. Ground testing requirements for the experiment are given in Paragraph 4.1.5.

4.1.1 Preliminary Design. The preliminary design for the liquid reorientation experiment is shown in Figures 32 through 34.

As shown in Figure 32, the flow schematic, the experiment consists of three acrylic reorientation tanks and a cylindrical supply tank with an O-ring sealed piston for liquid expulsion. Initially all three reorientation tanks are evacuated. The supply tank is filled with 5634 cm^3 of FC-77. At a liquid temperature of 25°C, 722 cm^3 of air are contained in the supply tank to permit the piston to move as the liquid expands due to environmental temperature changes. The air volume is sized to produce an isentropic pressure rise of 34.5 kPa for a 17°C temperature change in the liquid (i.e., if the liquid temperature increases from 25°C to 42°C). If the piston jams or for some other reason the air pressure exceeds 138 kPa, a relief valve will open and allow liquid to enter the largest of the reorientation tanks. The design is fail-safe since any leak in the system plumbing will permit air to leak into the system until system pressure reaches (at most) ambient pressure.

The experiment is operated in flight by opening the supply tank piston air-side vent and then opening one of the reorientation tank valves to allow liquid to enter the tank. The piston is driven by a pressure differential across the piston--the difference between the saturation pressure of FC-77 at ambient temperature--5.5-6.2 kPa (0.80-0.90 psia)--and ambient cabin pressure--94-110 kPa (13.6-16 psia). Control of the liquid volume entering each tank is accomplished by monitoring the displacement of the piston.

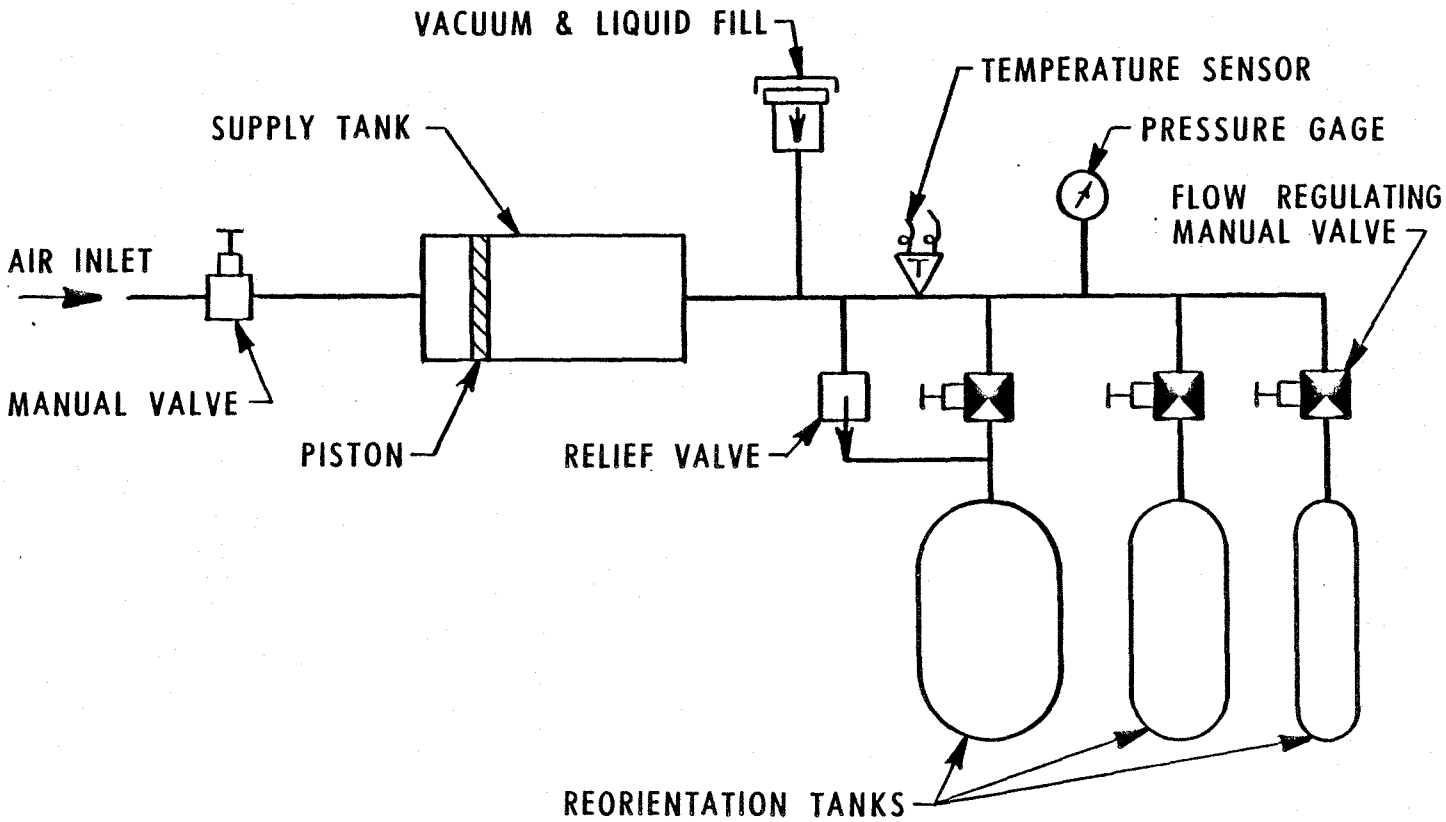

Figure 32 LIQUID REORIENTATION EXPERIMENT FLOW SCHEMATIC

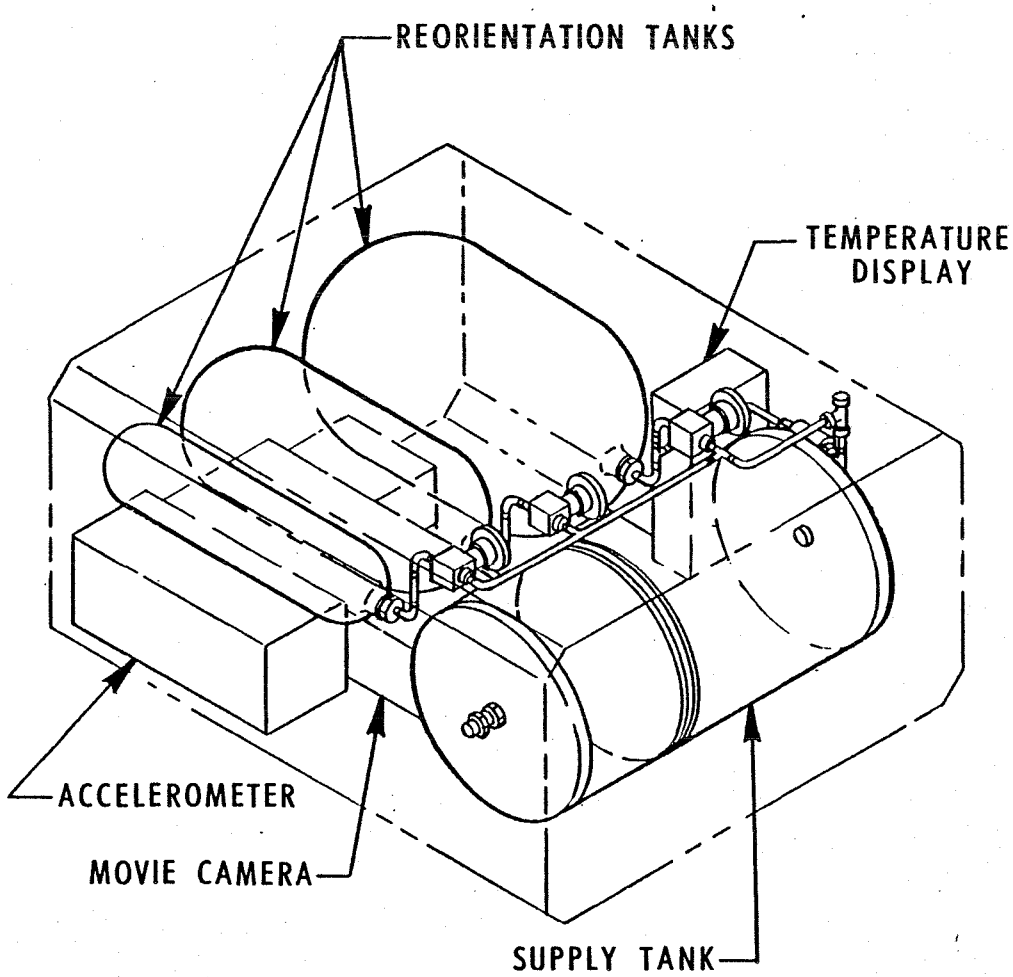

Figure 33 LIQUID REORIENTATION EXPERIMENT PACKAGE

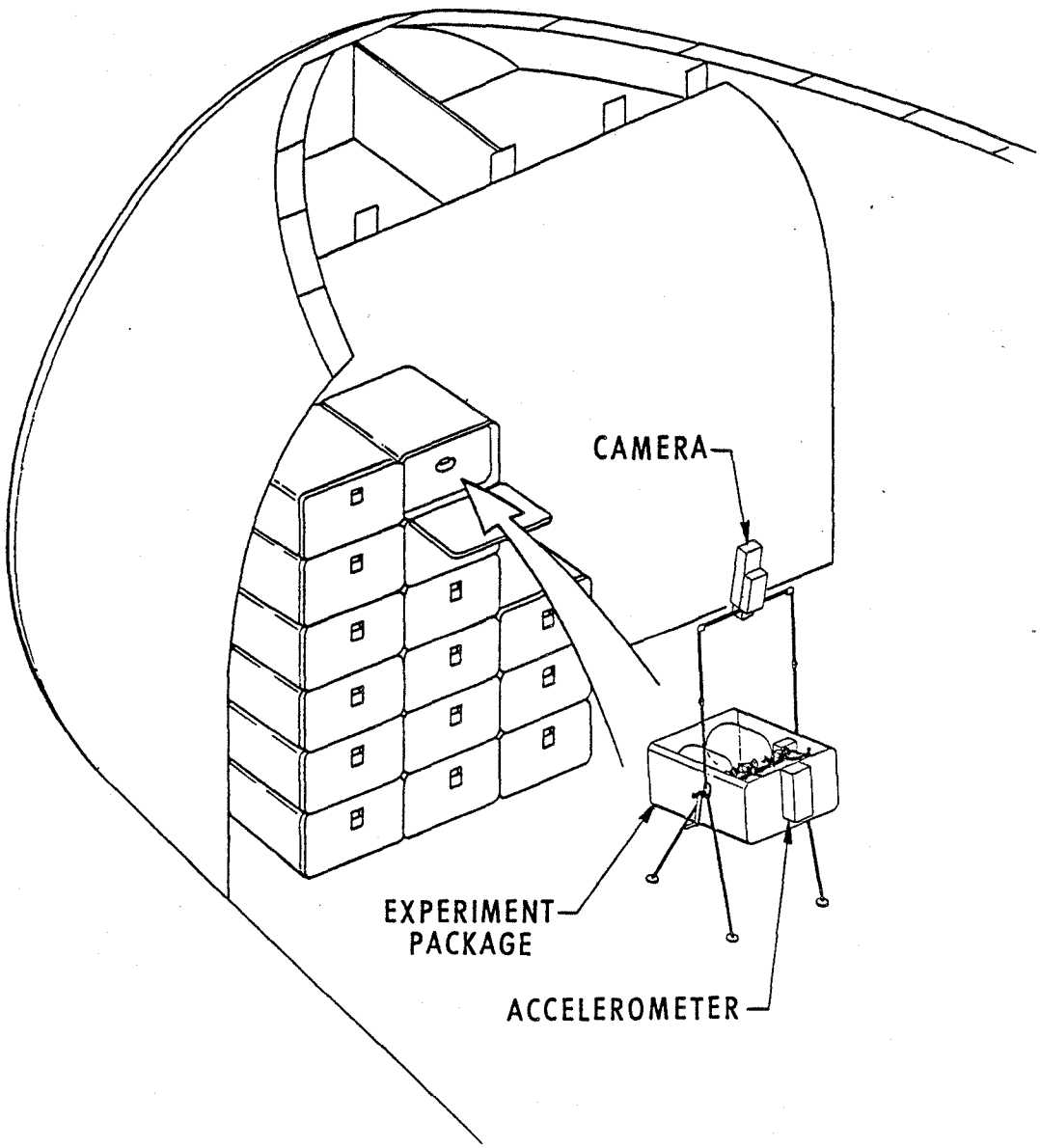

Figure 34 LIQUID REORIENTATION EXPERIMENT INSTALLATION

The valves selected for the liquid reorientation are manufactured by Nupro Valve Company. They are Shuttle flight qualified. The movie camera selected for the experiment is a Photo-Sonics miniature 16mm model 16mm-1VN. Conversations with Kodak have indicated that ASA 400 movie film can be used with lighting available in the middeck.

An accelerometer package is shown as part of the design given in Figure 32. This package will consist of three translational accelerometers, a clock, and a temperature sensing element (used for accelerometer calibration), all connected to individual liquid crystal displays. The design of this package has been prepared by KMS Fusion of Ann Arbor, Michigan. They have developed the accelerometer for the Aero Coefficient Instrumentation Package (ACIP) and High Resolution Triaxial Linear Accelerometer Package (HIRAP) Orbiter experiments and have extensive experience with low-level high resolution accelerometers.

The flight hardware for the experiment consists of two major assemblies:

- The tank assembly.
- The test stand assembly.

The tank assembly consists of the acrylic tanks, plumbing and the electronics packages. The entire assembly is embedded in foam (such as Poron) for structural support. Subassemblies, such as the camera or the test stand, are stored in cutouts in the foam. The entire assembly is encased in a thin plastic envelope that will retain FC-77 or acrylic fragments in the event of tank failure during take-off or landing. The plastic envelope is unsealed while in orbit only after the astronaut has verified (through transparent windows in the case) that the tanks are intact and liquid is not leaking. The design for the plastic outer case was not completed as part of the preliminary design effort.

The test stand, which is stored in the tank assembly and assembled in orbit, is designed to serve several purposes:

1. Support and Optimum Orientation of Test Tasks. The stand is taken out of the middeck drawer, unfolded, and attached to four pre-installed Velcro pads on the middeck floor. The experiment package is attached to the stand such that it can be rotated about the Y-axis of the Orbiter. This will allow the test tanks to be aligned with the acceleration vector produced by an Orbiter RCS +X firing.

2. Support of the Movie Camera. The stand includes a support for the movie camera.

3. Settling of the Fluid in the Test Tanks Prior to Start of a Reorientation Test. The stand includes a crank which is used to settle the fluid in the test tanks prior to the start of a reorientation run. Also included is a clutch which, following the settling, will uniformly decelerate the rotating experiment package without disturbing the liquid interfaces in the test tanks.

4.1.2 Design Analysis. The analyses carried out during the preliminary design effort were directed primarily at sizing the reorientation and supply tanks and estimating the time required to settle the liquid in the reorientation tanks before each test run. Structural or fluid system calculations were not carried out beyond what was considered necessary to obtain estimates of hardware costs, operating time and system safety.

4.1.2.1 Supply Tank. The supply tank was designed to meet the following criteria while minimizing the overall weight of the tank:

1. Deliver a total liquid volume of 5634 cm^3 according to Table XXII, which is based on the test matrix shown in Section 2.3. The volume of the reorientation tanks is given in Table XXII. The total volume of the supply tank is sized to fill all reorientation tanks 70 percent full with a safety factor of 1.2.

TABLE XXII LIQUID REORIENTATION LIQUID DELIVERY SCHEDULE

Tank	0-20% (cm^3)	20-50% (cm^3)	50-70% (cm^3)
1. L/D = 4.00	141	211	141
2. L/D = 2.45	353	530	353
3. L/D = 1.50	848	1272	848

2. Design must permit the filling of the smallest tank with a minimum accuracy of 10 percent (of maximum liquid volume). Since the maximum fill level is 70 percent, the maximum total inaccuracy is 7.0 percent of the volume of the smallest tank or 50 cm^3.

3. Piston must operate properly with a minimum external cabin pressure of 94 kPa and a nominal FC-77 saturation pressure of 6.2 kPa.

4. Tank must withstand an external pressure difference of 110 kPa (orbital operation).

5. Liquid expansion during ground and flight operations must not cause the design pressure of supply tank to be exceeded. Orbital atmospheric temperature range is $18^{\circ}C$ to $32^{\circ}C$.

6. The supply tank must be transparent since the position of the piston shows how much liquid has been expelled.

Material. The only plastic that has the necessary optical qualities and can be readily cast is acrylic. The properties of standard molding grade acrylic are:

Density: 1.19 g/cm^3
Tensile strength: 72 mPa (10500 psi)
Modulus: 2.96 (10^9) N/m^2 (0.45 (10^5) psi)
Coefficient of thermal expansion: 3.6 (10^{-5}) cm/cm - $^{\circ}C$
Refractive index: 1.49
Transmittance: 92 percent

Design Model. The nomenclature for the piston tank design model is shown in Figure 35.

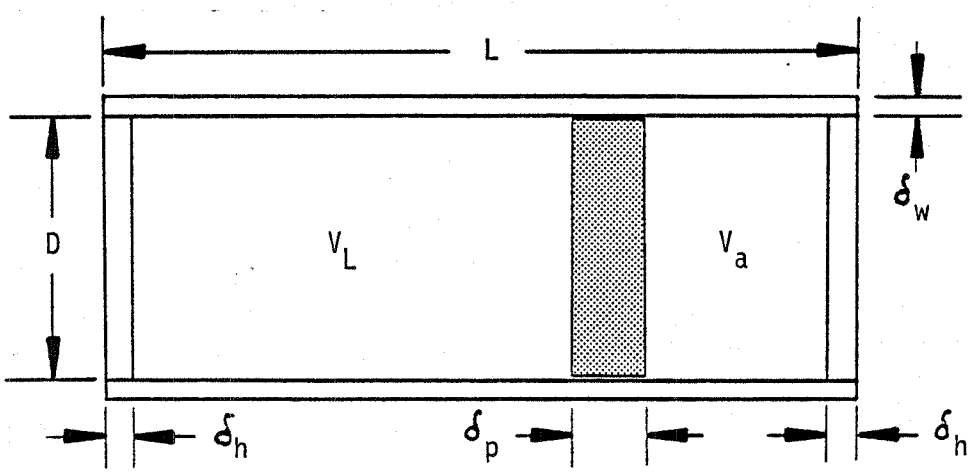

Figure 35 SUPPLY TANK DESIGN MODEL NOMENCLATURE

Assuming all components are of the same material, the weight of the piston tank is given by:

$$W = \pi D^2 \rho \left[L \left(\frac{\delta_w}{D} - \left(\frac{\delta_w}{D} \right)^2 \right) + \frac{\delta_p}{4} + \frac{\delta_h}{2} \right] \qquad \text{(Equation 5)}$$

The total internal volume of the tank is

$$V = (L - 2\delta_h - \delta_p) \frac{\pi D^2}{4} = V_a + V_L \qquad \text{(Equation 6)}$$

Assuming that the liquid expands while the air and liquid volumes are sealed off and that the change in liquid volume is ΔV_L, the change in air pressure can be calculated for an ideal gas assuming a polytropic process. That is

$$P_1 V_{a1}^n = P_2 V_{a2}^n \qquad \text{(Equation 7)}$$

where

n = 1.4 for an isentropic process (air)

1, 2 = initial and final states for pressure and volume

Since

$$V_{a1} - \Delta V_L = V_{a2} \qquad \text{(Equation 8)}$$

$$V_{a_1} = \frac{\Delta V_L}{1 - \left(\frac{P_1}{P_2} \right)^{1/n}} \qquad \text{(Equation 9)}$$

The assumption that the process is isentropic (i.e. adiabatic) is conservative since any heat transfer will be away from the air, resulting in a smaller pressure rise. Substituting Equation 9 for V_a in Equation 6 yields an expression for the tank length in terms of the initial and final pressures.

$$L = \left[\frac{\Delta V_L}{1 - \left(\frac{P_1}{P_2} \right)^{1/n}} + V_L \right] \frac{4}{\pi D^2} + \delta_p + 2\delta_h \qquad \text{(Equation 10)}$$

Substituting Equation 10 into Equation 5 gives an expression for the tank weight

$$W = \pi D^2 \rho \left[\left(\frac{\delta_w}{D} - \frac{\delta_w^2}{D^2} \right) \left\{ \left(\frac{4}{\pi D^2} \right) \left(\frac{\Delta V_L}{1 - \left(\frac{P_1}{P_2} \right)^{1/n}} + V_L \right) + \delta_p + 2\delta_h \right\} + \frac{\delta_p}{4} + \frac{\delta_h}{2} \right]$$

(Equation 11)

Minimizing the weight of the supply tank requires the determination of the allowable tank diameters and pressures. The allowable design space is shown in Figure 36.

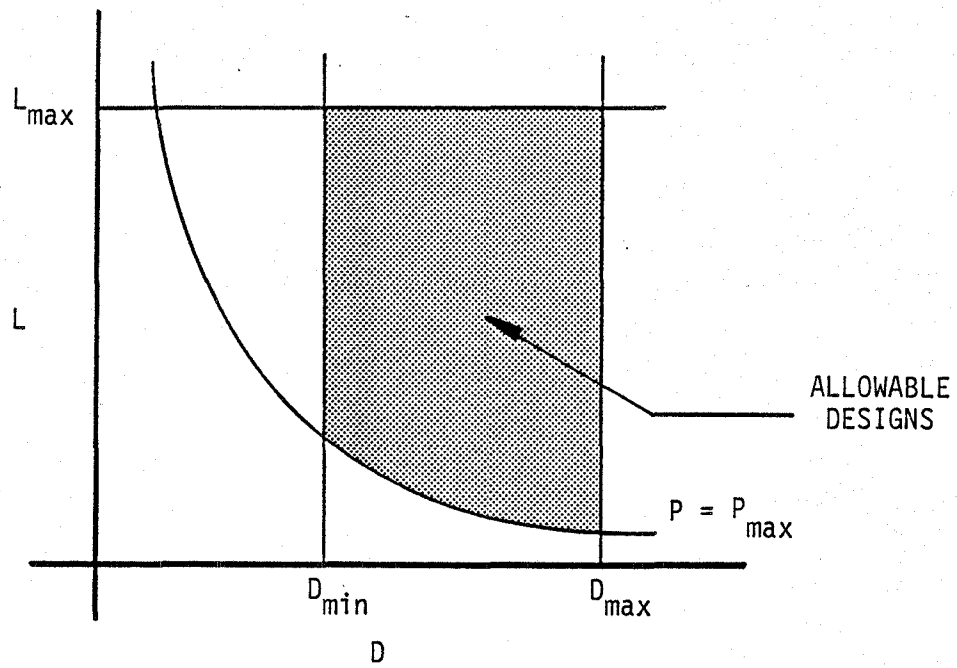

Figure 36 SUPPLY TANK DESIGN SPACE

The boundaries of the allowable design space are determined in the following manner:

Maximum Length. The maximum length is based on the maximum width of the locker internal envelope. From Reference 10, L_{max} = 432 mm.

Maximum Diameter. The maximum diameter is set by the accuracy required in the minimum volume pulse. From statistical considerations, assuming the tanks are sent into orbit 20 percent full, the error in filling the smallest tank is

$$e_v = \sqrt{\varepsilon_1^2 + \varepsilon_2^2}$$

(Equation 12)

where ε_1 is the error in the first volume pulse and ε_2 is the error in the second volume pulse. Actually $\varepsilon_1 = \varepsilon_2 = \varepsilon$ and is the result of the error in controlling the position of the piston.

$$e_v = \varepsilon\sqrt{2} \qquad \text{(Equation 13)}$$

or

$$\varepsilon = \frac{0.07V}{\sqrt{2}} \qquad \text{(Equation 14)}$$

where V is the volume of the smallest tank and $e_v = 0.07V$ from design criterion 2, that the error in filling the smallest tank must be less than 10 percent of the maximum liquid volume in the tank.

But ε is proportional to the error in position of the piston.

$$\varepsilon = \frac{\Delta x \ \pi D_{max}^2}{4} \qquad \text{(Equation 15)}$$

where Δx = piston positioning error. Combining Equation 14 and Equation 15 and solving for D_{max} yields:

$$D_{max} = 0.251\sqrt{\frac{V}{\Delta x}} \qquad \text{(Equation 16)}$$

With $V = 705\ cm^3$ and $\Delta x = 0.13$ cm (Assumes the piston position can be controlled $\pm$ 0.05 inches)

$$D_{max} = 18.4 \text{ cm} \qquad \text{(Equation 17)}$$

Minimum Diameter. The minimum piston diameter is set by the requirement that the piston operates with a minimum pressure differential of $\Delta P = 83$ kPa. The pressure force to drive the piston is

$$F_D = \frac{\Delta P \, \pi D^2}{4} \qquad \text{(Equation 18)}$$

The piston frictional force F_F at start up, resists F_D.

$$F_F = \pi D f_{RS} \qquad \text{(Equation 19)}$$

where f_{RS} is the O-ring static frictional force based on two O-rings compressed ten percent.

Typically the breakout friction is three times the running friction. For a ten percent compression of 70 durometer neoprene, the O-ring stress, σ, is approximately 345 kPa and the sliding friction coefficient is conservatively 0.325 for an O-ring width, w, of 0.254 cm:

$$f_{RS} = 6 \, w \sigma (0.325) = 1709 \frac{N}{m} \text{ (two O-rings)} \qquad \text{(Equation 20)}$$

For $F_D > 2F_F$ (i.e., safety factor of 2):

$$D > \frac{8 f_{RS}}{\Delta P} \qquad \text{(Equation 21)}$$

$$D_{min} = 16.51 \text{ cm} \qquad \text{(Equation 22)}$$

The wall thickness and head thicknesses of the cylinder are functions of pressure, as described below.

Head Thickness. The head thickness is calculated from Reference 13. The allowable head thickness is

$$\delta_h = D \sqrt{CP/SE} \qquad \text{(Equation 23)}$$

From Figure UG-34(u) of Reference 13, C = 0.33. Taking the allowable stress of acrylic to be ten percent of the ultimate, S equals 7240 kPa. For a bonded joint in plate acrylic, the strength is slightly less than the parent material, so that E = 0.9.

Therefore

$$\delta_h = 0.109 \sqrt{P} \qquad \text{(Equation 24)}$$

Wall Thickness. The wall thickness based on Reference 13 for internal pressurization is

$$\delta_w = \frac{PD}{2(S-0.6P)} \qquad \text{(Equation 25)}$$

For

P = 173 kPa
S = 7240 kPa
D = 18.67 cm
δ_{max} = 2.26 mm

For external pressurization, the buckling pressure for a short cylinder that is given on page 556 of Reference 19 is:

$$P = 0.807 \frac{2E\delta_w^2}{LD} \sqrt[4]{\left(\frac{1}{(1-\nu^2)^3}\right)\left(\frac{4\delta_w^2}{D^2}\right)} \qquad \text{(Equation 26)}$$

for

ν = 0 (conservative)
E = 3103 mPa
P = 1100 kPa (safety factor 10 for a 110 kPa maximum differential)
$\delta_w = 0.029\, L^{0.4}\, D^{0.6}$

Using Equation 25 and Equation 26 to calculate values for δ_h and δ_w in Equation 11 yields the curves shown in Figure 37. The weight of the tank is a minimum at a maximum pressure of 138 kPa (due to liquid expansion) for any diameter. The absolute minimum weight occurs at the minimum diameter and a peak pressure of 138 kPa. As a practical matter, the diameter of the cylinder was made 16.95 cm to accommodate a standard O-ring.

The optimum (minimum weight) tank therefore has the following characteristics

Length L = 32.32 cm
Diameter D = 16.95 cm

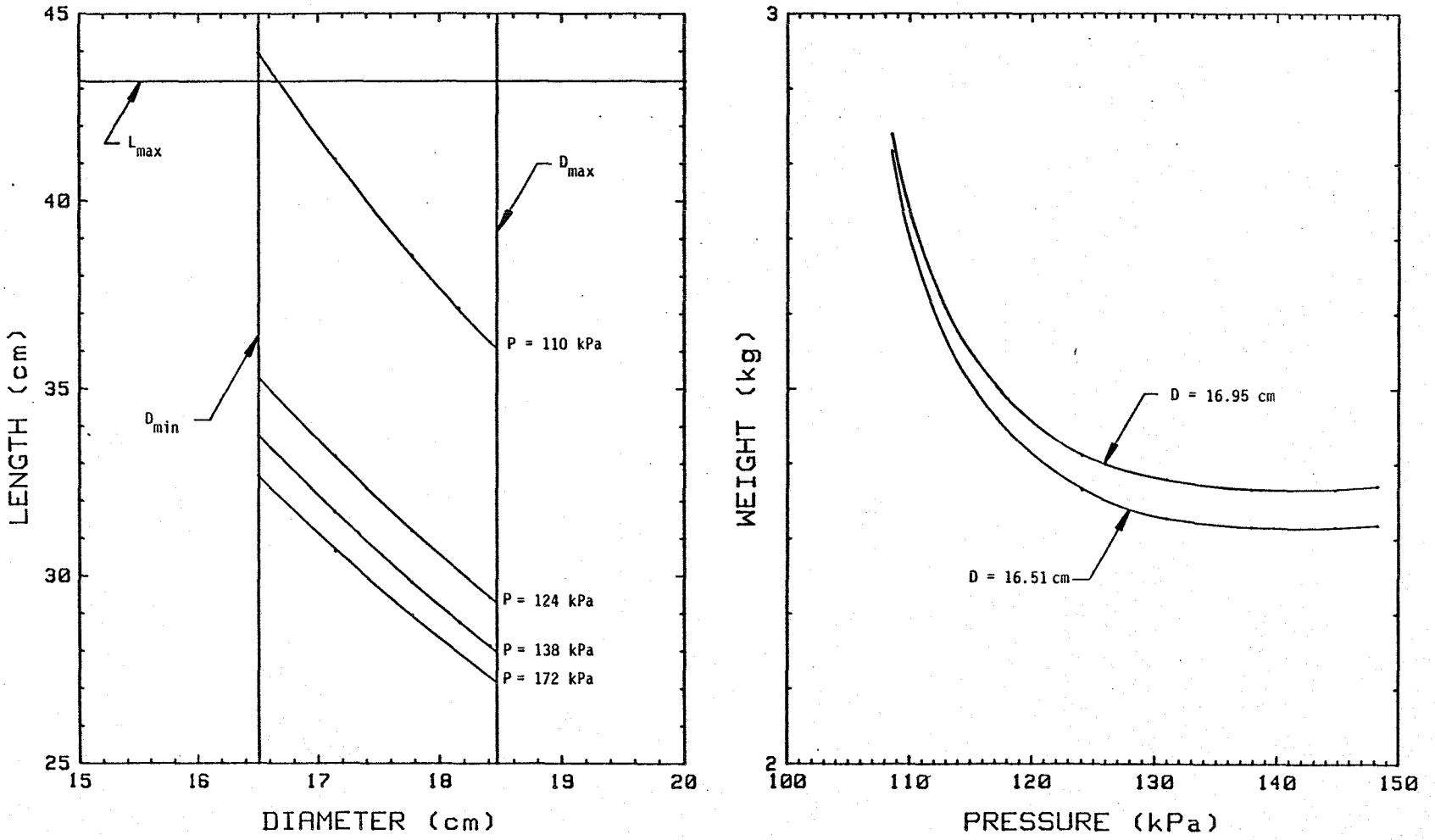

Figure 37 SUPPLY TANK DESIGN CURVES

Wall thickness δ_w = 0.635 cm

Head thickness δ_h = 1.448 cm

Design external pressure 110 kPa safety factor = 10

Design internal pressure 138 kPa safety factor = 10

Weight = 2.37 kg empty

4.1.2.2 Reorientation Tanks. The liquid reorientation experiment requires three transparent tanks for the observation of liquid motion during reorientation. The significant tank dimensions are summarized in Table XXIII.

TABLE XXIII LIQUID REORIENTATION TEST TANK DIMENSIONS

Tank	L/D	Internal Length (cm)	Internal Diameter (cm)	Volume (cm^3)
1	4.00	25.0	6.25	704
2	2.45	25.0	10.20	1766
3	1.50	25.0	16.67	4240

The design requirements for these tanks are:

1. Hemispherical heads with the internal dimensions shown in the Table XXIII.

2. Tank material must be optically clear with a minimum of distortion.

3. Temperature: 18°C to 32°C (Reference 16).
   Pressure: External pressurization - 41.4 kPa difference; internal pressurization - 110 kPa difference.

4. Steady-state acceleration to a maximum of 5 g's in each axis.

5. Crash load of 20 g's in Z-axis.

6. Rapid decompression (Reference 8).

Material Selection. As discussed in Section 4.1.2.1, acrylic is the only plastic that has the required optical properties. The material properties of the acrylic used for the reorientation tanks are the same as those for the supply tank.

Wall Thickness. For a cylinder under internal pressure, Section UG-27 of Reference 13 applies. The shell thickness of a cylindrical shell with a longitudinal joint is given by

$$\delta = \frac{PR}{SE - 0.6P} \qquad \text{(Equation 27)}$$

when $P < 0.385\ SE$.

The ultimate tensile strength of cast acrylic is 10,500 psi. For design purposes (consistent with ASME-BPV-X) one-tenth the ultimate was used as the allowable. From discussions with a tank vendor, a joint efficiency (based on test data) for bonded joints in cast acrylic is 0.6. For P = 110 kPa, Equation 27 becomes:

$$\delta = 0.026\ R \qquad \text{(Equation 28)}$$

The minimum wall thickness for internal pressure is given in Table XXIV.

TABLE XXIV MINIMUM TANK WALL THICKNESS FOR INTERNAL PRESSURIZATION

Tank	L/D	R (cm)	δ (cm)
1	4.00	3.125	0.081
2	2.45	5.100	0.133
3	1.50	8.335	0.217

Since the ASME Code is not readily applicable for external pressurization of acrylic tanks, we used the following equation for the buckling of short cylinders from Reference 19, page 556. The buckling pressure:

$$P = 0.807 \frac{E\delta^2}{LR} \sqrt[4]{\left(\frac{1}{(1 - \nu^2)^3}\right)\left(\frac{\delta^2}{R^2}\right)} \qquad \text{(Equation 29)}$$

Using a factor of safety of 10 on the buckling pressure (i.e., P = 110 kPa), Equation 29 was solved for δ. Poisson's ratio, ν, was assumed to be zero, since data is not available for design purposes (and it is a conservative assumption).

$$\delta = 0.045 (L_c)^{0.4} R^{0.6} \qquad \text{(Equation 30)}$$

Using the above equation, tank wall thicknesses for external pressurization were calculated. The results are presented in Table XXV.

TABLE XXV MINIMUM TANK WALL THICKNESS FOR EXTERNAL PRESSURIZATION

Tank	L/D	R (cm)	L (cm)	L_c* (cm)	t (cm)
1	4.0	3.125	25.0	18.75	0.288
2	2.45	5.100	25.0	14.80	0.351
3	1.50	8.335	25.0	8.33	0.375

*Cylindrical Length = L - 2R = L_c

Crash Loads. An analysis of the boss and thread tear-out loads resulting from the 20-g crash loads was performed. Table XXVI summarizes the results of the calculations. For preliminary design purposes, it was assumed that the tanks were 70 percent full of liquid FC-77 and that the entire crash load was resisted by the tank wall at the root of the boss (boss tear-out) or by the shear area of the boss threads (thread tear-out). As can be seen from Table XXVI, the bosses are adequately designed for the crash loads.

TABLE XXVI SUMMARY OF CRASH LOAD CALCULATIONS

Tank	L/D	70% Filled Tank Mass, kg	Axial Tear-out Load, N	Thread[1] Shear Factor of Safety	Boss[2] Tear-out Factor of Safety
1	4.00	6.53	1279	10.3	8.5
2	2.45	2.93	575	22.4	17.9
3	1.50	1.26	247	53.5	34.8

1. Thread shear area based on 7/16 UNF20 x 10.6 mm deep.
2. Boss root shear area equal to tank wall thickness times boss diameter (25.4 mm).

4.1.2.3 Flow Analysis. The liquid reorientation experiment piping was sized to ensure that liquid addition to any of the test tanks could be accomplished within 60 seconds. This criterion is easily met with the 0.635 cm (0.25 in) piping shown. In addition, the time required for full flow to be achieved after a valve is opened was determined to be less than ten seconds.

4.1.2.4 Test Stand Assembly. Analysis of the test stand was directed at determining two things:

- The rotational speed required to settle the liquid in the tank before reorientation.
- The maximum permissible deceleration after the settling rotation so that the liquid interface is not disturbed.

Rotational Speed Required For Settling. The rotational speed required to settle the fluid in the reorientation tanks prior to the start of a test was determined from the Bond Number. Reference 20 gives the minimum Bond Number required to disturb a liquid-vapor interface as 0.84. Using a conservative value of Bo = 2, the minimum centripetal acceleration required is:

$$a = \frac{2\beta}{R_o^2} \qquad \text{(Equation 31)}$$

The rotational speed required to produce the centripetal acceleration is:

$$\omega = \left(\frac{a}{R_1}\right) = \left(\frac{2\beta}{R_o^2 R}\right)^{1/2} \qquad \text{(Equation 32)}$$

Setting R_o = 3.12 cm (smallest test tank), R = 5.08 cm, and β = 8.43 cm^3/sec^2 for FC-77:

$$\omega = 0.584 \text{ rad/sec} \quad (0.19 \text{ revolutions/sec}) \qquad \text{(Equation 33)}$$

Deceleration. The time required to decelerate the experiment was also determined from the Bond Number = 0.84 criterion. In this case, the object is to make sure the fluid interface is not disturbed during the deceleration. The tangential deceleration required is therefore:

$$a_T = \frac{0.84\beta}{R_{o2}} \qquad \text{(Equation 34)}$$

The angular deceleration, α, is:

$$\alpha = \frac{a_T}{R} \qquad \text{(Equation 35)}$$

The total time required to decelerate the experiment is:

$$t = \frac{\omega}{\alpha} = \frac{RR_o^2}{0.84\beta} \qquad \text{(Equation 36)}$$

Setting R_o = 8.33 cm (largest test tank) and R = 30.08 cm, since the fluid is at the far end of the tank:

$$t = 172 \text{ sec.} \qquad \text{(Equation 37)}$$

4.1.3 Mission Analysis. Mission operation timelines were based on the experiment operation procedure shown in Table XXVII. The mission timeline reflects only the on-orbit operations: preparation, operation and disassembly.

TABLE XXVII EXPERIMENT OPERATING PROCEDURE - LIQUID REORIENTATION

Mission Phase	
1. Pre-flight Handling:	A. Final checkout of batteries, film and camera B. Evacuate tanks and plumbing, leak check C. Partially fill (20 percent) reorientation tanks and fill piston (supply) tank D. Package all equipment E. Stow experiment in middeck locker F. Install experiment attachments on middeck floor
2. Launch:	A. Rely on packaging to withstand launch loads and contain potential leakage, tank fragments, etc.
3. On-orbit Stowage:	A. Rely on packaging to withstand launch loads and contain potential leakage, tank fragments, etc.
4. On-orbit Experiment Preparation:	A. Remove package from locker B. Visually inspect package for leakage before opening (windows in package) C. Open package D. Assemble test stand E. Load camera and check out F. Install tank assembly into test stand

TABLE XXVII EXPERIMENT OPERATING PROCEDURE - LIQUID REORIENTATION (Concluded)

Mission Phase	
	G. Activate and check out accelerometer and temperature monitoring systems H. Adjust initial orientation of tank assembly to be aligned parallel to RCS thrust vector I. Fire RCS to determine actual thrust vector and record angular position J. Adjust metering scale on supply tank
5. On-orbit Experiment Operation:	A. Reorient liquid and position tank assembly B. Activate camera (t-20 seconds) C. Fire RCS (60 seconds) t = 0 D. Stop camera (t + 90 seconds) E. Fire RCS/verniers to null rotations F. Open supply tank air vent G.* Add prescribed volume increments to each reorientation tank (open and close appropriate manual valves) H. Close air vent I. Reorient liquid and position tank assembly K. Activate camera (t-20 seconds) L. Fire RCS (60 seconds) M. Stop camera (t + 90 seconds) N. Null rotation with RCS/verniers O. Open supply tank air vent P.* Add final volume increment to each tank Q. Close vent R. Reorient liquid and align tank package S. Start camera (t-20 seconds) T. Fire RCS (60 seconds) U. Null rotation - t + 90 seconds V. Stop camera - t + 120 seconds
6. On-orbit Experiment Disassembly:	A. Deactivate accelerometer and temperature sensor B. Remove tank assembly C. Disassembly test stand and stow D. Remove film, package and stow E. Repackage and seal for locker stowage F. Stow in locker
7. Re-entry and Landing:	A. Rely on packaging to withstand loads and contain potential leakage, tank fragments, etc.
8. Post Flight:	A. Remove locker package B. Remove test stand mounting attachments

*NOTE: Camera may be operated to photograph fill operation.

A preliminary mission time line is shown in Figure 38. The total time required for the experiment is approximately 30 minutes, and is determined primarily by the 10 minutes (total) required to settle the liquid and decelerate the experiment package.

4.1.4 Safety Analysis. The basic approach in the design of the liquid reorientation experiment was to minimize the total number of energy sources in the experiment and to ensure that no catastropic release of energy could occur.

There are three sources of mechanical energy:

- Evacuated reorientation tanks--may implode or leak
- Rotation of the experiment package to initialize the liquid interface.
- Thermal expansion of liquid.

Design features to control these energy sources are:

1. The tanks are designed to withstand buckling loads due to external pressurization with a safety factor of 10.

2. Tanks are completely encased in shock absorbing foam during launch and landing--an implosion would be completely contained by the packaging.

3. Leaks would be self-limiting since leakage would be into the fluid system and would stop once the system reached cabin pressure.

4. The packaging will have clear windows to permit inspection of the tanks for leakage or damage before the package is opened.

5. Film will be packaged in leakproof containers after the experiment is completed to prevent damage from leakage during landing, etc.

6. To prevent leakage of test liquid or dispersion of tank fragments into the middeck during testing, the entire package will be enclosed by a sheet of acrylic. Valves and switches will be accessible.

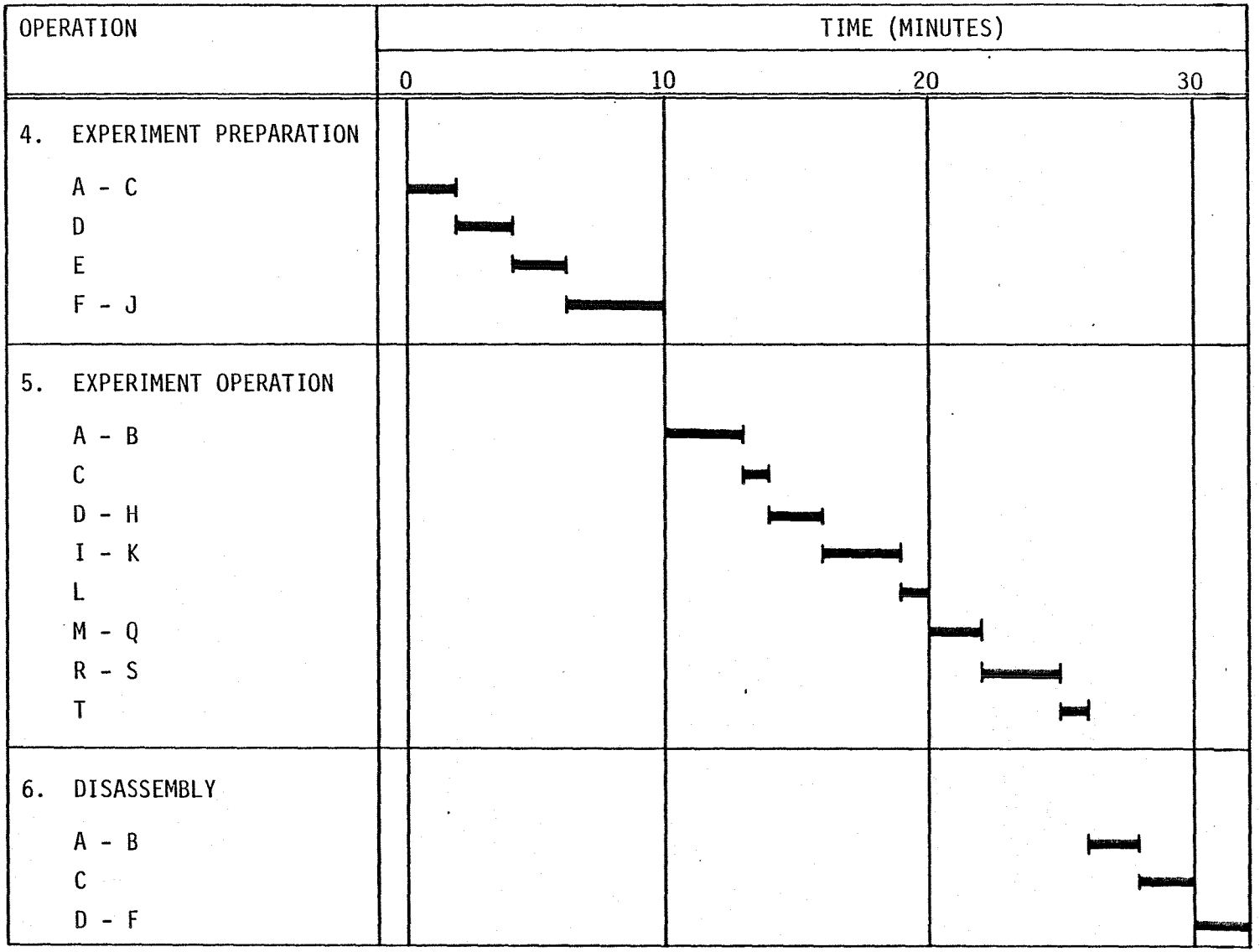

Figure 38 MISSION TIMELINE - LIQUID REORIENTATION EXPERIMENT

7. To prevent the experiment package or test stand from breaking loose during rotation, tethering of the test stand to the floor and package to the test stand will be provided.

8. Thermal expansion of the liquid is controlled by the supply tank air space which is sized so that under worst case temperature fluctuations the liquid can expand without the pressure exceeding approximately 138 kPa. In the event that the air cushion behind the piston is insufficient (or that the piston jams) a relief valve will open to permit liquid to flow into the largest reorientation tank and thus avoid over-pressurizing the system.

A detailed safety analysis was carried out for the liquid reorientation experiment to generate the basic data needed for a Phase Zero Safety Review—the safety matrix and the hazard lists consistent with the requirements of Reference 17. These documents were based on a Fault Hazard Analysis (FHA) carried out in accordance with Reference 18. The safety data is contained in Appendix A. Failure rates for some of the more conventional components were estimated from data in Reference 21. Failure rates of components unique to the reorientation experiment, such as the acrylic tanks and the accelerometer package, will require detailed analysis or testing to evaluate their reliability. Such evaluations were beyond the scope of the preliminary design effort.

Supply Tank Reliability. As an example of an analytic reliability approach which may be used during the detailed design, the reliability of the supply tank was calculated using the basic assumption that the loads on the tank and strength of the tank are normally distributed as shown in Figure 39.

The load and strength (load capability) distributions have means and standard deviations μ_L, μ_S, σ_L, and σ_S, respectively.

As discussed in Reference 22, the reliability of the tank is the probability that the strength will exceed the load. Defining a combined distribution

$$Y = S - L \qquad \text{(Equation 38)}$$

it can be shown that

$$\mu_Y = \mu_S - \mu_L \qquad \text{(Equation 39)}$$

and $$\sigma_Y = \sqrt{\sigma_S^2 + \sigma_L^2} \qquad \text{(Equation 40)}$$

The reliability, R, is then the probability that $Y > 0$,

$R = P(Y > 0)$ which Reference 22 gives as

$$R = \frac{1}{2\pi} \int_{z_o}^{\infty} e^{-z^2/2} dz \qquad \text{(Equation 41)}$$

with $$z_o = - \frac{\mu_S - \mu_L}{\sigma_S^2 + \sigma_L^2} \qquad \text{(Equation 42)}$$

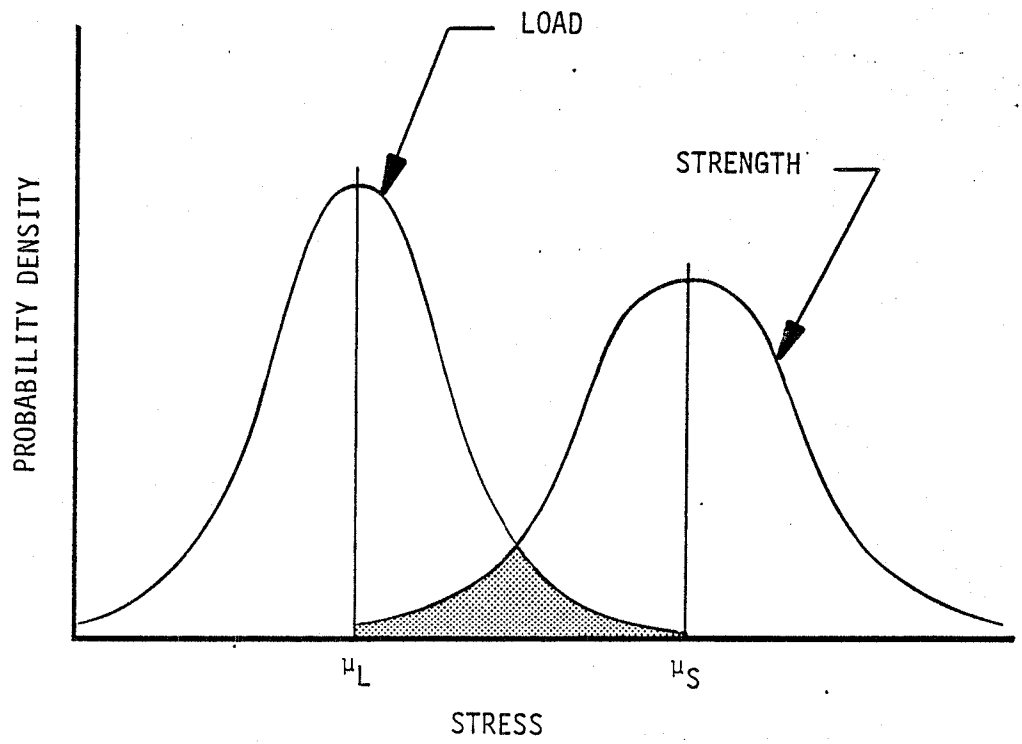

Figure 39 STRENGTH AND LOAD NORMAL DISTRIBUTION

The integral in (Equation 41) is just the tabulated cumulative normal function.

To evaluate z_o, the standard deviations σ_S and σ_L must be calculated (μ_S, μ_L are the design values for strength and load and are already known).

From Reference 23, the standard deviation can be approximated by

$$\sigma^2 = \left(\frac{\partial f}{\partial x_1}\right)^2 \sigma_{x_1}^2 + \cdots + \left(\frac{\partial f}{\partial x_n}\right)^2 \sigma_{x_n}^2 \qquad \text{(Equation 43)}$$

where f is a function of $x_1 \ldots x_n$ and σ_{x_n} is the known standard deviation of x_n.

For the supply tank, the limiting load could be considered to be the pressure at which buckling will occur. From Equation 26, the approximate buckling pressure for an externally pressurized cylinder is:

$$P = \frac{0.807\, E\, \delta^{2.5}}{L\, r^{1.5}} \qquad \text{(Equation 44)}$$

From Equation 43 the standard deviation can be approximated by

$$\sigma_S^2 = \left(\frac{0.807\delta^{2.5}}{L\, r^{1.5}}\right)^2 \sigma_E^2 + \left(\frac{2.018\, E\delta^{1.5}}{L\, r^{1.5}}\right)^2 \sigma_\delta^2 + \left(\frac{0.807\, E\delta^{2.5}}{L^2\, r^{1.5}}\right)^2 \sigma_L^2 + \left(\frac{1.211\, E\delta^{2.5}}{L\, r^{2.5}}\right)\sigma_r^2$$

(Equation 45)

From Section 4.1.2.1:

$L = 32.32$ cm
$r = 8.48$ cm
$\delta = 0.635$ cm
$E = 3103$ mPa

Assuming that the 3σ limits on all linear dimensions are the design tolerances, then

$$\sigma_\delta = \sigma_L = \sigma_r = 0.042 \text{ cm (design tolerance} = \pm 0.127 \text{ cm)} \qquad \text{(Equation 46)}$$

Also assuming that the 3σ limit on E is $\pm$ 20 percent, the standard deviation of the modulus is

$$\sigma_E = 207 \text{ mPa} \qquad \text{(Equation 47)}$$

From Equation 45:

$$\sigma_S = 0.18 \text{ mPa} \qquad \text{(Equation 48)}$$

The mean strength of the cylinder by design (due to buckling pressure), is $_S = 1.103$ mPa. The external pressure can range from 0 to 0.207 mPa. Therefore, the load mean and standard deviation are

$$\mu_L = 0.103 \text{ mPa} \qquad \text{(Equation 49)}$$
$$\sigma_L = 0.034 \text{ mPa} \qquad \text{(Equation 50)}$$

from (Equation 41) when $z_o = 5.46$, the reliability is

$$R > 0.99999 \qquad \text{(Equation 51)}$$

4.1.5 Ground Test Requirements. The ground test requirements for the liquid reorientation experiment were defined. The required ground testing was divided into four parts: Development testing, Component Acceptance testing, Qualification testing, and End Item Acceptance testing.

- Development Testing. Development tests are considered those tests that are normally conducted to evaluate new designs, verify analytical assumptions, fill in data voids, and subassembly and final assembly deisgn verification tests. Some examples of development tests are: material property tests to verify design values, and vibration and shock tests to verify support system damping characteristics and dynamic analyses, and component or subsystem performance tests. Development testing provides the level of confidence required to proceed with the final design, fabrication and qualification testing.

- Component Acceptance Testing (CAT). CAT tests are the tests required to verify that a component meets its specification requirements. These tests

include, but are not limited to, proof tests, thermal shock, leak checks, flow tests, dimensional verification and electrical checks.

- Qualification Testing. Qualification tests are those tests that are required to qualify the final system and its subassemblies for use. Examples of qualification tests are pressure vessel testing, vibration and shock tests during actual operating conditions, mission simulation, and pack and ship tests.

- End Item Acceptance Testing (EIAT). These tests are made on the final flight article prior to shipment. EIATs verify the integrity of the final assembly and verify that all subsystems are operating properly. EIATs are not required if the qualification unit also is to serve as the flight article, since there is no separate flight article.

Tables XXVIII through XXXI summarize the development, CAT, qualification and EIAT required for the liquid reorientation experiment. In addition, each area of testing was further subdivided into functional, environmental and performance testing.

TABLE XXVIII LIQUID REORIENTATION EXPERIMENT DEVELOPMENT TESTING

Component	Test	Description
Environmental Tests		
Supply Tank	Outflow Line Boss Tear-out	Ultimate load required to cause boss failure due to tear-out.
	Shock/Vibration	Subject tank with simulated load to handling, prelaunch, launch, re-entry and post-landing shock and vibration loads.
Reorientation Tanks	Supply Line Boss Tear-out	Same as supply tank.
	Shock/Vibration	Same as supply tank.
Test Stand	Cyclic	Subject stand to cyclic loads caused by rotating experiment.
	Clutch	Perform torque load tests on stand clutch.
	Bracket Tear-out	Ultimate load to cause bracket failure due to tear-out.
Performance Tests		
Supply Tank	Fluid Expulsion	Fill tank with FC-77 and perform outflow tests.
Reorientation Tanks	Fluid Inflow	Evacuate tank and perform no-vent fills.

TABLE XXIX LIQUID REORIENTATION EXPERIMENT
COMPONENT ACCEPTANCE TESTING

Component	Test	Description
Functional Tests		
Supply Tank	Proof Pressure (Internal)	Subject tank to a pressure of at least two times the operating pressure as per Reference 14.
	Proof Pressure (External)	Pressurize the tank surroundings to a minimum of two times the maximum surroundings pressure as per Reference 14.
	Leak Check	Determine if the tank leaks.
Reorientation Tanks	Proof Pressure	Pressurize the tank surroundings to a minimum of two times the maximum surroundings pressure as per Reference 14.
	Leak Check	Determine if the tanks leak.
Temperature Sensor and Readout	Ice Bath/Boiling	Check temperature sensor readout at ice bath, ambient and boiling water conditions.
Accelerometer	Operational	Perform electrical check on accelerometer unit. Check output for each axis and temperature readout.
Camera	Operational	Check operation of lens, film advance, etc.
Test Stand	Assembly/Operation	Assemble and check operation of stand.
Valves	Leak Test	Perform an external and internal leak test of valves at maximum operating and maximum differential pressure.
Batteries	Electrical	Check output of batteries, temperature rise during planned discharge cycle.

TABLE XXX LIQUID REORIENTATION EXPERIMENT QUALIFICATION TESTING

Component	Test	Description
Functional Testing		
Supply Tank	Burst	Pressurize inside of tank to design burst pressure, then continue pressurizing to tank rupture.
	Collapse	Pressurize exterior of tank to design collapse pressure, then continue pressurizing to tank collapse.
Reorientation Tanks	Collapse	Pressurize exterior of tanks to the design collapse pressure, then continue pressurizing to tank collapse.
Experiment Package	Proof Pressure (Internal)	Pressurize package to two times maximum operating pressure as per Reference 14.
	Proof Pressure (External)	Pressurize package surroundings to two times maximum surroundings pressure as per Reference 14.
	Leak Check	Determine if experiment package leaks.
Environmental Testing		
Experiment Package	Shock/Vibration	Subject assembled experiment package, filled with FC-77, to handling, prelaunch, launch, re-entry, and post-landing shock and vibration loads.
	Acceleration	Subject assembled experiment package, filled with FC-77, to anticipated acceleration loads.
	Pack and Ship	Pack and ship simulated package load in instrumented container to buyer.
Test Stand	Shock/Vibration	Subject test stand to handling and on-orbit shock and vibration loads.
	Acceleration	Subject test stand to the anticipated on-orbit loads.

TABLE XXX LIQUID REORIENTATION EXPERIMENT
QUALIFICATION TESTING (Concluded)

Component	Test	Description
Performance Testing		
Experiment Package	Mission Simulation	Perform mission simulation test on the experiment package, including evacuation, fill, setup in the test stand, fluid transfer, settling by rotation and disassembly and storage.

TABLE XXXI LIQUID REORIENTATION EXPERIMENT -
END ITEM ACCEPTANCE TESTING

Assembly	Test	Description
Experiment Package	Proof Pressure (Internal)	Pressurize package to 1.5 times the maximum operating pressure per Reference 14.
	Proof Pressure (External)	Pressurize package surroundings to 1.5 times maximum surroundings pressure as per Reference 14.
	Leak Check	Determine if package leaks.
	Flow	Conduct flow tests on experiment package.
	Electrical	Perform check on package electrical systems.

4.2 Pool Boiling Experiment. The preliminary design of the pool boiling experiment is described in the following paragraphs. Paragraph 4.2.1 describes the design, including fluid and electrical schematics. Paragraph 4.2.2 gives the details of the analyses supporting the experiment design and includes analyses of the heaters, test cells and data requirements. The mission analyses, including the experiment operating procedures and mission timelines, are given in Paragraph 4.2.3. The safety analysis is given in Paragraph 4.2.4. Ground testing requirements for the experiment are given in Paragraph 4.2.5.

4.2.1 Pool Boiling Experiment Preliminary Design. Figure 40 gives the preliminary design of the nine pool boiling experiment test cells. Plumbed to each acrylic test cell is an overflow tank, toggle valve, relief valve, charging valve, pressure switch and pressure transducer. The flow schematic of these components is shown in Figure 41.

The installation of the experiment in the middeck is shown in Figure 42. The experiment DACS and power supplies form a separate unit and are stored in a second middeck locker shown in the figure. During on-orbit experimentation, the test cell units are removed from their storage locker and placed in a test fixture so that they can be aligned with the RCS thrust vector. Connections to the DACS and power supply are made by shielded cables to the panel connections on the DACS/power locker.

Prior to launch, each test cell and associated plumbing is evacuated through the charging valve. The appropriate test fluid is then loaded into each cell, while the overflow tank remains evacuated, with the toggle valve closed. After each cell is filled, the toggle valves are opened slightly to allow test fluid vapor to fill the overflow tank and to allow the pressure to equalize, after which they are closed again. By following this procedure, the test cells remain full of liquid with virtually no entrained vapor, assuring vapor bubbles are not present at the start of the test. The relief valve prevents over-pressurization of the test cells, by allowing test fluid to flow from the cell to the overflow tank.

Just prior to the start of a test, the toggle valves of the cells to be tested are opened, allowing pressure equalization and allowing the cells to operate in the presence of a test fluid vapor volume of approximately ten percent. This assures that an almost constant pressure is maintained over the course of the test, as well as assuring saturated conditions

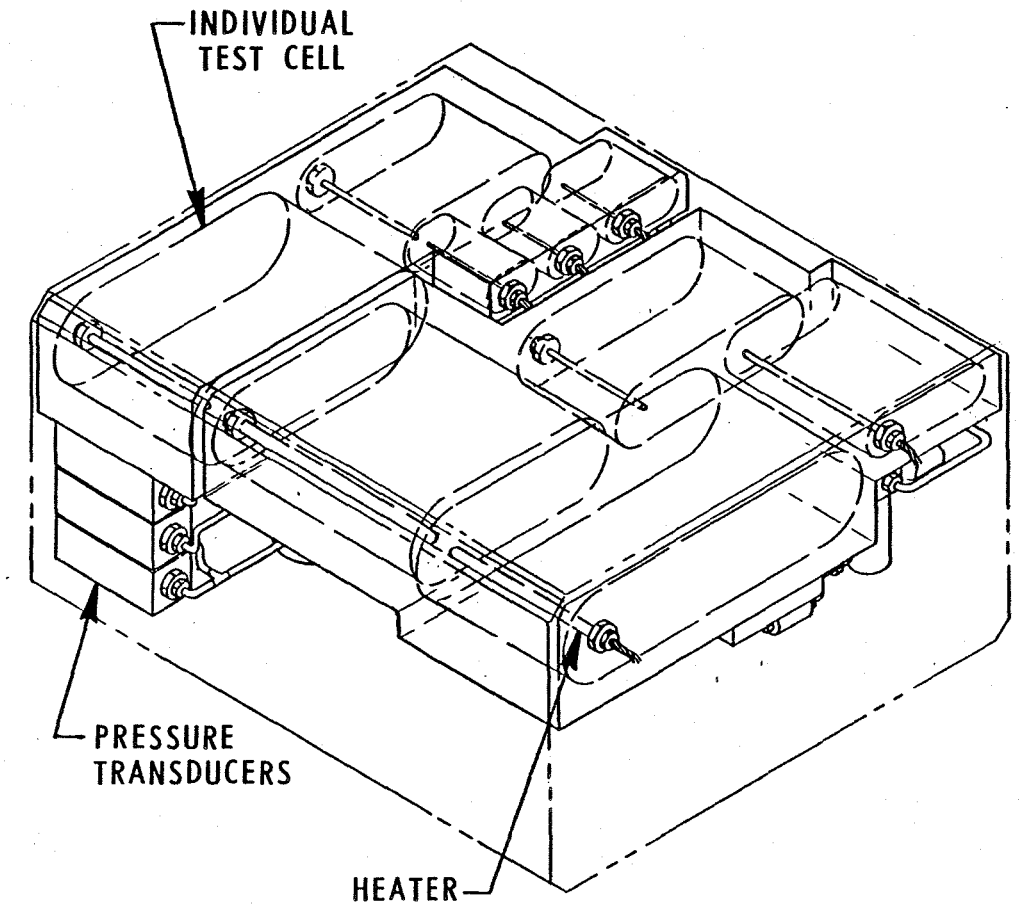

Figure 40 POOL BOILING EXPERIMENT PACKAGE

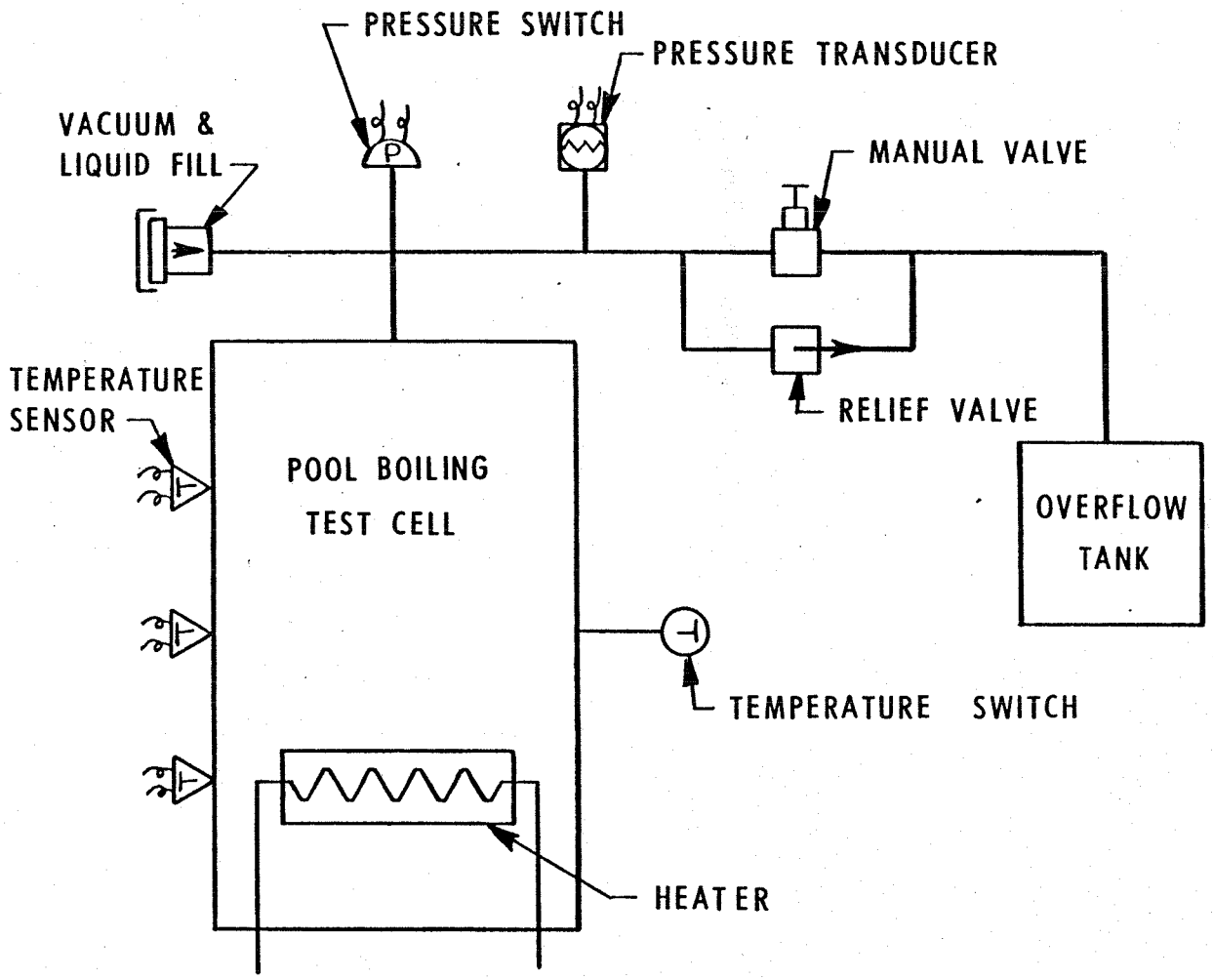

Figure 41 POOL BOILING EXPERIMENT FLOW SCHEMATIC

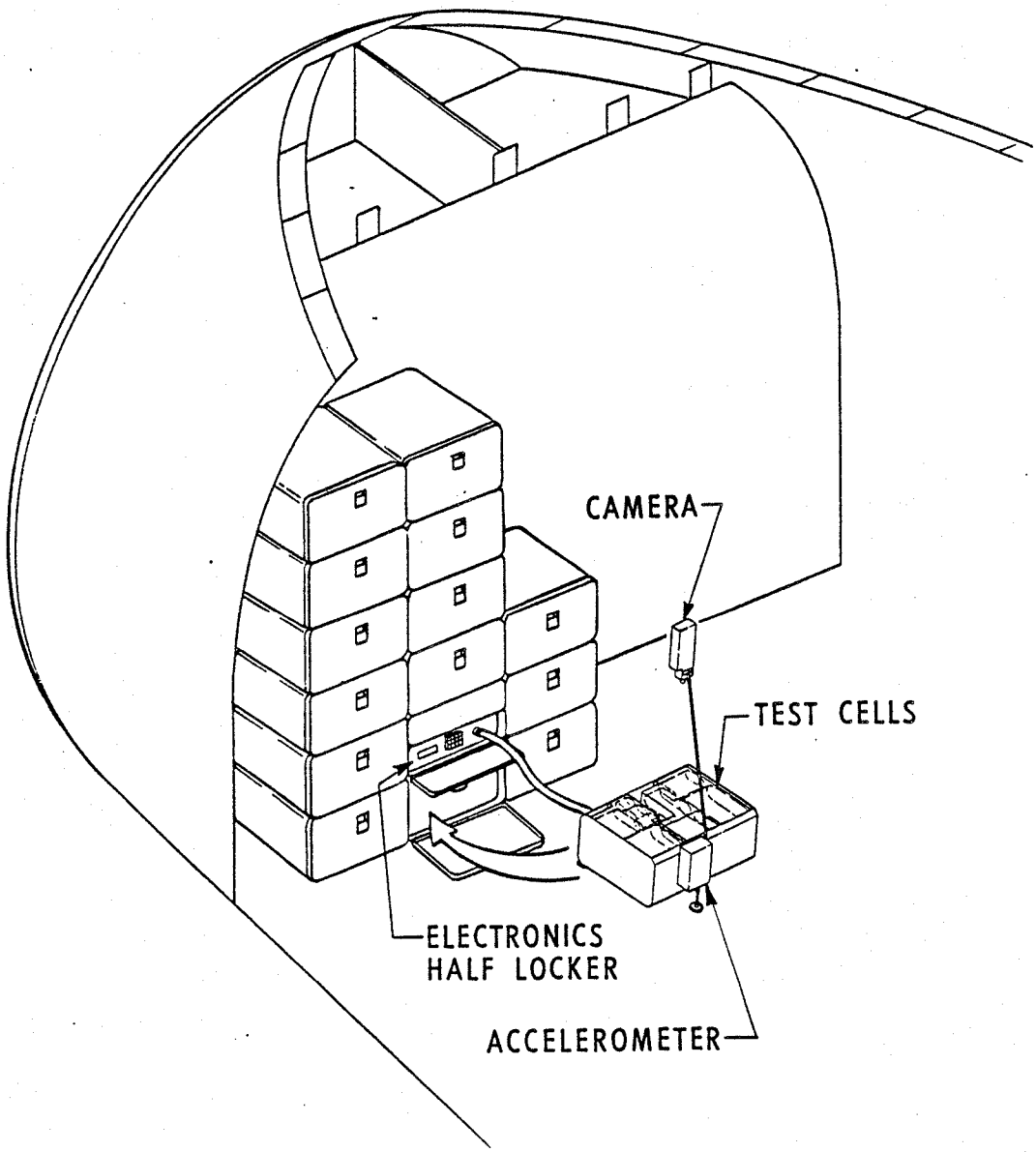

Figure 42 POOL BOILING EXPERIMENT INSTALLATION

at the start of the test. After the first test on a cell is complete (using RCS thrust firings), the toggle valve is closed to prevent liquid from escaping into the overflow tank. The valve is opened again just prior to the start of the second test of a cell (using drag -g acceleration).

Figures 43, 44 and 45 show the design of the 8.00 mm, 3.18 mm and 0.51 mm heaters. The two larger heaters are designed such that power is fed through the center support rod to the end of the heater, through the 0.025 mm titanium foil wall and back through the 7/8-inch hex nut of the heater. The center support is spring-loaded with an O-ring to provide a preload on the titanium foil so the foil does not go into compression when heated. The center rod also serves as the support for the noncontacting infrared temperature sensors. In the smallest diameter heater, there is insufficient space for a center support and noncontacting sensors, requiring the straight-through design shown in Figure 45.

The pool boiling experiment stand is designed to mount on the middeck floor in the same manner as the stand used for the liquid reorientation experiment. The forward end of the stand is hinged to allow the astronaut or mission specialist to turn the underside of the cells up, exposing the valves that need to be controlled.

The electrical schematic for the pool boiling experiment is shown in Figure 46 and shows the heater power camera and DACS connections.

4.2.2 Pool Boiling Experiment Design Analysis. Detailed design analyses were made of the pool boiling heater power requirements, structural, thermal mass, heat boss characteristics, and temperature instrumentation. The size, geometry and construction material of the test cells were determined. Finally, the hardware data quantity and data rate for the pool boiling DACS were defined. The level of detail for the analyses was only sufficient to support cost and schedule estimates for detailed design, fabrication and testing.

Heater Power Requirements. The power requirements per unit length were calculated by determining the film boiling heat transfer rate at a 500°C temperature excess (temperature excess is defined as the temperature difference between the heater wall and the fluid

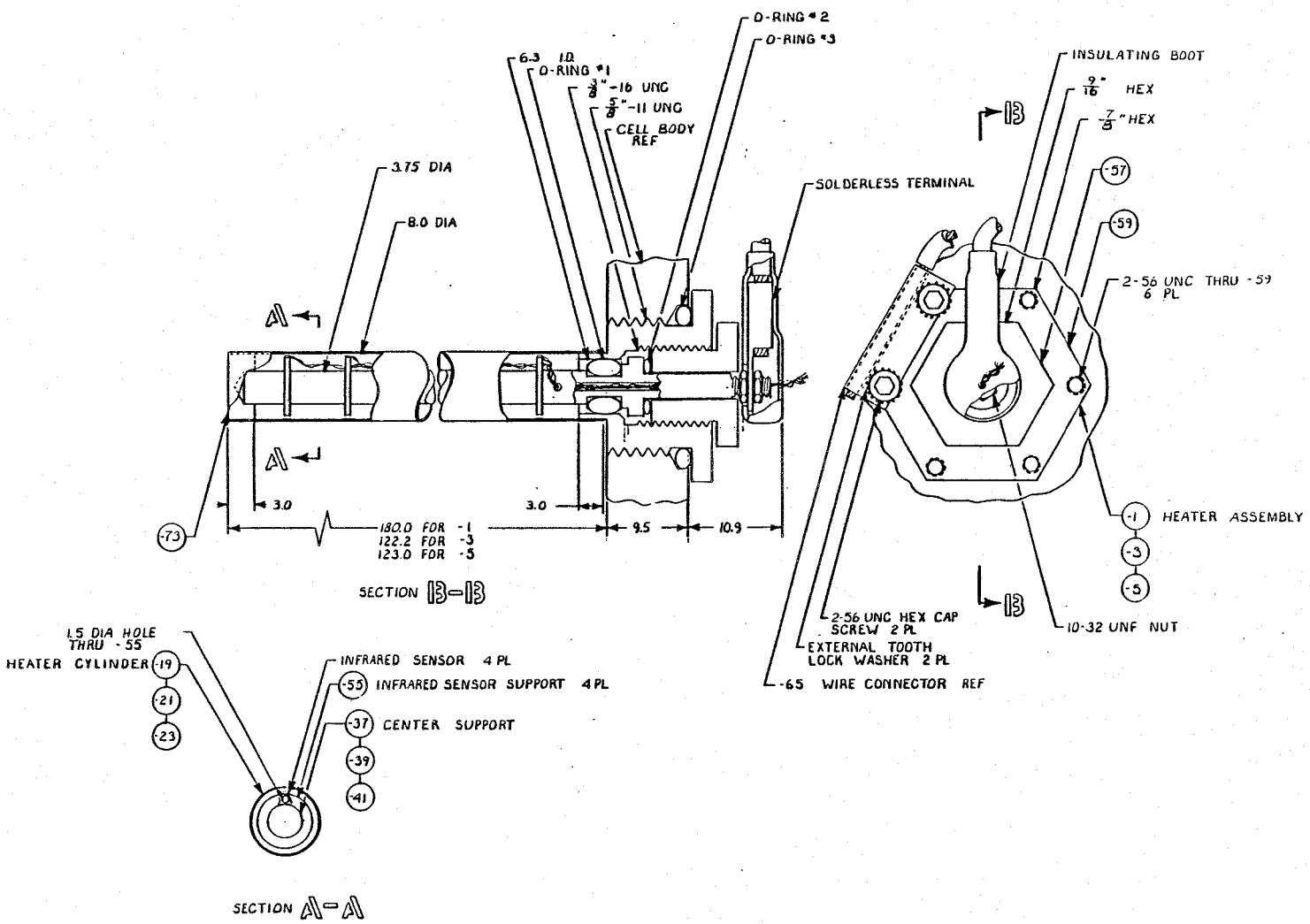

Figure 43 8.00 mm DIAMETER HEATER DESIGN

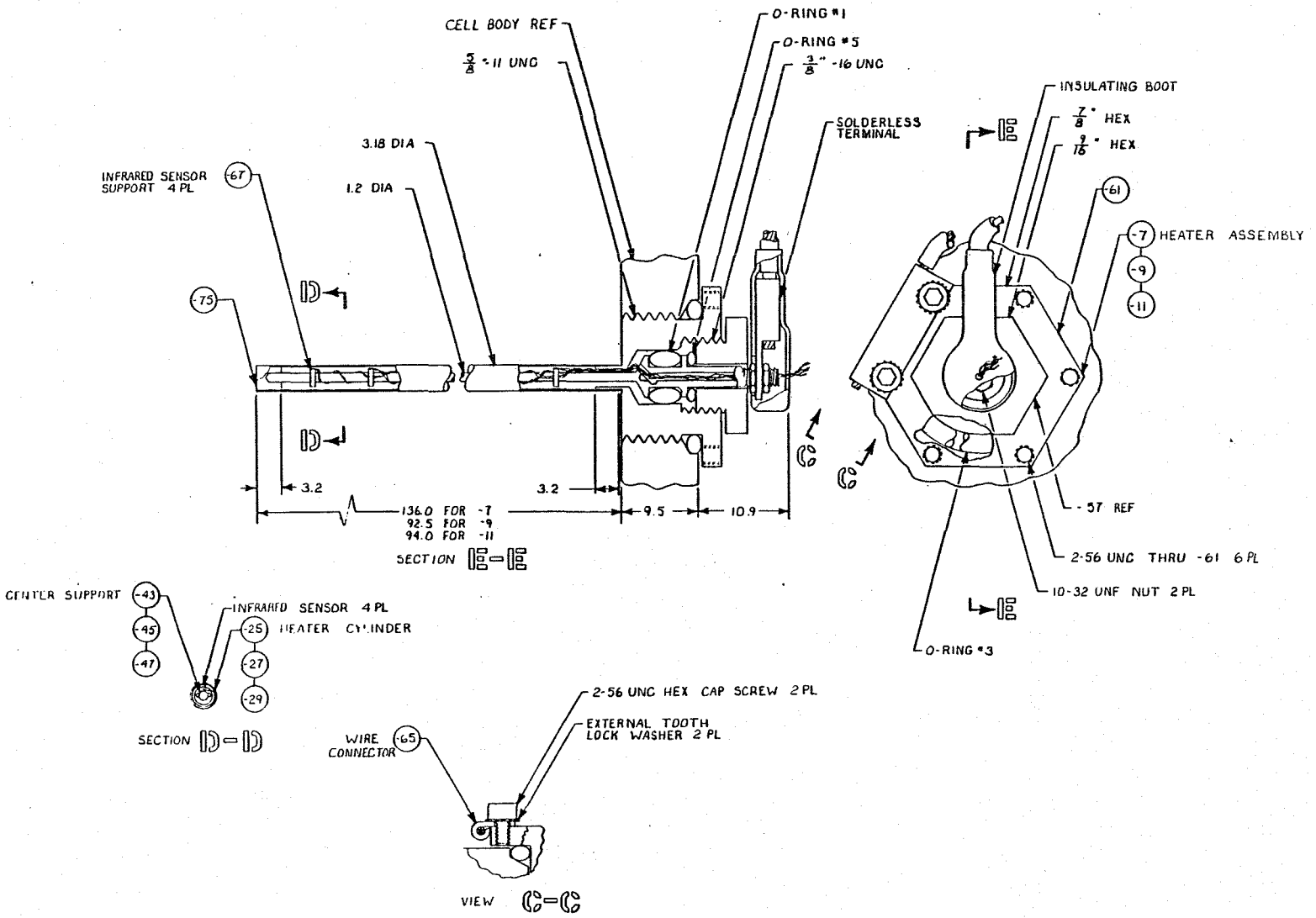

Figure 44 3.18 mm DIAMETER HEATER DESIGN

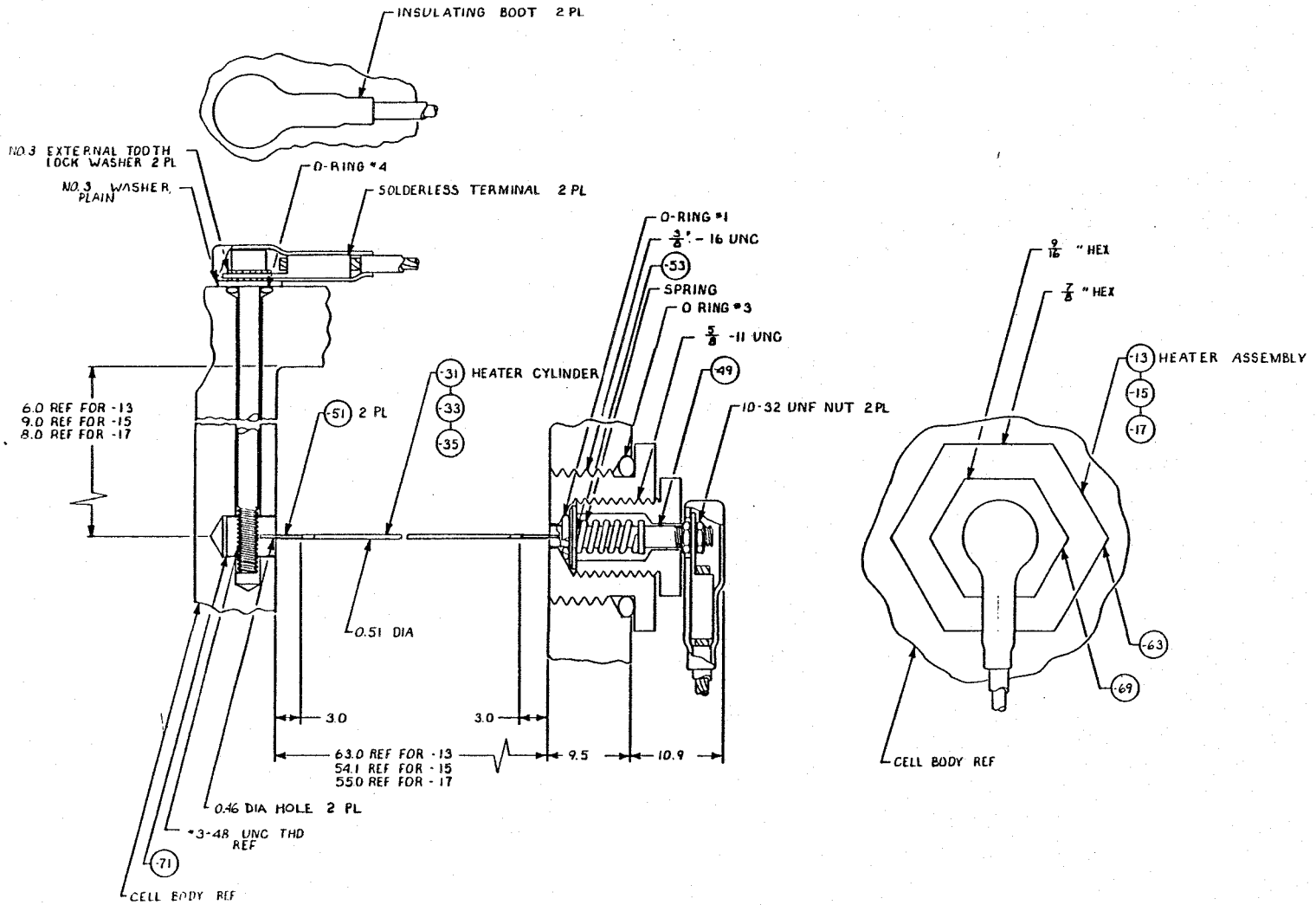

Figure 45 0.51 mm DIAMETER HEATER DESIGN

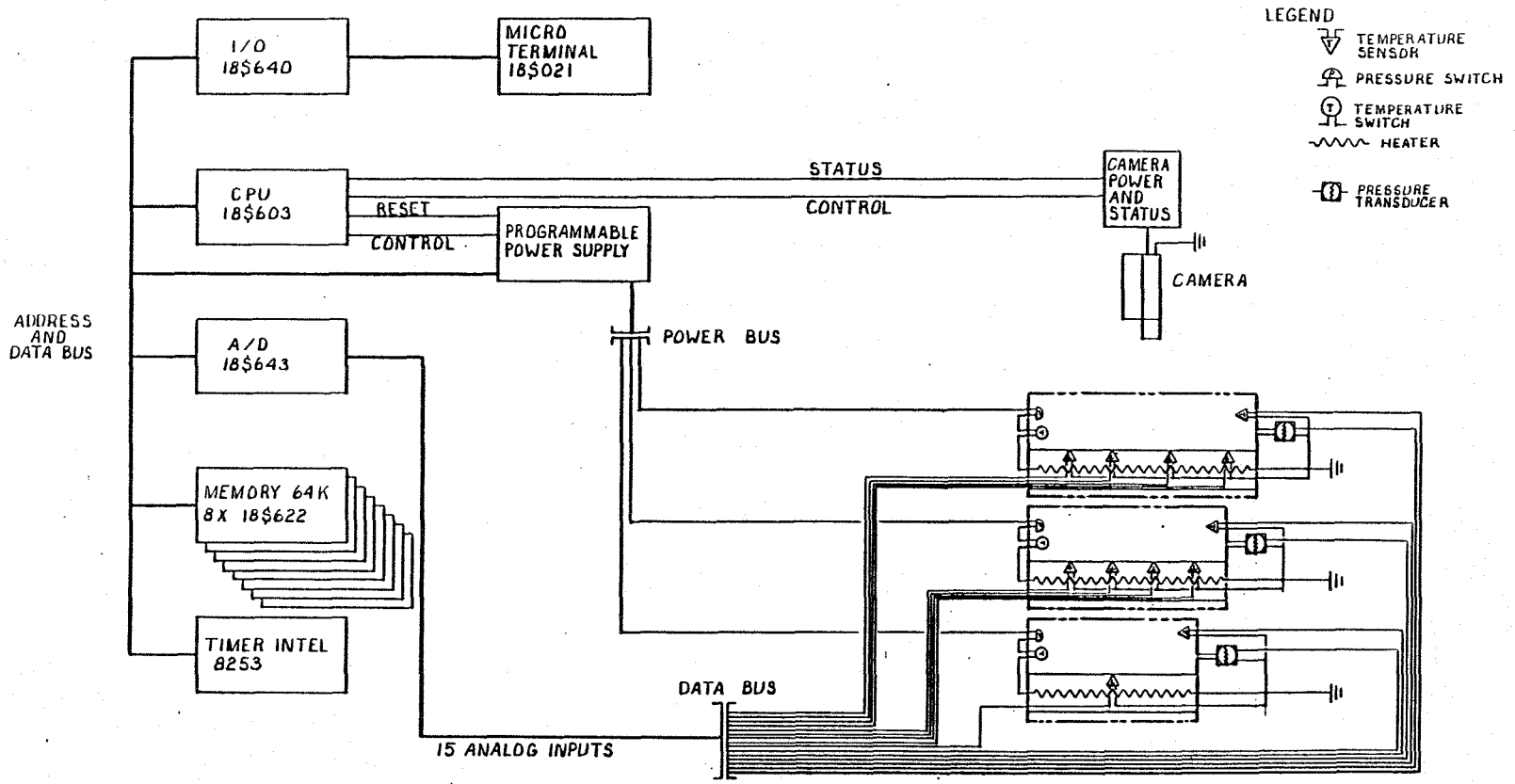

Figure 46 POOL BOILING EXPERIMENT DACS SCHEMATIC

saturation temperature.). From Reference 24, the film boiling heat transfer coefficient was determined from

$$Nu = \frac{hD}{k_g} = 0.7\ Ra^{*1/4}/(2R')^{1/3} \qquad \text{(Equation 52)}$$

The modified Rayliegh Number, Ra* is defined by:

$$Ra^* = \rho_g(\rho_f-\rho_g)\, h_{fg}^*\, g\, D^3/\mu_g k_g\, \Delta T \qquad \text{(Equation 53)}$$

The heater power requirements per unit length for each heater were determined from:

$$Q/L = h\pi D\, \Delta T \qquad \text{(Equation 54)}$$

The results of these calculations are summarized in Table XXXII.

TABLE XXXII POOL BOILING HEATER WIRE POWER PER UNIT LENGTH

Test Point	Test Fluid	Heater Diameter (cm)	R' @10^6g	R' 0.008g	Heater Power Per Unit Length (W/cm)
1	Water	0.800	0.0015	0.1314	5.58
2	Water	0.318	0.00058	0.0522	3.79
3	Water	0.051	0.000093	0.0083	1.75
4	Ethanol	0.800	0.0024	0.2143	5.50
5	Ethanol	0.318	0.00095	0.0851	3.75
6	Ethanol	0.051	0.00015	0.0136	1.75
7	Freon 113	0.800	0.0037	0.3337	2.63
8	Freon 113	0.318	0.0015	0.1324	1.79
9	Freon 113	0.051	0.00024	0.0212	1.33

Heater Wire Structural Analysis. Calculations were made to determine the minimum allowable heater tube wall thickness. Three failure modes were considered: (1) Bending due to buoyant forces, (2) buckling due to buoyant forces, and (3) yielding due to the pressure increase inside the heater during operation. The heater wall thickness, δ, required to withstand bending due to buoyant forces, was determined from:

$$\delta \geq \frac{5\rho_f L^2 g}{12\sigma_y g_c} \qquad \text{(Equation 55)}$$

This equation was developed by combining the equation for the 5 g buoyant force load:

$$w = 5\,\rho_f \pi R_o^2\, g/g_c \qquad \text{(Equation 56)}$$

with the equation for the yield stress:

$$\sigma_y = \frac{MR_o}{I} = \frac{wL^2 R_o}{12\,\pi R_o^3\,\delta} \qquad \text{(Equation 57)}$$

The tube wall thickness required to avoid buckling due to buoyant forces was determined from Reference 21:

$$\delta = \left[\frac{1-\nu^2}{1.14E}\,M\right]^{1/2} \qquad \text{(Equation 58)}$$

During heater operation, the pressure inside the tube will rise due to the heating of the gas (i.e., nitrogen) inside the tube. The wall thickness required to avoid yielding due to this pressure rise was determined from:

$$\delta = \frac{P_a\left(\frac{T_{max}}{T_a} - 1\right) R_o}{\sigma_y} \qquad \text{(Equation 59)}$$

Table XXXIII gives minimum wall thicknesses required to meet the three loads considered, for a variety of candidate materials. For all materials, it is apparent from the table that the minimum wall thickness is determined by material fabrication and handling requirements and not by structural loads.

TABLE XXXIII MINIMUM WALL THICKNESS REQUIREMENTS

Material	E GPa	σ_y mPa	$\delta_{bending}$ (μm)	$\delta_{buckling}$ (μm)	$\delta_{pressure}$ (μm)
Aluminum	69	34	10.9	7.1	20.3
Copper	117	69	5.6	5.3	10.2
Nickel	207	138	2.8	4.1	5.1
Platinum	145	14	27.4	4.8	50.8
Silver	76	55	6.9	6.6	12.7
Titanium	103	276	1.3	5.6	2.5

Maximum Heater Thermal Mass. A major consideration in the selection of the heater material and wall thickness is that the thermal mass of the heater be small enough so that several "steady state" data points may be obtained during each 45 second test run.

For a heated system with negligible internal thermal resistance (i.e., uniform temperature) the temperature response may be represented by

$$\frac{dT}{dt} + \frac{hA}{\rho CV} T = \frac{Q(t)}{\rho CV} \qquad \text{(Equation 60)}$$

The time constant of this system is:

$$\tau = \frac{\rho CV}{hA} \qquad \text{(Equation 61)}$$

and, for a hollow cylindrical heater with outer radius D_o and a wall thickness of δ, Equation 61 can be rewritten as:

$$\tau = \frac{(\rho C)(D_o \delta - \delta^2)}{hD_o} \qquad \text{(Equation 62)}$$

To give some notion of the magnitude of this number, consider a heater composed of vacuum deposited metal on a glass substrate:

$(\rho C) = 2200 \frac{kJ}{m^3\ ^oC}$ (glass)

$h = 20.8 \frac{W}{m^2\ ^oC}$ (R -113, film boiling)

$D_o = 0.800$ cm

$\delta = 1.27$ mm

$\tau = 452$ seconds

Obviously, this is unacceptable. Obtaining 95 percent of the steady state temperature would require three time constants or 1356 seconds for a single point.

The maximum acceptable time constant for the heater is a function of the number of test points needed during a 45-second test run. Suppose the heater input power is ramped to

some level and then held for a specified period of time for each data point, as shown in Figure 47.

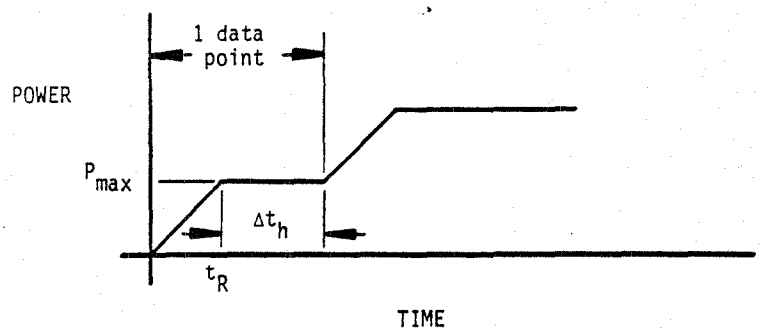

Figure 47 HEATER WIRE INPUT POWER VERSUS TIME

Mathematically this can be expressed as:

$$Q(t) = \begin{cases} \frac{P_{max} t}{t_R} & 0 \leq t \leq t_R \\ P_{max} & t_R \leq t \end{cases} \qquad \text{(Equation 63)}$$

At any time, an equilibrium temperature can be defined ($\frac{dT}{dt} = 0$)

$$T_{eq} = \frac{Q(t)}{\rho C V} \tau \qquad \text{(Equation 64)}$$

Equation 60 can be solved (assuming constant h and the initial condition T = 0).

$$\frac{T}{T_{eq}} = \begin{cases} \frac{t}{t_R} - \frac{\tau}{t_R} + \frac{\tau e^{-t/\tau}}{t_R} & 0 \leq t \leq t_R \qquad \text{(Equation 65)} \\ 1 + \frac{\tau}{t_R}(1 - e^{t_R/\tau})e^{-t/\tau} & t_R \leq t \qquad \text{(Equation 66)} \end{cases}$$

Table XXXIV presents the tabular values of the solution to Equation 60 and shows that if the power is ramped up in one time constant (to avoid inducing hydrodynamic instabilities by a sudden application of power) and the power is held constant for two time constants,

the heater equilibrium temperature will be within ten percent of the equilibrium temperature. Thus, each data point will require three time constants as shown in Figure 48.

TABLE XXXIV SOLUTION OF HEATER TRANSIENT RESPONSE EQUATION

	t_R/τ					
t/τ	0	1	2	3	4	5
1	0.632	0.368	0.368	0.368	0.368	0.368
2	0.865	0.767	0.568	0.568	0.568	0.568
3	0.950	0.914	0.841	0.683	0.683	0.683
4	0.982	0.969	0.941	0.883	0.755	0.755
5	0.993	0.988	0.978	0.957	0.910	0.801

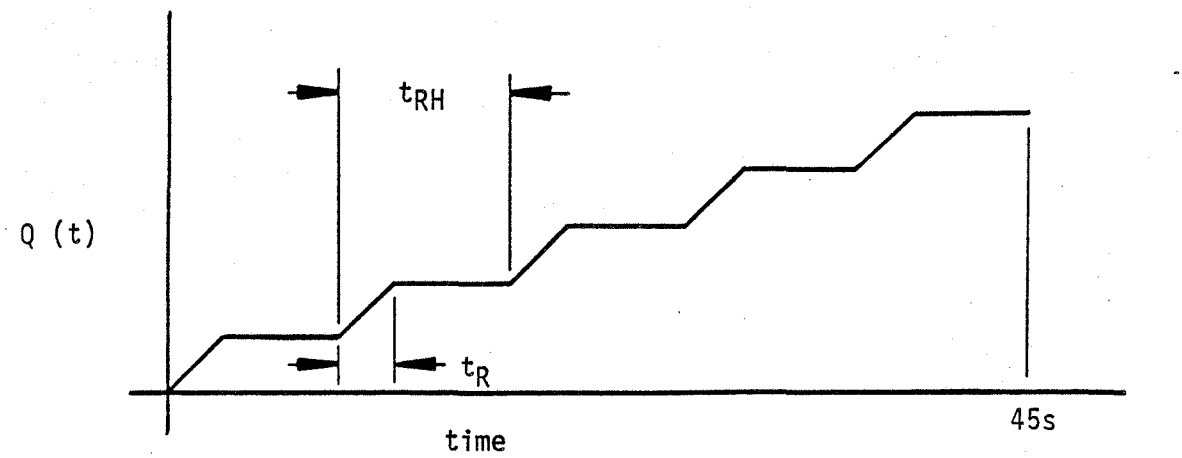

Figure 48 TIME REQUIRED FOR ONE DATA POINT

For N data points during the 45 second experiment period,

$$3N = 45, \text{ or} \qquad \text{(Equation 67)}$$

$$\tau = \frac{15}{N} \qquad \text{(Equation 68)}$$

Assuming that five data points are the minimum needed to generate a heat flux versus temperature curve, the maximum acceptable time constant is three seconds.

Assuming that the minimum material thickness is 0.025 mm (i.e., metal foil formed into a cylinder), the maximum heater ρC is:

$$\frac{hD_o\,\tau}{(D_o\,\delta - \delta^2)} = \rho C \qquad \text{(Equation 69)}$$

Using the smallest heat transfer coefficient (for R-113), Equation 69 was used to determine the maximum acceptable ρC products for each heater size. The results are given in Table XXXV.

TABLE XXXV MAXIMUM ρC PRODUCTS

Heater Radius (mm)	h, R-113 ($W/m^{3o}C$)	ρC ($kJ/m^{3o}C$)
4.00	20.8	2469
1.59	35.9	4274
0.254	164.7	20464

Material Selection. Only pure metals were considered suitable for the heater, since results obtained with alloys may not be entirely reproducible. Thus, the material selection consisted of finding elemental metals that had low enough values of (ρC) and also had satisfactory electrical properties.

The resistance of the heater is

$$R = \frac{jL}{A} \qquad \text{(Equation 70)}$$

It is desirable to maximize the heater resistance (which for a given geometry means maximizing j) to minimize the heater current and hence minimize losses of the heater power cable.

Potentially acceptable heater materials are tabulated in Table XXXVI.

TABLE XXXVI HEATER WIRE MATERIALS

Material	C ($kJ/m^{3o}C$)	j ($\mu\Omega$-cm)	α (cm/cm ^oC)	k ($W/m\ ^oC$)
Titanium	2340	42	2.59	17.0
Aluminum	2430	2.65	7.28	222
Silver	2460	1.59	6.06	419

The obvious choice for the heater material is titanium, since the resistivity is higher than either of the other metals. In addition, titanium has a lower coefficient of thermal expansion than either of the other metals which will reduce problems with thermal buckling.

Heater Length. The minimum heater length was determined from the allowable percentage of the heater power which could be lost by conduction from the ends of the heater.

The steady state temperature distribution along the heater is determined by

$$\frac{d^2T}{dx^2} - \frac{hP}{kS} T = -\frac{Q}{kS} \qquad \text{(Equation 71)}$$

The solution to Equation 71 is (assuming $T = 0$ at the ends of the heater and $\frac{dT}{dx} = 0$ at the heater midpoint):

$$T = \frac{Q}{hP} \left[1 - \left(\frac{e^{-mx} e^{mL} + e^{mx}}{1 + e^{mL}} \right) \right] \qquad \text{(Equation 72)}$$

Defining η as

$$\eta = \frac{\text{heat transferred to fluid}}{\text{heat input to heater}}$$

$$\eta = \frac{hP \int_0^L T dx}{QL} \qquad \text{(Equation 73)}$$

or

$$\eta = 1 - \frac{2}{mL(e^{-mL} + 1)} \qquad \text{(Equation 74)}$$

since for the proposed heaters $e^{-mL} \simeq 0$

$$L = \frac{2}{(1-\eta)} \sqrt{\frac{k\,\delta(1-\delta/D_o^2)}{h}} \qquad \text{(Equation 75)}$$

For $\eta = 0.95$ and $\delta = 0.025$ mm (heater material thickness), the minimum required heater lengths are given in Table XXXVII.

TABLE XXXVII MINIMUM HEATER LENGTHS

D_o (cm)	R-113 L (cm)	H_2O L (cm)	Ethanol L (cm)
0.800	18.16	12.42	12.52
0.318	13.82	9.45	9.55
0.051	6.30	5.41	5.49

Heater Temperature Instrumentation. To avoid adding thermal mass to the heater, and hence increasing the heater time constant or forcing a decrease in the heater material thickness, it is desirable to use noncontact temperature sensors inside the heater. The sensors proposed are infrared sensitive thermistors (Thermoflakes manufactured by Thermometrics). The thermistors are approximately 1 millimeter square and 50 microns thick and have an adequate response in the expected temperature range 20-500°C. Use of these thermistors will require development testing to determine accuracy and optimum hardware configurations.

Test Cell Size. The test cell inside dimensions were determined from consideration of the size the vapor jets developed during boiling. From Reference 4, the diameter of a vapor jet, D_j, for boiling from a horizontal cylinder is:

$$D_j = 2(R + \delta) \qquad \text{(Equation 76)}$$

The vapor blanket thickness, δ, is related to a dimensionless vapor blanket thickness, Δ :

$$\delta = \frac{\Delta}{(g(\rho_f - \rho_g)/\sigma)^{1/2}} \qquad \text{(Equation 77)}$$

Δ is related to R' through the following

$$\Delta = \left[2.54R' + 6.48R' \exp(-3.44R'^{1/2}) \right]^{2/3} - R' \qquad \text{(Equation 78)}$$

Table XXXVIII gives values for R', Δ and D_j for the pool boiling test matrix.

TABLE XXXVIII R', Δ AND D_j FOR THE POOL BOILING TEST MATRIX

Cell	Fluid	R (mm)	R' @ 0.008g	Δ	D_j (mm)
1	Water	4.00	0.1314	0.563	42.3
2	Water	1.59	0.0522	0.383	26.5
3	Water	0.26	0.0083	0.146	9.6
4	Ethanol	4.00	0.2143	0.667	32.9
5	Ethanol	1.59	0.0851	0.474	20.9
6	Ethanol	0.26	0.0136	0.192	7.9
7	R113	4.00	0.3337	0.760	26.2
8	R113	1.59	0.1324	0.564	16.7
9	R113	0.26	0.0212	0.245	6.5

The width, W, of the cells was taken as $2D_j$. The cell heights, H, are the largest multiple of the disturbed wave length of the vapor jets which allows all of the cells to be fitted in one middeck locker. Reference 4 gives the disturbed wave length of a vapor jet as πD_j; H was set equal to $1.9\ \pi D_j$. The cells' lengths are set by the required heater lengths. All dimensions meeting these criteria are summarized in Table XXXIX; the cell dimensions are defined in Figure 49.

Material Selection for Test Cells. Considerations in selection of the test cell material include the following:

1. Ease of fabrication, minimization of the number of joints and sealed openings

2. Good visibility of boiling process
3. Minimum weight and volume

TABLE XXXIX TEST CELL DIMENSIONS

Cell	Fluid	D (mm)	L (mm)	W (mm)	H (mm)
1	Water	8.00	124	85	266
2	Water	3.18	94	53	167
3	Water	0.51	54	19	60
4	Ethanol	8.00	125	66	207
5	Ethanol	3.18	96	42	131
6	Ethanol	0.51	55	16	50
7	R113	8.00	182	52	165
8	R113	3.18	138	33	105
9	R113	0.51	63	63	41

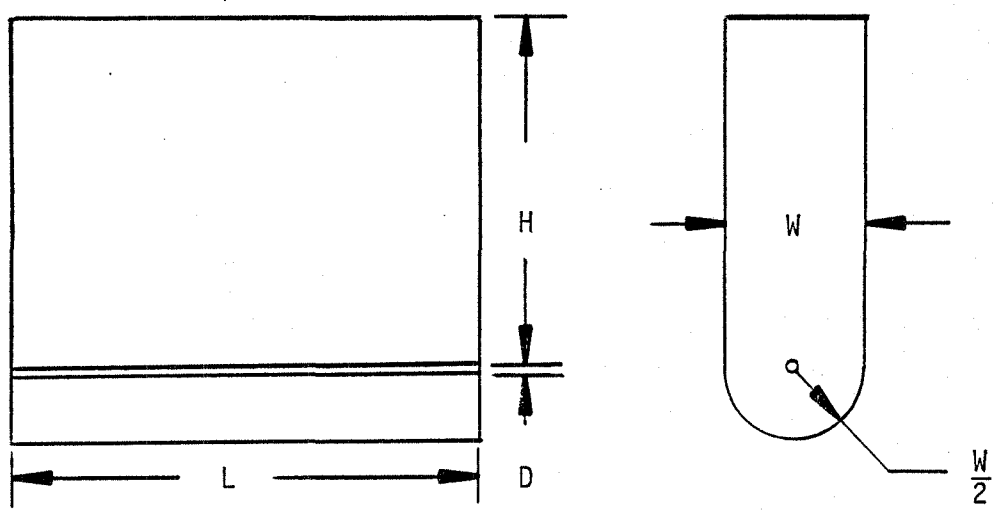

Figure 49 CELL DIMENSIONS DEFINITION

Assuming that the sides of the cell can be modeled as a flat plate that is uniformly loaded by pressure, then for a plate of fixed dimensions, the maximum stress and maximum deflection are given by

$$\sigma_m = \frac{K_\sigma}{\delta^2} \qquad y_m = \frac{K_y}{E^3}$$ (Equations 79, 80)

For a fixed maximum deflection

$$\frac{\delta}{\delta_R} = \sqrt[3]{\frac{E_R}{E}}$$ (Equation 81)

where δ_R and E_R are the thickness and modulus of a reference material.

If the plate design is stress limited, then

$$\frac{\delta}{\delta_R} = \sqrt{\frac{\sigma dR}{\sigma_d}}$$ (Equation 82)

where σ_{dR} and σ_d are the design limit stresses for the reference material and the material of interest. The actual value of $\frac{\delta}{\delta_R}$ is the greater of Equations 81 or 82.

The total volume of the box will be proportional to the wall thickness of the "plates" forming the sides of box.

$$\frac{V}{V_R} = \frac{\delta}{\delta_R}$$ (Equation 83)

The weight of the box will be proportional to both the wall thickness and density:

$$\frac{W}{W_R} = \left(\frac{\delta}{\delta_R}\right)\left(\frac{\rho}{\rho_R}\right)$$ (Equation 84)

Using aluminum 7075 (T6) as the reference material, the relevant parameters for several candidate materials are tabulated in Table XL.

TABLE XL TEST CELL MATERIAL EVALUATION

Material	σ_{yield} (MPa)	σ_d (MPa)	E (GPa)	ρ (kg/m^3)	$\sqrt[3]{\frac{E_R}{E}}$	$\sqrt{\frac{\sigma_{dR}}{\sigma_d}}$	$\frac{V}{V_R}$	$\frac{W}{W_R}$
7075 T6 Aluminum	503	151.7	68.9	2720	1.0	1.0	1.0	1.0
6061 T4 Aluminum	145	89.6	68.9	2720	1.0	0.77	1.0	1.0
304 Stainless Steel	207	51.7	193.1	8030	0.71	1.71	1.71	4.96
Brass	365	89.6	110.3	8580	0.86	1.30	1.30	4.03
Magnesium AZ31B-H24	145	110.3	44.8	1770	1.15	1.17	1.17	0.75
Copper	69	17.2	117.2	8970	0.84	2.97	2.97	9.61
Acrylic	69	6.9	3.4	1190	2.71	4.70	4.70	2.02
Polycarbonate	69	6.9	2.1	1190	3.22	4.70	4.70	2.02

The results shown in Table XL make it evident that metallic cells made from magnesium or aluminum have the minimum weight (or volume). However, they require the addition of a window and necessarily permit a limited view of the boiling process.

An all-acrylic or polycarbonate cell avoids the problems inherent in fabricating a window joint. In addition, an all-plastic cell minimizes the potential for electrical shock and permits more complete viewing of the boiling process (i.e., from the end of the heater as well as from the side of the heater.)

Of the two possible plastics, acrylic has much superior optical qualities and is only slightly more difficult to machine, and therefore was selected as the test cell material.

DACS. The DACS consists of a microcomputer assembled from off-the-shelf components: 64 kilobytes of static memory for storage of data, an A/D converter and an I/O board. Heater power is supplied from a programmable power supply capable of supplying 30 amperes at 0 - 3 volts DC. The supply will be controlled by the DACS via reset and control lines. The design of the power supply was beyond the scope of this study.

The DACS is based on the RCA COSMAC 1802 microprocessor. The primary advantages of this microprocessor are low power consumption, full military operating temperature range, and an architecture optimized for data logging and control.

The DACS will consist of the following standard boards (each board is 11.4 x 19.1 cm).

1	CDP18S603	- Central Processor
1	CDP18S643	- 16-Channel Analog to Digital Converter
8	CDP18S622	- 8 Kilobyte Static RAM Memory with on-board battery backup power
1	CDP18S640	- 1/0 Control
1	CDP18S021 (or Equivalent)	- MICRO Terminal

Total maximum power consumption is approximately 4 watts, with approximately 40 per cent of the power being dissipated in the I/0 control board (i.e., a function which could be minimized for reduced power consumption).

Data Rate: Analog signals from the test cells (heater temperature, liquid temperature and pressure) are routed to the A/D converter, converted to 8-12 bit digital values and then stored in memory. (A useful feature of the 1802 microprocessor is the capability for direct access to memory without interrupting executing program operation.) The total time required for conversion of a single reading is 300 microseconds maximum (assuming 8 bit conversion with a 2 MHz CPU clock.) At this conversion speed, the data rate is approximately 3 KHz. This data rate could completely fill the available memory in approximately 20 seconds.

The power to the heaters will be increased in five steps, with "steady state" temperatures present only in the last second of the time at each power level. For nine test cells, at two gravity levels, five power levels, and monitored for one second at each power level, the maximum data rate without exceeding the 64 K memory is: $\sim$ 680 Hz (assuming $\sim$ 3 K bytes for program storage).

The total number of readings to be taken during each one-second measurement interval is:

9	heater temperatures
3	liquid temperatures
3	cell pressures
3	heater powers* - multiplexed to A/D
18	Total readings

*Heater power could be implicit and not measured - the power supply is adjusted before flight to deliver a specified power at a specific time.

At the 680 Hz data rate, all the test cells could be sampled 37 times during the one-second measurement period.

The camera could simultaneously be operated under control by the DACS to synchronize the photographic record with the measured data. For example, the camera could be driven at 100 frames per second to obtain nearly three photographic records of every data point. The amount of film required would be 46 meters.

Experiment Timer: Timing of program operations is controlled by an Intel 8253 programmable timer. This frees the CPU from menial timing chores and permits simultaneous control of multiple tasks. The timer consists of three independent,

programmable timers and can be directly interfaced to the 1802 system (the timer is simply considered as another memory location). The interconnections are shown in Figure 50.

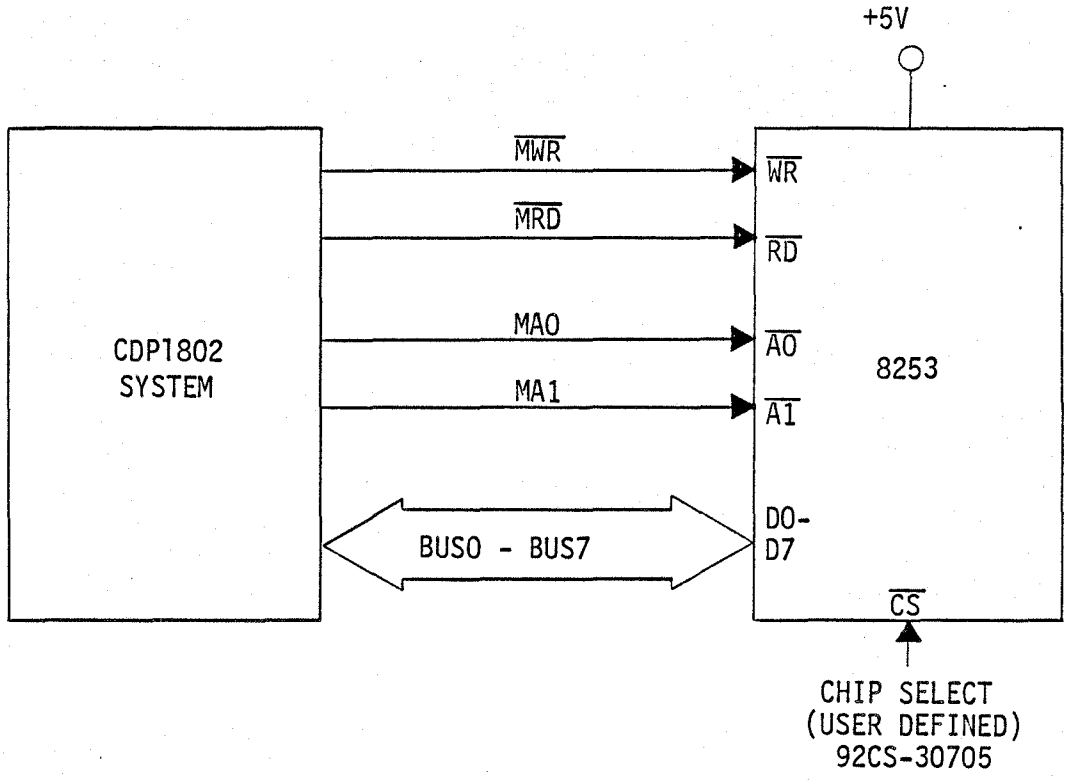

Figure 50 TIMER - DACS SYSTEM INTERCONNECTIONS

Independent Pressure and Temperature Control. Shutdown of the heater power in the event of excessive test cell temperature or pressure is provided by temperature and pressure switches independent of the microcomputer. The status of these switches may be monitored by the microprocessor to provide an accurate picture of the experiment status.

4.2.3 Mission Analysis. Mission operation timelines for the pool boiling experiment were based on the experiment operation procedure shown in Table XLI. The mission timeline reflects only the on-orbit operations: preparation, operation and disassembly.

TABLE XLI POOL BOILING EXPERIMENT OPERATING PROCEDURE

1. Pre-flight Handling:	A. Final checkout of batteries, film, camera, and DACS B. Evacuate all tanks, leak check and fill with liquid C. Package all equipment D. Stow all equipment in two middeck lockers E. Install middeck attachments on middeck floor
2. Launch:	A. Rely on packaging to withstand launch loads and contain potential leakage, etc.
3. On-orbit Stowage:	A. Rely on packaging to withstand launch loads and contain potential leakage, etc.
4. On-orbit Experiment Stowage:	A. Remove tanks and support stand from stowage locker B. Visually inspect for leakage before opening C. Open package D. Assemble test stand E. Load camera and check out; install F. Make all electrical connections to tank set and camera G. Activate and check out accelerometer package H. Run DACS diagnostics I. Adjust initial orientation of test stand to be aligned parallel with RCS thrust vector J. Fire RCS to determine actual thrust vector and align test stand
5. On-orbit Experiment Operation:	A. Open vacuum space valves--all three tanks for run B. Activate DACS for first run C. Fire RCS on command (t = 0) D. Stop RCS (t = 45 seconds) - null rotation E. Verify DACS shutdown of experiment F. Wait for convection to stop G. Activate DACS for low-g experiment H. Verify DACS shutdown I. Shut vacuum space valves on three test tanks J. Disconnect DACS K. Connect DACS to next set of test tanks L. Repeat Steps A through J for last two tank sets
6. On-orbit Experiment Disassembly:	A. Disassemble test stand and stow B. Stow camera, film, and test tanks C. Place DACS in power-down data-save mode
7. Re-entry and Landing:	A. Rely on packaging to withstand loads and contain potential leakage, etc.
8. Post Flight:	A. Remove storage locker package B. Remove DACS C. Store data from RAM on permanent medium (tape, etc.) D. Remove test stand mounting attachments

A preliminary mission timeline for the pool boiling experiment is shown in Figure 51. The total time required for the experiment is approximately 38 minutes.

4.2.4 Safety Analysis. The approach taken in the design of the pool boiling experiment was to make the experiment essentially fail-safe. The test cells are operated at subatmospheric pressure and leaks would come from the cabin into the test cell. This would ruin the experiment but would not present a safety hazard. The possibility of an uncontrolled pressure rise leading to test cell rupture is remote because:

1. Boiling is at subatmospheric pressure and tests conducted at Beech have shown that saturated boiling in a closed cell does not result in increases in cell pressure - as long as some small vapor volume exists.
2. If the cell leaks and approaches atmospheric pressure, boiling would probably not occur since the cell liquid would be greatly subcooled.
3. A pressure switch will shut off power if pressure in the cell exceeds design limits. Once the power is off, cell pressure cannot increase.
4. At some pressure below the cell rupture pressure, the thin-walled heater will collapse providing additional expansion volume to reduce pressure.
5. A relief valve will permit liquid flow from the cell into the overflow tank to relieve pressure.

Problem areas that do require further analysis during the detailed design are the following:

1. Excessive temperature rise at the heater/cell wall junction. This may result in a weakening or distortion of the cell and progressive failure.
2. Excessive touch temperature on the test cell surface. The surface temperature of the test cell may exceed 45°C as a result of stratification or vapor formation in the test cell. Predicting the location of the peak temperature to locate sensors so that the heater can be shut down is difficult, if not impossible. This will need to be resolved during detailed design.

A FHA and the Phase Zero safety review documents for the pool boiling experiment were completed and are given in Appendix B.

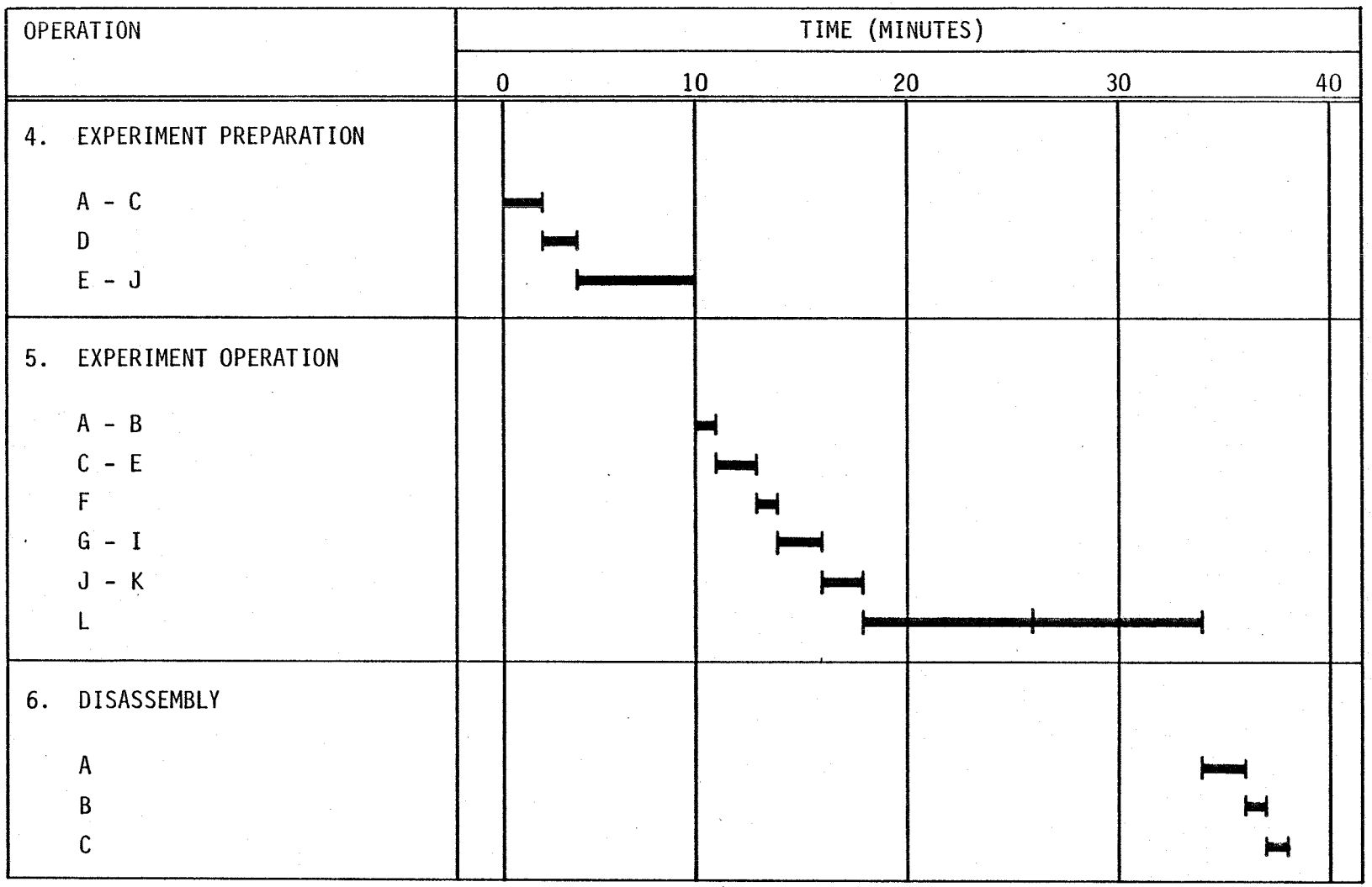

Figure 51 POOL BOILING EXPERIMENT MISSION TIMELINE

4.2.5 Ground Test Requirements. The ground test requirements for the pool boiling experiment were defined. As was the case for the liquid reorientation experiment, ground testing was divided into: (1) development (Table XLII), (2) component acceptance testing (Table XLIII), (3) qualification testing (Table XLIV), and (4) end item acceptance testing (Table XLV). These test areas are further divided into functional, environmental and performance testing.

TABLE XLII POOL BOILING EXPERIMENT DEVELOPMENT TESTING

Component	Test	Description
Functional Tests		
Heaters	Temperature Calibration	Electrically power heaters in appropriate fluid and calibrate temperature sensors.
Environmental Tests		
Test Cells and Heaters	End Plate Tensile	Ultimate load required to cause end plate-cell joint failure.
	Shock/Vibration	Subject cells filled with fluid to handling, prelaunch, launch, re-entry and post-landing shock and vibration loads.
Test Stand	Support Tear-out	Ultimate load to cause support bracket failure.
Performance Tests		
Test Cells and Heaters	Burnout	Electrically power heater in appropriate fluid to burnout conditions.
DACS	Experiment Control Program	Power DACS and check the logic of the experiment control program, including all abort modes.

TABLE XLIII POOL BOILING EXPERIMENT
COMPONENT ACCEPTANCE TESTING

Component	Test	Description
Functional Tests		
Test Cells	Proof Pressure (Internal)	Subject cells to a pressure of at least two times the operating pressure as per Reference 14.
	Proof Pressure (External)	Pressurize the cells surroundings to a minimum of two times the maximum surroundings pressure as per Reference 14.
	Leak Check	Determine if the cells leak.
Overflow Tanks	Acceptance	Same as test cells above.
Heaters	Electrical	Perform electrical check on heaters and temperature sensors.
	Resistance	Check resistance of heater assembly.
	Dielectric Strength	Check dielectric strength of heater insulator.
Valves	Leak Test	Perform an external and internal leak test of valves at maximum operating and maximum differential pressure.
Test Stand	Assembly/Operation	Assemble and check operation of stand.
Accelerometer	Operational	Perform electrical check on accelerometer unit. Check output for each axis and temperature readout.
Camera	Operational	Check operation of lens, film advance, etc.
Batteries	Electrical	Check output of batteries, temperature rise during discharge cycle.
DACS	Electrical	Perform electrical check on DACS.
Pressure Transducers	Calibration	Check calibration of pressure transducers on zero and full scale output.
Temperature Sensors	Calibration	Check calibration of temperature sensors at ice bath ambient and boiling water conditions.

TABLE XLIV POOL BOILING EXPERIMENT QUALIFICATION TESTING

Component	Test	Description
Functional Tests		
Test Cells	Burst	Pressurize inside of cells to design burst pressure, then continue pressurizing cell rupture.
	Collapse	Pressurize cell surroundings to design collapse pressure, then continue pressurizing to cell collapse.
Overflow Tank	Qualification	Same as above.
Experiment Package	Proof Pressure (Internal)	Pressurize package to two times maximum operating pressure as per Reference 14.
	Proof Pressure (External)	Pressurize cell package surroundings to two times maximum surroundings pressure as per Reference 14.
	Leak Check	Determine if experiment cell package leaks.
Environmental Tests		
Experiment Packages	Shock/Vibration	Subject assembled experiment packages, filled with the test fluids, to handling, prelaunch, launch, re-entry, and post-landing shock and vibration loads.
	Acceleration	Subject assembled experiment packages, filled with the test fluids, to anticipated acceleration loads.
	Pack and Ship	Pack and ship simulated package loads in instrumented container to buyer.
Test Stand	Shock/Vibration	Subject test stand to handling and on-orbit shock and vibration loads.
	Acceleration	Subject test stand to the anticipated on-orbit loads.

TABLE XLIV POOL BOILING EXPERIMENT
QUALIFICATION TESTING (Concluded)

Component	Test	Description
Performance Tests		
Experiment Packages	Mission Simulation	Perform mission simulation test on the experiment packages, including evacuation, fill, setup in the test stand, boiling, disassembly and storage.

TABLE XLV POOL BOILING EXPERIMENT -
END ITEM ACCEPTANCE TESTING

Assembly	Test	Description
Experiment Package	Proof Pressure (Internal)	Pressurize package to 1.5 times the maximum operating pressure per Reference 14.
	Proof Pressure (External)	Pressurize surroundings to 1.5 times maximum surroundings pressure.
	Electrical	Perform electrical check on assembled heaters.
DACS/Power Supply Assembly	Electrical/ Diagnostics	Perform electrical of DACS run fully configured system through diagnostic check.

4.3 Flow Boiling Experiment. The preliminary design of the flow boiling experiment is given in the following paragraphs. Paragraph 4.3.1 describes the design, including flow and electrical schematics for the flow boiling experiment. Paragraph 4.3.2 details the analyses supporting the design of the experiment and includes detailed analyses of the test section, condenser, flow loop pressure drop and pump requirements, and the DACS requirements. The mission analyses, including the experiment operating procedure, and the mission timeline are given in Paragraph 4.3.3, and the flow boiling safety analysis is given in Paragraph 4.3.4. Finally, the ground testing requirements for the flow boiling experiment are given in Paragraph 4.3.5.

4.3.1 Flow Boiling Preliminary Design. Figures 52, 53 and 54 show the flow schematic, locker layout and middeck installation of the flow boiling experiment. Shown in Figure 53 are all the major components of the Freon and cooling water flow loop, including the test section quality meter, condenser, pumps, and Freon accumulator. The flow boiling experiment condenser is designed to connect to Orbiter cooling water via flex lines to middeck quick disconnects that are available on the 099 and 102 Orbiters (References 8 and 25). The Freon flows through the test section in the $\pm$Y direction of the Orbiter. The tilt in its orientation is provided to align the upper face of the section with the Orbiter RCS +X thrust vector. The flow will be photographed from above the test section, where the flow boiling DACS locker is to be located. The fluid temperature instrumentation of the quartz tube test section will be provided by the axial wire support which is strung through the center of the tube (shown in Figure 55). The square outer sheath of the test section is fabricated from acrylic, and serves as an insulation system for the test section as well as a protective cover and secondary fluid containment system.

The wall temperature of the test section is measured by monitoring the resistance of test section heaters. Twenty individual vacuum deposited thin film heaters form the heat source and provide uniform test section heating, as detailed in Figure 56. Since only five wall and fluid temperature measurements are required, only every fourth heater will contain resistance measurement capability.

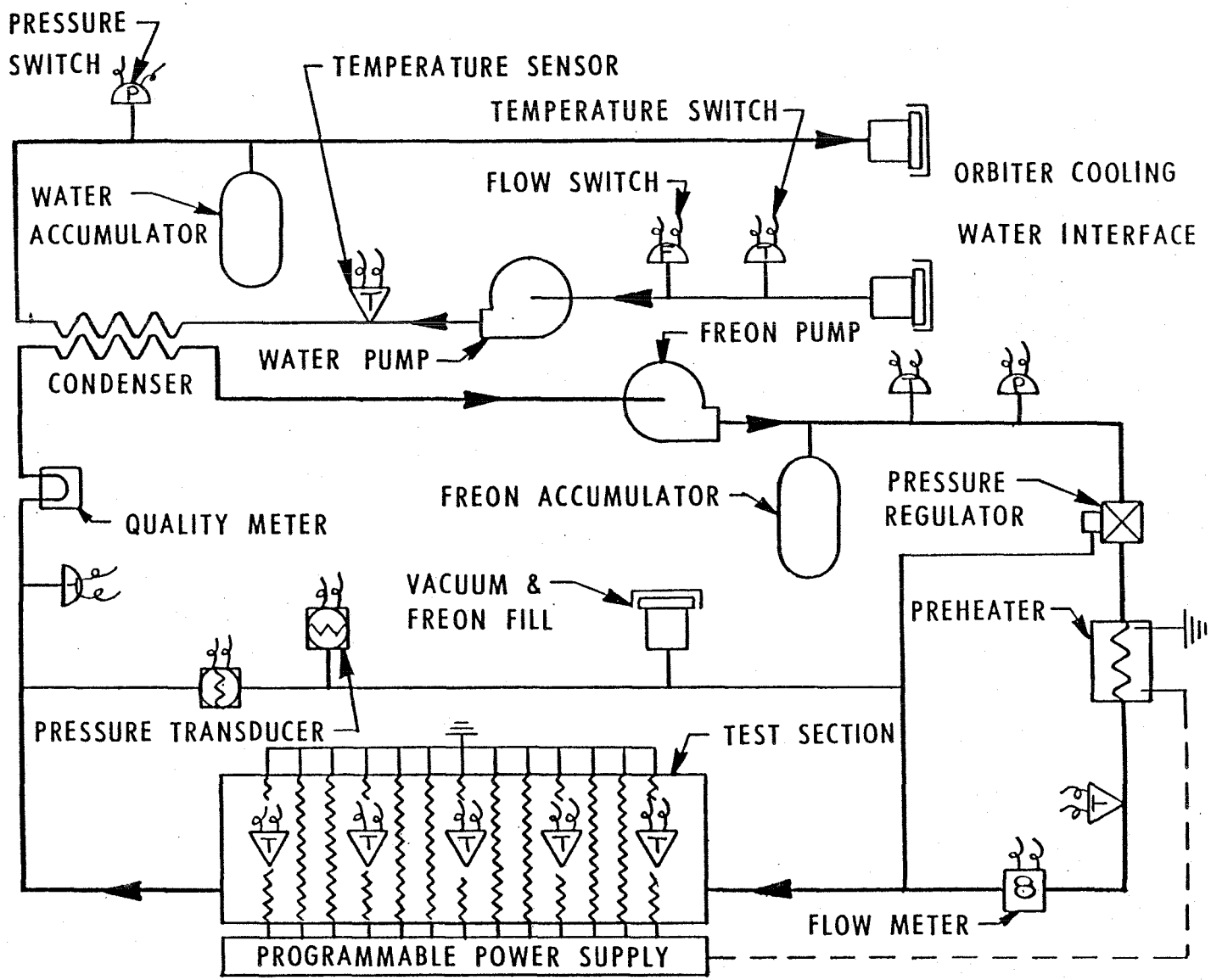

Figure 52 FLOW BOILING EXPERIMENT PRELIMINARY DESIGN FLOW SCHEMATIC

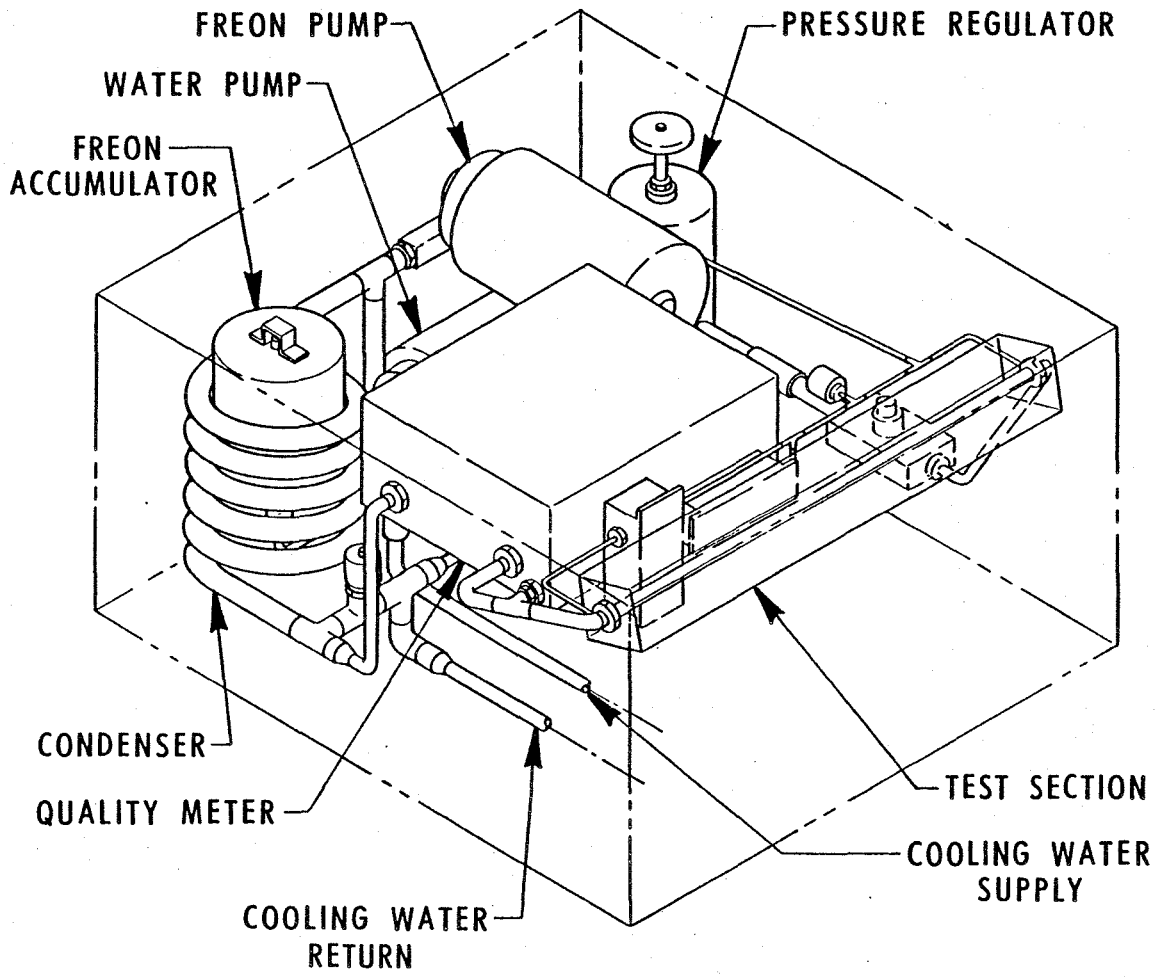

Figure 53 FLOW BOILING EXPERIMENT LOCKER LAYOUT

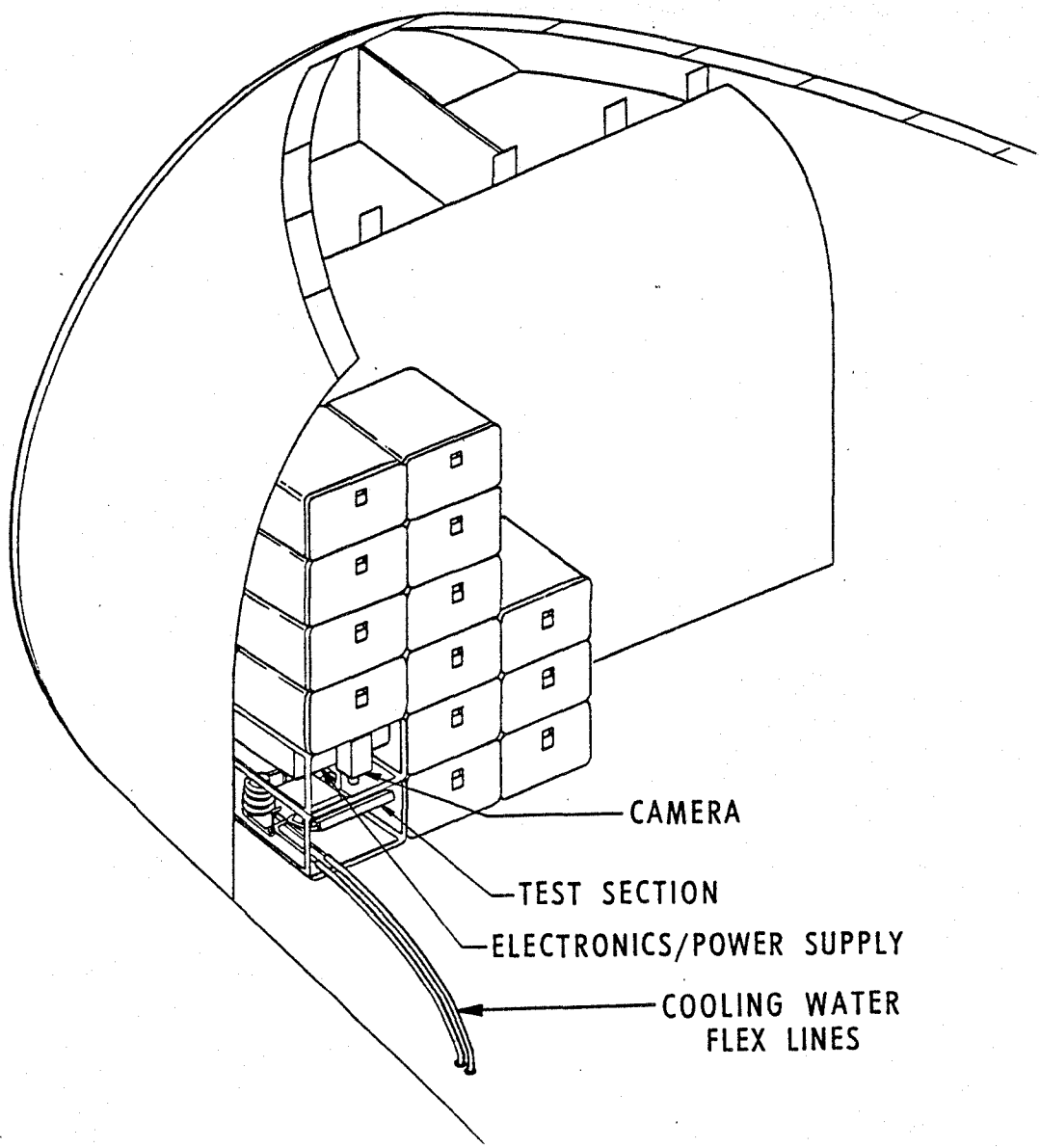

Figure 54 FLOW BOILING EXPERIMENT INSTALLATION

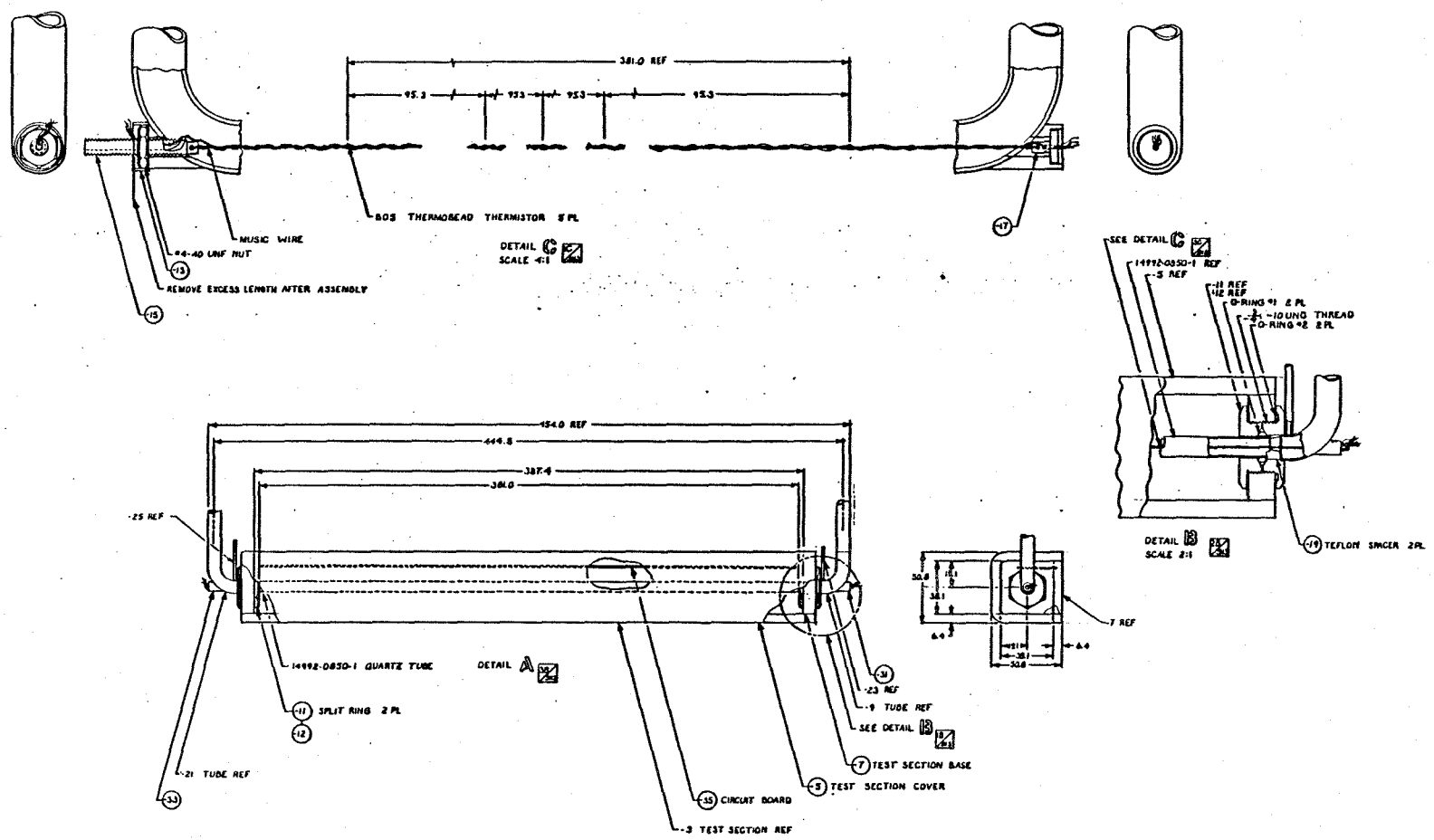

Figure 55 FLOW BOILING EXPERIMENT TEST SECTION DETAILS

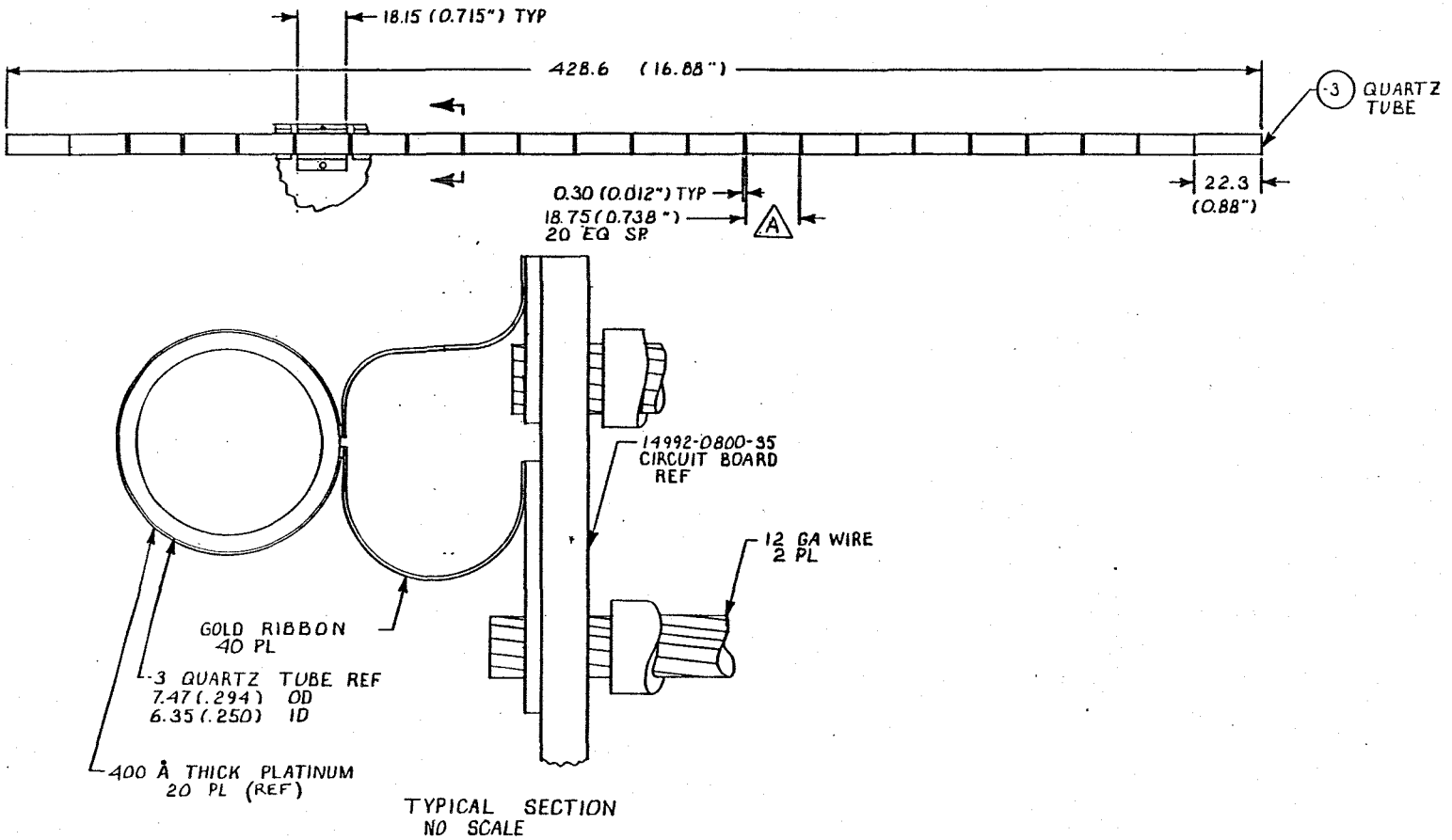

Figure 56 FLOW BOILING EXPERIMENT TEST SECTION HEATER DETAILS

The electrical schematic is shown in Figure 57. The DACS will control the Freon pump speed to produce the required inlet flow rate to the test section, and will control the cooling water pump speed and preheater power to produce the desired inlet temperature. The astronaut/mission specialist will adjust the inlet pressure regulator to achieve the required inlet pressure. The DACS will also control the power provided to the individual test section heaters through the programmable power supply. Due to the uncertainty in the heater film deposition thickness, each heater will be individually calibrated and controlled.

4.3.2 Flow Boiling Experiment Design Analyses. Detailed design analyses were made of the test section's structural, thermal and pressure drop characteristics, the condenser thermal and pressure drop characteristics and of the DACS hardware data quantity and rate requirements.

Test Section Minimum Wall Thickness. The minimum test section wall thickness required to meet the bending load was determined. The bending load is determined from the 5g quasi-static load on the test section when it is filled with Freon 11. The load per unit length, w is:

$$w = \frac{5\rho_f \pi R_o^2 g}{g_c} \qquad \text{(Equation 85)}$$

The equation for the bending stress, σ, is

$$\sigma = \frac{MR_o}{I} = \frac{wL^2 R_o}{12\pi R_o^3 \delta} \qquad \text{(Equation 86)}$$

Combining the two above equations and solving for the wall thickness yields:

$$\delta = \frac{5\rho_f L^2 g}{12\sigma g_c} \qquad \text{(Equation 87)}$$

Setting σ = 3.5 mPa which is for quartz at a factor of safety of 10, L = 0.3814 m and ρ_f = 1488 kg/m^3:

$$\delta = 0.253 \text{ mm} \qquad \text{(Equation 88)}$$

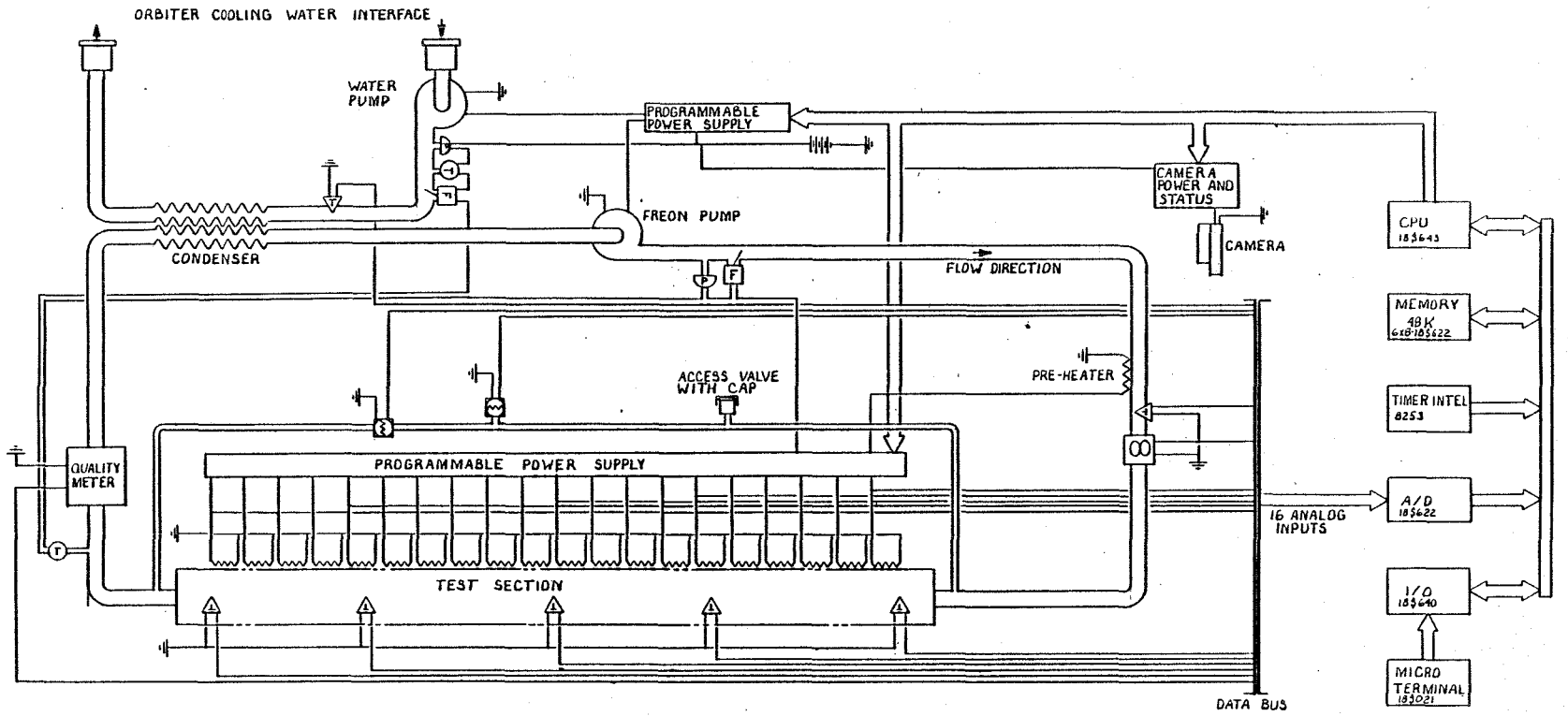

Figure 57 FLOW BOILING EXPERIMENT ELECTRICAL SCHEMATIC

Test Section Heat Transfer Coefficient. Two-phase heat transfer coefficients for the test section in normal gravity were determined from a correlation developed by Chen (Reference 26). The correlation relies upon the superposition principle. That is, the two-phase heat transfer coefficient is the summation of the contributions of boiling and forced convection:

$$h_{TP} = h_b + h_c \qquad \text{(Equation 89)}$$

The forced convection contribution is determined from a modified Dittus-Boelter equation:

$$h_c = 0.023 \left[\frac{G(1-x)D}{\mu_f}\right]^{0.8} \left[\frac{\mu_f C_{pf}}{k_f}\right]^{0.4} \left(\frac{k_f}{D}\right) (F) \qquad \text{(Equation 90)}$$

where F is a function only of the Lockhart-Martinelli parameter, X_{tt}:

$$F = f(X_{tt}). \qquad \text{(Equation 91)}$$

Subsequently:

$$X_{tt} = \left(\frac{1-x}{x}\right)^{0.9} \left(\frac{\rho_g}{\rho_f}\right)^{0.5} \left(\frac{\mu_f}{\mu_g}\right)^{0.1} \qquad \text{(Equation 92)}$$

Figure 7.5 of Reference 26 gives F as a function of X_{tt}.

The boiling contribution is determined from

$$h_b = 0.00122 \left[\frac{k_f^{0.79} C_{pf}^{0.45} \rho_f^{0.49}}{\sigma^{0.5} \mu_f^{0.29} h_{fg}^{0.24} \rho_g^{0.24}}\right] \Delta T_{SAT}^{0.24} \Delta P_{SAT}^{0.75} (S) \qquad \text{(Equation 93)}$$

where S is a function only of the two-phase Reynolds number:

$$S = F(Re_{TP}) \qquad \text{(Equation 94)}$$

and

$$Re_{TP} = \frac{G(1-x)D}{\mu_f} (F)^{1.25} \qquad \text{(Equation 95)}$$

Figure 7.6 of Reference 26 gives S as a function of Re_{TP}.

Table XLVI gives the results of using the above equations for calculating the Freon 11 h_{TP}, and $\dot{q}$, the total heat flux, for G = 10 kg/m^2-s and a quality, x = 0.01. Table XLVII gives similar results for x = 0.6.

TABLE XLVI FREON 11 TWO-PHASE HEAT TRANSFER
FOR G = 10 kg/m^2-s AND x = 0.01

T_{SAT} (^oC)	P_{SAT} (Pa)	h_b (W/m^2-^oC)	h_c (W/m^2-^oC)	h_{TP} (W/m^2-^oC)	$\dot{q}$ W/m^2)
0.455	1520	707	31	738	336
1.200	4053	1862	31	1893	2272
1.930	6586	3004	31	3035	5857

TABLE XLVII FREON 11 TWO-PHASE HEAT TRANSFER
FOR G = 10 kg/m^2-s AND x = 0.6

T_{SAT} (^oC)	P_{SAT} (Pa)	h_b (W/m^2-^oC)	h_c (W/m^2-^oC)	h_{TP} (W/m^2-^oC)	$\dot{q}$ W/m^2)
0.455	1520	650	270	920	419
1.200	4053	1713	270	1983	2380
1.930	6586	2763	270	3033	5854

Tables XLVI and XLVII show the clear dominance of the boiling contribution on the overall two-phase heat transfer coefficient for normal gravity, an expected result at these low mass velocities.

The effect of gravity on h_c, the convection contribution, is expected to be small. The boiling contribution, h_b, to overall two-phase heat transfer may be significantly affected by low gravity. To estimate these effects, the correlation for film boiling given by Bakhru and Lienhard (Reference 2) was used to determine h_b in Equation 89. Thus,

$$h_b = \left(\frac{k_g}{D}\right) 0.7 \left[\frac{\rho_g(\rho_f-\rho_g)\, h^*_{fg}\, gD^3}{\mu_g k_g}\right]^{1/4} \left[\frac{\sigma}{D^2 g\,(\rho_f-\rho_g)}\right]^{1/6} \left(\frac{1}{\Delta T}\right)^{1/4} \quad \text{(Equation 96)}$$

Table XLVIII gives values of h_b, h_{TP}, and $\dot{q}$ for x = 0.01 in earth normal gravity using the values of h_b calculated from Equation 96. Values of h_c were determined from Equation 90 for G = 10 kg/m^{2}s. Comparing these values with those given in Table XLVI shows that very similar but lower values of h_{TP} are obtained, indicating that h_{TP} determined by these correlations is conservative for normal gravity.

TABLE XLVIII TWO-PHASE HEAT TRANSFER FOR NORMAL GRAVITY USING h_b CALCULATED FROM EQUATION 96

T (^oC)	h_b (W/m^2 ^oC)	h_c (W/m^2 ^oC)	h_{TP} (W/m^2 ^oC)	$\dot{q}$ (W/m^2)
1	1361	31	1392	1392
2	1144	31	1175	2351
3	1034	31	1065	3195
4	962	31	993	3973

Table XLIX gives values of h_b, h_{TP} and $\dot{q}$ for x = 0.01 and g = $10^{-6} g_o$ (orbiter drag -g). Values for h_c were again determined using Equation 90 for G = 10 kg/m^{2}s. Interpolating Table XLIX for $\dot{q}$ = 15510 W/m^2, h_{TP} = 170 W/m^2-^{o}C. This value of h_{TP} was considered a reasonable minimum upon which to base the preliminary design of the test section.

TABLE XLIX TWO-PHASE HEAT TRANSFER FOR $g/g_o = 10^{-6}$

T (^oC)	h_b (W/m^2 ^oC)	h_c (W/m^2 ^oC)	h_{TP} (W/m^2 ^oC)	$\dot{q}$ (W/m^2)
20	203	31	234	4687
40	171	31	202	8079
60	155	31	186	11130
80	144	31	175	13982
100	136	31	167	16700

Test Section Thermal Mass Requirements. The thermal mass of the flow boiling test section must be small enough so that steady state data can be obtained at the end of a 60 second test.

For a heater system with negligible internal thermal resistance the temperature response may be represented by

$$\frac{dT}{dt} + \frac{h_{TP}A}{\rho CV} T = \frac{Q(t)}{\rho CV} \qquad \text{(Equation 97)}$$

The time constant, τ, for this system is

$$\tau = \frac{\rho CV}{h_{TP}A} \qquad \text{(Equation 98)}$$

which for the hollow tube test section is

$$\tau = \frac{\rho C(D_o^2 - D_i^2)}{4D_i h_{TP}} \qquad \text{(Equation 99)}$$

It was shown in Paragraph 4.2.2 for the pool boiling experiment that if heater power is ramped for 1 τ and then held at a constant value for 2τ, the heater temperature will be within ten percent of its equilibrium temperature. Since the flow boiling test section is directly analogous to the pool boiling heater, the maximum time constant, τ_{max}, to achieve 90 percent of equilibrium heat transfer is 20 seconds. Solving Equation 99 for the outer diameter yields:

$$D_o = \sqrt{\frac{4h_{TP}\tau_{max}}{C} D_i + D_i^2} \qquad \text{(Equation 100)}$$

Inserting $\rho C = 2200$ kJ/m^{3-o}C (quartz), $h_{TP} = 170$ W/m^{2-o}C and $D_i = 6.35$ mm gives $D_o = 8.92$ mm. The maximum wall thickness is:

$$\delta = \frac{D_o - D_i}{2} = 1.29 \text{ mm} \qquad \text{(Equation 101)}$$

Test Section Insulation System. The insulation concept for the flow boiling test section is shown in Figure 58, and consists of an acrylic sheath surrounding the test section. The space between is filled with dry air or nitrogen. Heat is added to the exterior of the quartz tube. The thermal network for this design is also shown in Figure 58. The sheath is assumed to be transparent to infared radiation. If the sheath is assumed to be at the same temperature as the surrounding middeck, then the equation for the heat flow out of the test section, Q_{leak}, is:

$$Q_{leak} = \frac{T_{to} - T_o}{R_g} \qquad \text{(Equation 102)}$$

and

$$R_g = \left[\frac{1}{R_a} + \frac{1}{R_r}\right]^{-1} = \frac{\ln \frac{D_s}{D_o}}{2\pi k_a L + h_r \pi D_o \, L \ln \frac{Ds}{D_o}} \qquad \text{(Equation 103)}$$

The radiation heat transfer coefficient is determined (assuming radiation is to a black body) from:

$$h_r = 4\, \varepsilon_t \sigma (T_{to}^2 + T_o^2)(T_{to} + T_o) \qquad \text{(Equation 104)}$$

The equation for the heat flow into the test section, Q_{fluid}, is:

$$Q_{fluid} = \frac{T_{to} - T_f}{R_f + R_t} \qquad \text{(Equation 105)}$$

where

$$R_f = \frac{1}{h_{TP} \pi D_i L} \qquad \text{(Equation 106)}$$

$$R_t = \frac{\ln \frac{D_o}{D_i}}{2\pi k_t L} \qquad \text{(Equation 107)}$$

Defining, η, a heating efficiency as:

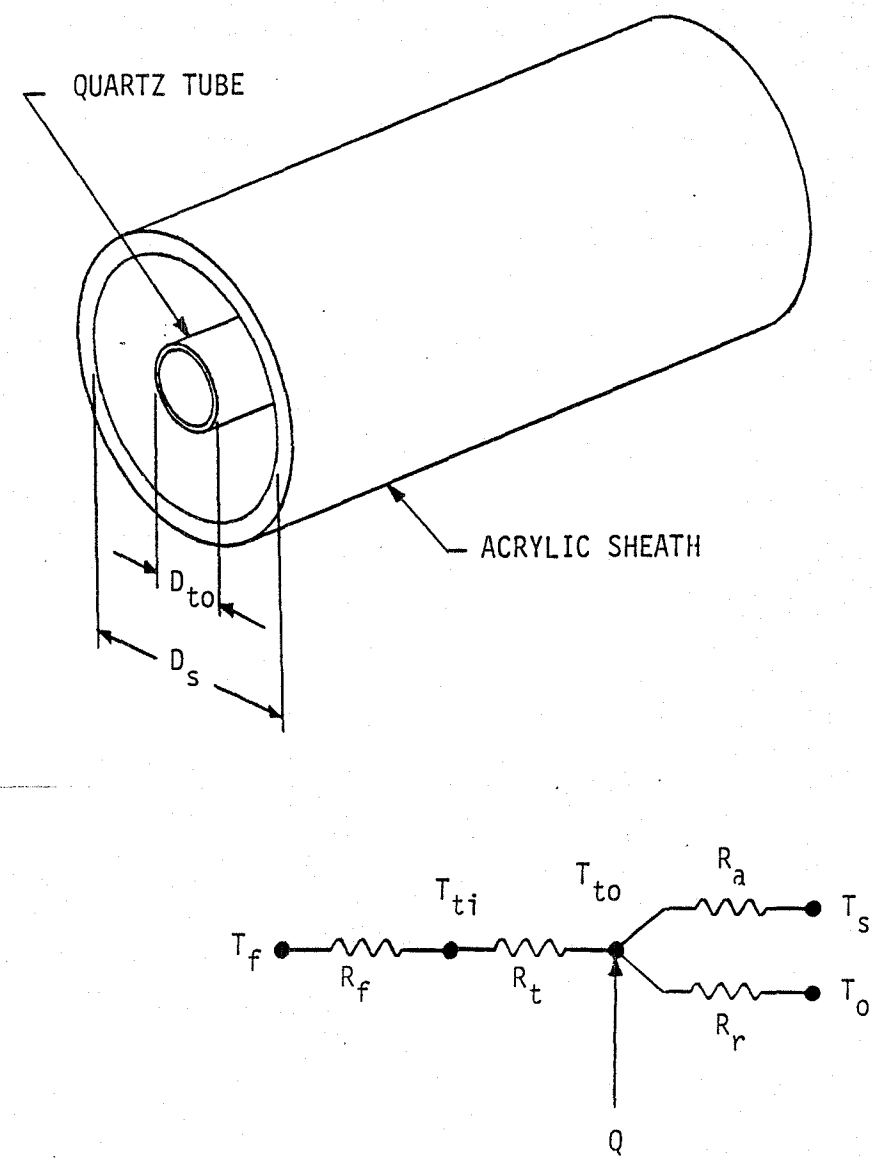

Figure 58 FLOW BOILING TEST SECTION INSULATION SYSTEM DESIGN AND THERMAL NETWORK

$$\eta = \frac{Q_{fluid}}{Q} = 1 - \frac{Q_{leak}}{Q} \qquad \text{(Equation 108)}$$

where Q = total power supplied to test section. For our system the fluid temperature T_f will equal the middeck temperature, T_o. Combining Equations 102, 105 and 108, then yields:

$$\eta = \frac{R_g}{R_f + R_g + R_t} \qquad \text{(Equation 109)}$$

Equation 109 can be used to examine the effect of tube wall thickness on the heating efficiency. Table L gives values for η as a function of tube wall thickness for D_s = 38.1 mm, and h_{TP} = 170 $W/m^2\ ^oC$.

TABLE L HEATING EFFICIENCY AS A FUNCTION OF TUBE WALL THICKNESS

Tube Wall Thickness (mm)	Heating Efficiency
0.00	0.90
0.56	0.87
1.29	0.84

Table L shows that between 10 and 16 percent of the input power will be lost to the middeck. The majority of this heat loss is due to radiation.

The test section wall thickness was selected as 0.56 mm as a compromise between ease of fabrication and the heating efficiency.

Test Section Heating System. Two approaches were considered for the design of the test section heating system: (1) vacuum deposition of a thin film, or (2) spiral wrap of a heater wire.

Vacuum Deposition. Calculations were made to determine the required thickness of a thin film of metal that would serve the dual purpose of a test section heater and electrical

resistance temperature measurement device (RTD). For the thin film to serve as an RTD, circumferential bands with small spaces between will be required, as shown in Figure 59. For one band the heat flux per unit area is:

$$\dot{q} = \frac{\dot{Q}}{A} = \frac{E^2}{\pi D_o w R} \qquad \text{(Equation 110)}$$

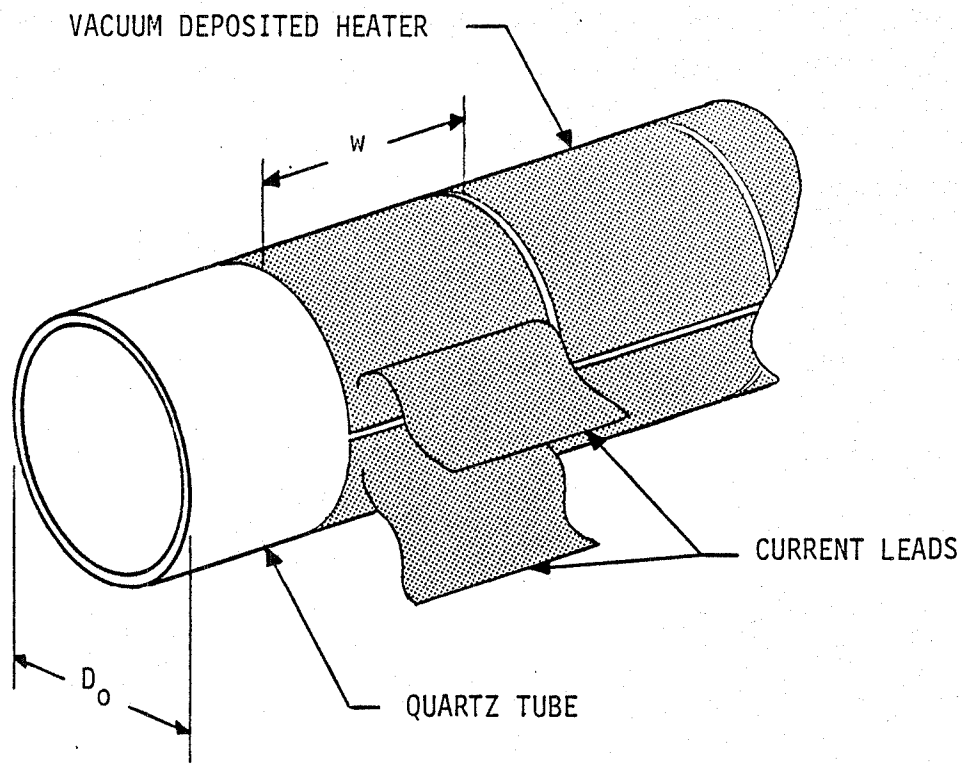

Figure 59 FLOW BOILING VACUUM DEPOSITED HEATER CONCEPT

The resistance, R, of the band can be related to the electrical resistivity of the material, j, and the film thickness, δ:

$$R = \frac{\pi D_o j}{\delta w} \qquad \text{(Equation 111)}$$

Combining Equations 110 and 111 and solving for the voltage yields:

$$E = \sqrt{\frac{\pi^2 D_o^2 j \dot{q}}{\delta}} \qquad \text{(Equation 112)}$$

To determine the voltage for a candidate material, it is necessary to select the film thickness. To allow light to pass through the film, the film should be as thin as possible. This also has the added benefit of increasing the voltage, and consequently reducing the current for a given heat flux. However, since vacuum deposition techniques can only be controlled to $\pm$ 50 Å, the percentage of uncertainty in the film thickness will increase as the average deposition thickness decreases. Selecting δ = 400 Å as the practical minimum film thickness, we used Equation 112 to determine the voltage for several candidate materials. The results are summarized in Table LI. Also shown in Table LI is the current and resistance for an assumed band width w = 19 mm.

TABLE LI VOLTAGE, CURRENT AND RESISTANCE FOR A 400 Å FILM TEST SECTION HEATER

Material	j ($\mu\Omega$-cm)	E (v)	I (a)	R (Ω)
Chromium	12.90	5.25	1.32	3.98
Gold	2.35	2.24	3.09	0.73
Nickel	6.84	3.82	1.81	2.11
Platinum	10.60	4.76	1.46	3.27
Silver	1.59	1.84	3.75	0.49

Table LI shows that, of the materials considered, platinum or chromium because of their lower currents and higher resistances, would be more desirable materials than gold or silver. Of the two, platinum has a better known resistance-versus-temperature curve and therefore was the preferred material for the heater.

Spiral Wrap. Calculations were also made to determine the characteristics of a test section heater consisting of spiral wrap of a heater wire. Figure 60 shows the sketch of the wire wrap design. The heater spacing, w, must allow nearly uniform heating of the tube wall.

$$\dot{q} = h_{TP} (T - T_f) = \text{constant} \qquad \text{(Equation 113)}$$

If h_{TP} and T_f are constant over the distance w (a reasonable assumption for small w) then T must be constant over w. This problem is analogous to a fin with an insulated tip. The variation in wall temperature over w is:

$$\frac{T - T_f}{T_o - T_f} = \frac{\cosh\left\{ m(\frac{w}{2} - x)\right\}}{\cosh \frac{mw}{2}} \qquad \text{(Equation 114)}$$

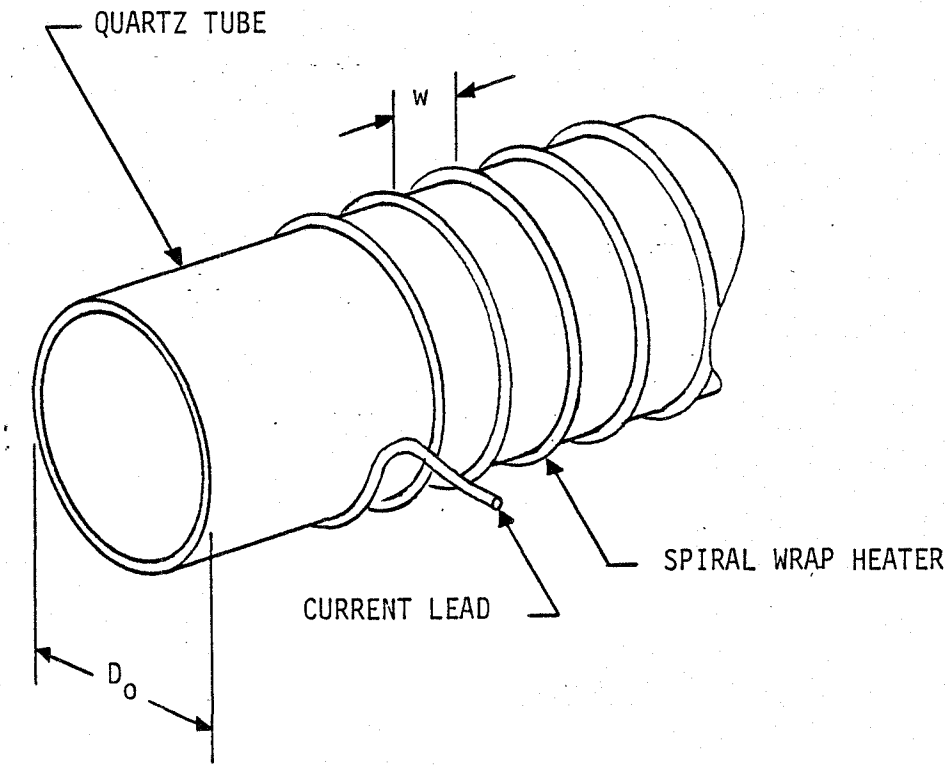

Figure 60 FLOW BOILING SPIRAL WRAP HEATER CONCEPT

The maximum temperature deviation occurs at x = w/2. If an acceptable temperature error limit is defined as $\theta_e = T_o - T_{w/2}$ and $\theta_o = T_o - T_f$ then:

$$\frac{\theta_o - \theta_e}{\theta_o} = \frac{1}{\cosh \frac{mw}{2}} \qquad \text{(Equation 115)}$$

Rearranging and solving for w:

$$w = \frac{2}{m} \cosh^{-1} \left\{ \frac{\theta_o}{\theta_o - \theta_e} \right\} \qquad \text{(Equation 116)}$$

θ_o is related to the required heat flux by:

$$\theta_o = \frac{\dot{q}}{h_{TP}\, \eta_f} \qquad \text{(Equation 117)}$$

where η_f the fin efficiency is:

$$\eta_f = \frac{\tanh (mw/2)}{mw/2} \qquad \text{(Equation 118)}$$

For a given acceptable temperature deviation (θ_e), heat transfer coefficient (h_{TP}) and heat flux ($\dot{q}$), Equations 116, 117 and 118 can be simultaneously solved to yield w. This was done for $\theta_e = 0.5^{\circ}C$, $\dot{q} = 15510\ w/m^2$ and minimum and maximum h_{TP} of 170 and 9000 $W/m^2\text{-}^{\circ}C$, respectively. For the minimum h_{TP} case, the required spacing is w = 0.35 mm; for the maximum h_{TP} case, w = 0.36 mm.

Since the required spacing, w, is quite small, the heater wire diameters which will allow light to pass through must be very small. The relationship between wire diameter and voltage is determined by relating the voltage for one complete turn to the heat flux spacing and the resistance:

$$E = \sqrt{\frac{\dot{q}}{R \pi D_i w}} \qquad \text{(Equation 119)}$$

The resistance for one turn is related to the wire diameter by

$$R = \frac{4\, D_o j}{D_w^2} \qquad \text{(Equation 120)}$$

Combining Equations 119 and 120 and solving for the voltage yields:

$$E = \sqrt{\frac{4\dot{q}\ \pi D_o D_i j w}{D_w^2}} \qquad \text{(Equation 121)}$$

If the spiral wrap heaters are made from platinum so that they can be used as an RTD in addition to a heater, then it will be necessary to design several multiple turn heaters axially along the test section. Table LII summarizes the number of heaters and the number of turns in each heater made from platinum versus wire diameter, where it was assumed the voltage to each heater was 28 volts DC. Also shown is percent of the field of view obstructed.

TABLE LII PLATINUM SPIRAL HEATER DESIGN REQUIREMENTS

Wire Diameter (mm)	Number of Turns Per Heater	Number of Heaters	View Obstruction (%)
0.0127	19	57	3.6
0.0254	38	28	7.2
0.0508	76	14	14.5

In actuality the spiral wrap heater design would probably have to be made by vacuum or electro-depositing platinum on the tube, followed by etching the spiral pattern on the tube. This is due to the difficulty in handling and attaching these extremely small wires to the quartz tube.

Preferred Design Approach. In conversations with several potential fabricators of the two heater designs, we found that the thin film vacuum deposition approach was a more workable design than the spiral wrap design. Therefore this design was selected as the preferred approach.

Test Section Pressure Drop. A computer algorithm was used to determine the flow boiling test section pressure drop. The equation to determine the pressure derivative for separated flow is (from Reference 26):

$$-\frac{dP}{dz} = \frac{\frac{2f_f G^2(1-x)^2 v_f}{D}\phi_f^2 + G^2\frac{dx}{dz}\left[\left\{\frac{2xv_g}{\alpha} - \frac{2(1-x)}{(1-\alpha)}v_f\right\} + \frac{d\alpha}{dx}\left\{\frac{(1-x)^2}{(1-\alpha)^2}v_f - \frac{x^2 v_g}{\alpha^2}\right\}\right]}{1 + G^2\left[\frac{x^2}{\alpha}\left(\frac{dv_g}{dP}\right) + \frac{d\alpha}{dP}\left\{\frac{(1-x)^2}{(1-\alpha)^2}v_f - \frac{x^2 v_g}{\alpha^2}\right\}\right]} \qquad \text{(Equation 122)}$$

For most systems, including ours, the term $d\alpha/dP\ \{\cdot\}$ in the denominator can be assumed to be zero. Thus the Equation simplifies to:

$$-\frac{dP}{dz} = \frac{\frac{2f_f G^2(1-x)^2 v_f}{D}\phi_f^2 + G^2\frac{dx}{dz}\left[\left\{\frac{2x_g}{\alpha} - \frac{2(1-x)}{(1-\alpha)}v_f\right\} + \frac{d\alpha}{dx}\left\{\frac{(1-x)^2}{(1-\alpha)^2}v_f - \frac{x^2 v_g}{\alpha^2}\right\}\right]}{1 + G^2\left\{\left(\frac{x^2}{\alpha}\right)\left(\frac{dv_g}{dP}\right)\right\}} \qquad \text{(Equation 123)}$$

For each increment in position (i.e., Δz), the change in quality, Δx, is determined by:

$$\Delta x = \frac{4\dot{q}}{GDh_{fg}}\Delta z \qquad \text{(Equation 124)}$$

It follows that $dx/dz = 4\dot{q}/GDh_{fg}$

The friction factors for liquid, f_f, and vapor, f_g, are determined from:

$$f = 0.079\,(Re)^{-0.25} \qquad \text{(Equation 125)}$$

where

$$Re_f = \frac{G(1-x)D}{\mu_f} \quad \text{(liquid Reynolds number)} \qquad \text{(Equation 126)}$$

and

$$Re_g = \frac{GxD}{\mu_g} \quad \text{(gas Reynolds number)} \qquad \text{(Equation 127)}$$

ϕ_f^2, the two-phase multiplier, is calculated from:

$$\phi_f^2 = 1 + \frac{20}{X} + \frac{1}{X^2} \qquad \text{(Equation 128)}$$

where X, the Lockhart - Martinelli parameter is calculated from:

$$X^2 = \frac{dP/dz/_f}{dP/dz/g} = \frac{f_f (1-x)^2 v_f}{f_g x^2 v_g} \qquad \text{(Equation 129)}$$

The void fraction, α, is calculated from (Reference 26):

$$\alpha = 1 - \frac{1}{\phi_f} \qquad \text{(Equation 130)}$$

and $d\alpha/dx$ is approximated by $\Delta\alpha/\Delta x$. Finally, dv_g/dP is approximated by $\Delta v_g/\Delta P$.

The results of the computer calculations for a mass velocity, G = 640 kg/m^2-s, the heat flux, q = 15510 W/m^2, and inlet quality, x = -0.011, are given in Figure 61. Shown in the figure is the fluid quality, overall pressure, overall pressure derivative, and also the pressure and pressure derivative due to the friction alone, all as a function of position along the test section. As can be seen from the figure, the overall pressure drop through the test section is 0.0152 atm (1.54 kPa, 0.223 psi). Since this is for the maximum test section flow rate and heat flux condition, the pressure drop for a lower flow rate or heat flux will always be less than 0.0152 atm.

Condenser Thermal Analysis. The objective of the condenser thermal analysis was to determine the overall heat transfer coefficient. Heat transfer coefficients were determined for the two-phase Freon 11 and water sides for the concentric tube heat exchanger design given in Figure 62. The Freon side coefficient for two-phase were determined at this minimum test loop flow rate of 3.167 x 10^{-4} kg/sec (10 kg/m^{2}s through the test section from equations developed by Akers et al., and given in Reference 27.

$$\frac{h_{TP}D}{k_L} = 13.8\ Pr_f^{1/3} \left[\frac{h_{fg}}{C_{P_f}\Delta T}\right]^{1/6} \left[\frac{DG_g}{\mu_f}\left(\frac{\rho_f}{\rho_g}\right)1/2\right]^{1/5} \qquad \text{(Equation 131)}$$

For the water side of the condenser at a flow rate of 0.0265 kg/s, heat transfer coefficients were determined from the Dittus-Boelter equation:

MASS VELOCITY..... 640.00 KG/M**2-S
TUBE DIAMETER..... 6.35 MM
HEAT FLUX..... 15510.00 W/M**2

POSITION (MM)	QUALITY	PRESSURE (ATM)	DPDZ (ATM/M)	FRICTIONAL PRESSURE (ATM)	DPDZF (ATM/M)
0.0	-0.0110	0.9100	-0.007	0.9100	-0.007
15.2560	-0.0097	0.9099	-0.007	0.9099	-0.007
30.5120	-0.0084	0.9098	-0.007	0.9098	-0.007
45.7680	-0.0071	0.9097	-0.007	0.9097	-0.007
61.0240	-0.0059	0.9096	-0.007	0.9096	-0.007
76.2800	-0.0046	0.9095	-0.007	0.9095	-0.007
91.5360	-0.0033	0.9094	-0.007	0.9094	-0.007
106.7920	-0.0020	0.9093	-0.007	0.9093	-0.007
122.0480	-0.0007	0.9092	-0.007	0.9092	-0.007
137.3040	0.0006	0.9083	-0.076	0.9091	-0.011
152.5600	0.0019	0.9074	-0.040	0.9089	-0.014
167.8160	0.0031	0.9069	-0.034	0.9087	-0.016
183.0720	0.0044	0.9063	-0.045	0.9084	-0.018
198.3280	0.0057	0.9056	-0.045	0.9081	-0.021
213.5840	0.0070	0.9049	-0.046	0.9078	-0.024
228.8400	0.0083	0.9042	-0.048	0.9074	-0.027
244.0960	0.0096	0.9035	-0.050	0.9070	-0.029
259.3520	0.0108	0.9027	-0.051	0.9065	-0.032
274.6080	0.0121	0.9019	-0.053	0.9060	-0.035
289.8640	0.0134	0.9011	-0.055	0.9055	-0.038
305.1200	0.0147	0.9002	-0.057	0.9049	-0.040
320.3760	0.0160	0.8994	-0.060	0.9043	-0.043
335.6320	0.0173	0.8984	-0.062	0.9036	-0.045
350.8880	0.0186	0.8975	-0.064	0.9029	-0.048
366.1440	0.0198	0.8965	-0.066	0.9021	-0.051
381.4000	0.0211	0.8955	-0.068	0.9013	-0.053

Figure 61 FLOW BOILING TEST SECTION PRESSURE VERSUS POSITION

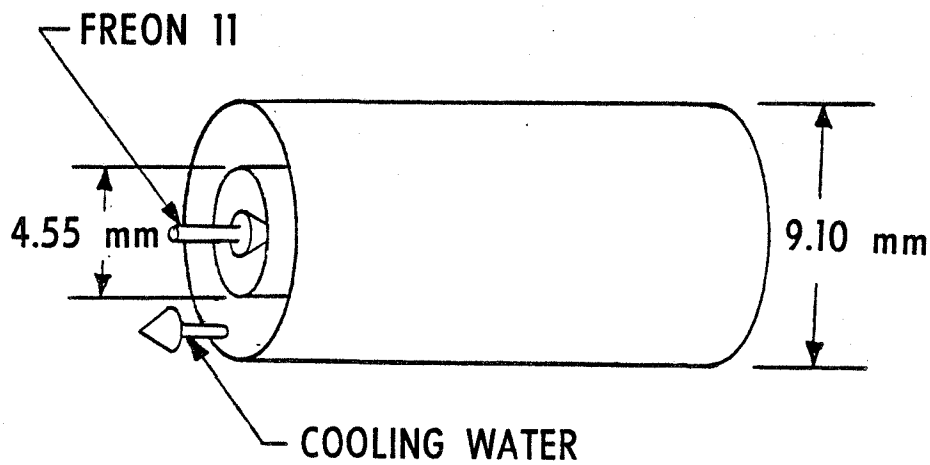

Figure 62 CONCENTRIC TUBE CONDENSER CONCEPTUAL DESIGN

$$\frac{hD_h}{k_L} = 0.023\ Re_L^{0.8} Pr_L^{0.3} \qquad \text{(Equation 132)}$$

For the Freon side of the condenser in the subcooled liquid region, the flow is laminar. The heat transfer coefficient was calculated from Reference 28:

$$\frac{h_{1\phi}D_h}{k_L} = 3.66 \qquad \text{(Equation 133)}$$

Overall heat transfer coefficients for the two-phase and single-phase sections of the condenser were determined from:

$$U_{TP} = \left(\frac{1}{h_{TP}} + \frac{1}{h_w}\right)^{-1} = 1450\ \frac{W}{m^{2o}C} \qquad \text{(Equation 134)}$$

$$U_{1\phi} = \left(\frac{1}{h_{1\phi}} + \frac{1}{h_w}\right)^{-1} = 70\ \frac{W}{m^{2o}C} \qquad \text{(Equation 135)}$$

The total amount of heat to be removed in the two-phase section, Q_{TP}, was assumed to be 118 watts, the maximum heater power available. To provide sufficient subcooling, 5 watts, $Q_{1\phi}$, should be removed from the Freon in the single-phase section. The required heat transfer area was calculated.

$$A_{TP} = \frac{Q_{TP}}{U_{TP}\ \Delta T_{LMTP}} = 8.144 \times 10^{-3} m^2 \qquad \text{(Equation 136)}$$

$$A_{1\phi} = \frac{Q_{1\phi}}{U_{1\phi}\ \Delta T_{LM1\phi}} = 8.977 \times 10^{-3} m^2 \qquad \text{(Equation 137)}$$

$$A = A_{TP} + A_{1\phi} = 0.01712\ m^2 \qquad \text{(Equation 138)}$$

Where ΔT_{LMTP} and $\Delta T_{LM1\phi}$ are the log mean temperature differences for the two-phase and single-phase sections of the condenser, respectively, and were $10^{o}C$ and $8^{o}C$, respectively. These temperature differences are relatively conservative since test loop saturation temperature will be in the range of 22 to $25^{o}C$ while cooling water

temperature can range from 10 to 15°C (References 23 and 7). The total length of the condenser was determined from

$$L = \frac{A}{\pi D} = 1.20 \text{ m} \qquad \text{(Equation 139)}$$

Condenser Pressure Drop. The pressure drop through the condenser was determined for all four flow boiling flow rates at the corresponding maximum inlet quality. The pressure drop computer algorithm (Equations 122 - 130) were used to calculate the pressure drop through the condenser. The heat flux along the condenser length was assumed to be constant at $q = U_{TP}\ \Delta T_{LMTP} = -14490\ W/m^2$. The results are given in Figures 63, 64, 65 and 66. The maximum pressure drop occurs at the maximum mass velocity ($G = 1248\ kg/m^2\text{-s}$), an expected result. If it is assumed that none of the vapor velocity pressure is recovered, then the maximum pressure drop is 0.099 atm (10.0 kPa, 1.46 psi).

System Pressure Drop. The pressure drop through the remaining components in the Freon loop was calculated at the maximum loop flow rate. The pressure drop through the quality meter was calculated from:

$$\Delta P = 3.306 \times 10^7\ \dot{m}^{1.75} \qquad \text{(Equation 140)}$$

where ΔP the pressure drop through the quality meter in Pa and in the flow rate in kg/s. Equation 140 is based on the equation for the quality meter pressure drop given in the manufacturer's literature:

$$\Delta P = 0.026\ \dot{m}^{1.75} \qquad \text{(Equation 141)}$$

where ΔP in psi and $\dot{m}$ in lbm/min for liquid water flow. The constant in Equation 140 is derived from the constant in Equation 141 by multiplying by the ratio of the fluid densities, the ratio of the fluid viscosities to the one-fourth power, and the dimensional constants.

The pressure drop in the remaining loop plumbing was based on the equivalent length of pipe. Pressure drop was determined from:

MASS VELOCITY..... 1248.00 KG/M**2-S
TUBE DIAMETER..... 4.55 MM
HEAT FLUX..... -14490.00 W/M**2

POSITION (MM)	QUALITY	PRESSURE (ATM)	DPDZ (ATM/M)	FRICTIONAL PRESSURE (ATM)	DPDZF (ATM/M)
0.0	0.0220	0.8800	-0.236	0.8800	-0.275
48.0000	0.0193	0.8691	-0.211	0.8673	-0.249
96.0000	0.0166	0.8594	-0.183	0.8558	-0.223
144.0000	0.0139	0.8512	-0.153	0.8456	-0.196
192.0000	0.0112	0.8444	-0.122	0.8367	-0.168
240.0000	0.0085	0.8392	-0.088	0.8292	-0.138
288.0000	0.0058	0.8356	-0.050	0.8231	-0.100
336.0000	0.0031	0.8340	-0.006	0.8184	-0.076
384.0000	0.0004	0.8336	0.042	0.8152	-0.049
432.0000	-0.0023	0.8330	-0.033	0.8134	-0.033
480.0000	-0.0049	0.8314	-0.033	0.8119	-0.033
528.0000	-0.0076	0.8298	-0.033	0.8103	-0.033
576.0000	-0.0103	0.8282	-0.033	0.8087	-0.033
624.0000	-0.0130	0.8266	-0.033	0.8071	-0.033
672.0000	-0.0157	0.8250	-0.033	0.8055	-0.033
720.0000	-0.0184	0.8234	-0.033	0.8039	-0.033
768.0000	-0.0211	0.8218	-0.033	0.8023	-0.033
816.0000	-0.0238	0.8202	-0.033	0.8007	-0.033
864.0000	-0.0265	0.8186	-0.033	0.7991	-0.033
912.0000	-0.0292	0.8170	-0.033	0.7975	-0.033
960.0000	-0.0318	0.8154	-0.033	0.7959	-0.033
1008.0000	-0.0345	0.8138	-0.033	0.7943	-0.033
1056.0000	-0.0372	0.8122	-0.033	0.7927	-0.033
1104.0000	-0.0399	0.8106	-0.033	0.7911	-0.033
1152.0000	-0.0426	0.8090	-0.033	0.7895	-0.033
1200.0000	-0.0453	0.8074	-0.033	0.7879	-0.033

Figure 63 FLOW BOILING CONDENSER PRESSURE VERSUS POSITION FOR G = 1248 kg/m^2-s

MASS VELOCITY..... 156.00 KG/M**2-S
TUBE DIAMETER..... 4.55 MM
HEAT FLUX..... -14490.00 W/M**2

POSITION (MM)	QUALITY	PRESSURE (ATM)	DPDZ (ATM/M)	FRICTIONAL PRESSURE (ATM)	DPDZF (ATM/M)
0.0	0.2550	0.8800	-0.041	0.8800	-0.052
48.0000	0.2334	0.8781	-0.038	0.8776	-0.049
96.0000	0.2118	0.8763	-0.035	0.8753	-0.045
144.0000	0.1902	0.8747	-0.032	0.8732	-0.040
192.0000	0.1686	0.8732	-0.028	0.8714	-0.036
240.0000	0.1470	0.8719	-0.025	0.8697	-0.032
288.0000	0.1254	0.8708	-0.021	0.8682	-0.028
336.0000	0.1038	0.8698	-0.018	0.8670	-0.024
384.0000	0.0822	0.8690	-0.014	0.8659	-0.019
432.0000	0.0607	0.8684	-0.010	0.8651	-0.015
480.0000	0.0391	0.8680	-0.006	0.8644	-0.010
528.0000	0.0175	0.8678	-0.003	0.8640	-0.006
576.0000	-0.0041	0.8678	-0.001	0.8638	-0.001
624.0000	-0.0257	0.8678	-0.001	0.8638	-0.001
672.0000	-0.0473	0.8677	-0.001	0.8637	-0.001
720.0000	-0.0689	0.8677	-0.001	0.8637	-0.001
768.0000	-0.0904	0.8676	-0.001	0.8636	-0.001
816.0000	-0.1120	0.8676	-0.001	0.8636	-0.001
864.0000	-0.1336	0.8676	-0.001	0.8636	-0.001
912.0000	-0.1552	0.8675	-0.001	0.8635	-0.001
960.0000	-0.1768	0.8675	-0.001	0.8635	-0.001
1008.0000	-0.1984	0.8675	-0.001	0.8635	-0.001
1056.0000	-0.2200	0.8674	-0.001	0.8634	-0.001
1104.0000	-0.2415	0.8674	-0.001	0.8634	-0.001
1152.0000	-0.2631	0.8673	-0.001	0.8633	-0.001
1200.0000	-0.2847	0.8673	-0.001	0.8633	-0.001

Figure 64 FLOW BOILING CONDENSER PRESSURE VERSUS POSITION FOR G = 156 kg/m^2-s

MASS VELOCITY..... 78.00 KG/M**2-S
TUBE DIAMETER..... 4.55 MM
HEAT FLUX..... -14490.00 W/M**2

POSITION (MM)	QUALITY	PRESSURE (ATM)	DPDZ (ATM/M)	FRICTIONAL PRESSURE (ATM)	DPDZF (ATM/M)
0.0	0.5200	0.8800	-0.023	0.8800	-0.034
48.0000	0.4768	0.8789	-0.022	0.8784	-0.032
96.0000	0.4336	0.8779	-0.021	0.8769	-0.030
144.0000	0.3904	0.8769	-0.019	0.8755	-0.027
192.0000	0.3472	0.8760	-0.017	0.8742	-0.025
240.0000	0.3040	0.8752	-0.016	0.8731	-0.022
288.0000	0.2608	0.8745	-0.014	0.8721	-0.020
336.0000	0.2176	0.8739	-0.012	0.8712	-0.017
384.0000	0.1744	0.8734	-0.010	0.8704	-0.014
432.0000	0.1312	0.8729	-0.007	0.8698	-0.011
480.0000	0.0881	0.8726	-0.005	0.8694	-0.008
528.0000	0.0449	0.8724	-0.002	0.8690	-0.004
576.0000	0.0017	0.8723	0.001	0.8689	-0.001
624.0000	-0.0415	0.8723	-0.000	0.8689	-0.000
672.0000	-0.0847	0.8723	-0.000	0.8688	-0.000
720.0000	-0.1279	0.8723	-0.000	0.8688	-0.000
768.0000	-0.1711	0.8723	-0.000	0.8688	-0.000
816.0000	-0.2142	0.8723	-0.000	0.8688	-0.000
864.0000	-0.2574	0.8722	-0.000	0.8688	-0.000
912.0000	-0.3006	0.8722	-0.000	0.8688	-0.000
960.0000	-0.3438	0.8722	-0.000	0.8687	-0.000
1008.0000	-0.3870	0.8722	-0.000	0.8687	-0.000
1056.0000	-0.4302	0.8722	-0.000	0.8687	-0.000
1104.0000	-0.4733	0.8721	-0.000	0.8687	-0.000
1152.0000	-0.5165	0.8721	-0.000	0.8687	-0.000
1200.0000	-0.5597	0.8721	-0.000	0.8686	-0.000

Figure 65 FLOW BOILING CONDENSER PRESSURE VERSUS POSITION FOR G = 78 kg/m^2-s

MASS VELOCITY..... 19.50 KG/M**2-S
TUBE DIAMETER..... 4.55 MM
HEAT FLUX..... -14490.00 W/M**2

POSITION (MM)	QUALITY	PRESSURE (ATM)	DPDZ (ATM/M)	FRICTIONAL PRESSURE (ATM)	DPDZF (ATM/M)
0.0	0.5980	0.8800	-0.002	0.8800	-0.005
48.0000	0.4252	0.8799	-0.002	0.8798	-0.004
96.0000	0.2524	0.8799	-0.001	0.8796	-0.003
144.0000	0.0795	0.8798	-0.001	0.8795	-0.001
192.0000	-0.0933	0.8798	-0.000	0.8795	-0.000
240.0000	-0.2661	0.8798	-0.000	0.8795	-0.000
288.0000	-0.4389	0.8798	-0.000	0.8795	-0.000
336.0000	-0.6118	0.8798	-0.000	0.8795	-0.000
384.0000	-0.7846	0.8798	-0.000	0.8795	-0.000
432.0000	-0.9574	0.8798	-0.000	0.8795	-0.000
480.0000	-1.1302	0.8798	-0.000	0.8795	-0.000
528.0000	-1.3031	0.8798	-0.000	0.8795	-0.000
576.0000	-1.4759	0.8798	-0.000	0.8795	-0.000
624.0000	-1.6487	0.8798	-0.000	0.8795	-0.000
672.0000	-1.8215	0.8797	-0.000	0.8794	-0.000
720.0000	-1.9944	0.8797	-0.000	0.8794	-0.000
768.0000	-2.1672	0.8797	-0.000	0.8794	-0.000
816.0000	-2.3400	0.8797	-0.000	0.8794	-0.000
864.0000	-2.5128	0.8797	-0.000	0.8794	-0.000
912.0000	-2.6856	0.8797	-0.000	0.8794	-0.000
960.0000	-2.8585	0.8797	-0.000	0.8794	-0.000
1008.0000	-3.0313	0.8797	-0.000	0.8794	-0.000
1056.0000	-3.2041	0.8797	-0.000	0.8794	-0.000
1104.0000	-3.3769	0.8797	-0.000	0.8794	-0.000
1152.0000	-3.5498	0.8797	-0.000	0.8794	-0.000
1200.0000	-3.7226	0.8797	-0.000	0.8794	-0.000

Figure 66 FLOW BOILING CONDENSER PRESSURE VERSUS POSITION FOR G = 19.5 kg/m^2-s

$$\Delta P = 4f \frac{L}{D} \rho \frac{V^2}{2}$$ (Equation 142)

A summary of the Freon loop pressure drop at the maximum loop flow rate is:

Test Section	1.54 kPa	(0.22 psi)
Condenser	10.00 kPa	(1.46 psi)
Quality Meter	36.09 kPa	(5.23 psi)
Remaining Plumbing	20.88 kPa	(3.03 psi)
Total	68.51 kPa	(9.94 psi)

DACS. The DACS for the flow boiling experiment consists of a microcomputer assembled from off-the-shelf components, 48 kilobytes of static memory for storage of data and program instructions, A/D converter and I/O board. Heater power is supplied from a programmable power supply capable of supplying 20 individual outputs at 2 amperes and 0 - 6 volts DC each. The supply will be controlled by the DACS via reset and control lines.

The DACS is based on the RCA COSMAC 1802 microprocessor. The primary advantages of this microprocessor are low power consumption, full military operating temperature range, and an architecture optimized for data logging and control.

The DACS will consist of the following standard boards (each board is 11.4 x 19.1 cm).

1	CDP18S603	- Central Processor
1	CDP18S643	- 16-Channel Analog to Digital Converter
6	CDP18S622	- 8 Kilobyte Static RAM Memory with on-board battery backup power
1	CDP18S640	- I/0 Control
1	CDP18S021 (or Equivalent)	- MKRO Terminal

Total maximum power consumption for this system is approximately 4 watts, with approximately 40 percent of the power being dissipated in the I/0 control board (i.e., a function which could be minimized for reduced power consumption).

Data Rate: Analog signals from the experiment (test section wall and fluid temperatures and pressures) are routed to the A/D converter, converted to 8-12 bit digital values and then stored in memory. The total time required for conversion of a single reading is 350

microseconds maximum (assuming 8 bit conversion with a 2 mHz CPU clock and 50 s for multiplexing of the test section temperatures). At this conversion speed, the data rate is approximately 3 KHz. This data rate could completely fill the available memory in approximately 17 seconds.

For the 15 test conditions, assuming data is taken for one second at each condition, the maximum data rate without exceeding the 48K memory is: 1860 Hz (assuming 20K bytes for program storage).

The total number of readings to be taken which comprise one data point is:

5	Wall temperatures - multiplied to A/D
5	Fluid temperatures - multiplied to A/D
1	Heater power*
1	Pressure drop
1	Inlet pressure
1	Inlet temperature
1	Flow rate
1	Quality
16	Total readings

*Heater power could be implicit and not measured - the power supply would be adjusted to deliver a specified power at a specific time. In addition, since all 20 heater powers are the same, only one heater power needs to be stored.

At the 1860 Hz data rate, all the test cells could be sampled up to 116 times during the one-second measurement period.

The camera could simultaneously be operated under control by the DACS to synchronize the photographic record with the measured data. For example, the camera could be driven at 100 frames per second for the last 10 seconds of every test condition to obtain a photographic record of every data point (data taken at 100 times per second). The total amount of film required would be 114 m (375 ft).

Experiment Timer: Timing of program operations is controlled by an Intel 8253 programmable timer. This frees the CPU from menial timing chores and permits simultaneous control of multiple tasks. The timer consists of three independent, programmable timers and can be directly interfaced to the 1802 system (the timer is simply considered as another memory location).

4.3.3 Mission Analysis. Mission operation timelines for the flow boiling experiment were based on the experiment operation procedure shown in Table LIII. The mission timeline reflects only the on-orbit operations: preparation, operation and disassembly. A preliminary mission timeline for the flow boiling experiment is shown in Figure 67. The total time required for the experiment is approximately 40 minutes.

4.3.4 Safety Analysis. The approach taken in the design of the flow boiling experiment was to make the experiment as fail-safe as possible. The possibility of an uncontrolled pressure rise in the experiment is remote due to pressure temperature and flow switches which will shut down the pumps and heaters of the experiment independent of the DACS. An uncontrolled leak of Freon 11 caused by fracture of the quartz tube test section cannot occur since the acrylic sheath provides a complete secondary seal. The FHA and Phase Zero safety review documentation for the flow boiling experiment is given in Appendix C.

4.3.5 Ground Test Requirements. The ground test requirements for the flow boiling experiment were defined. As was the case for the liquid reorientation experiment, ground testing was divided into: (1) development testing (Table LIV), (2) component acceptance testing (Table LV), (3) qualification testing (Table LVI) and (4) end item acceptance testing (Table LVII). These test areas were then further divided into functional, environmental and performance testing.

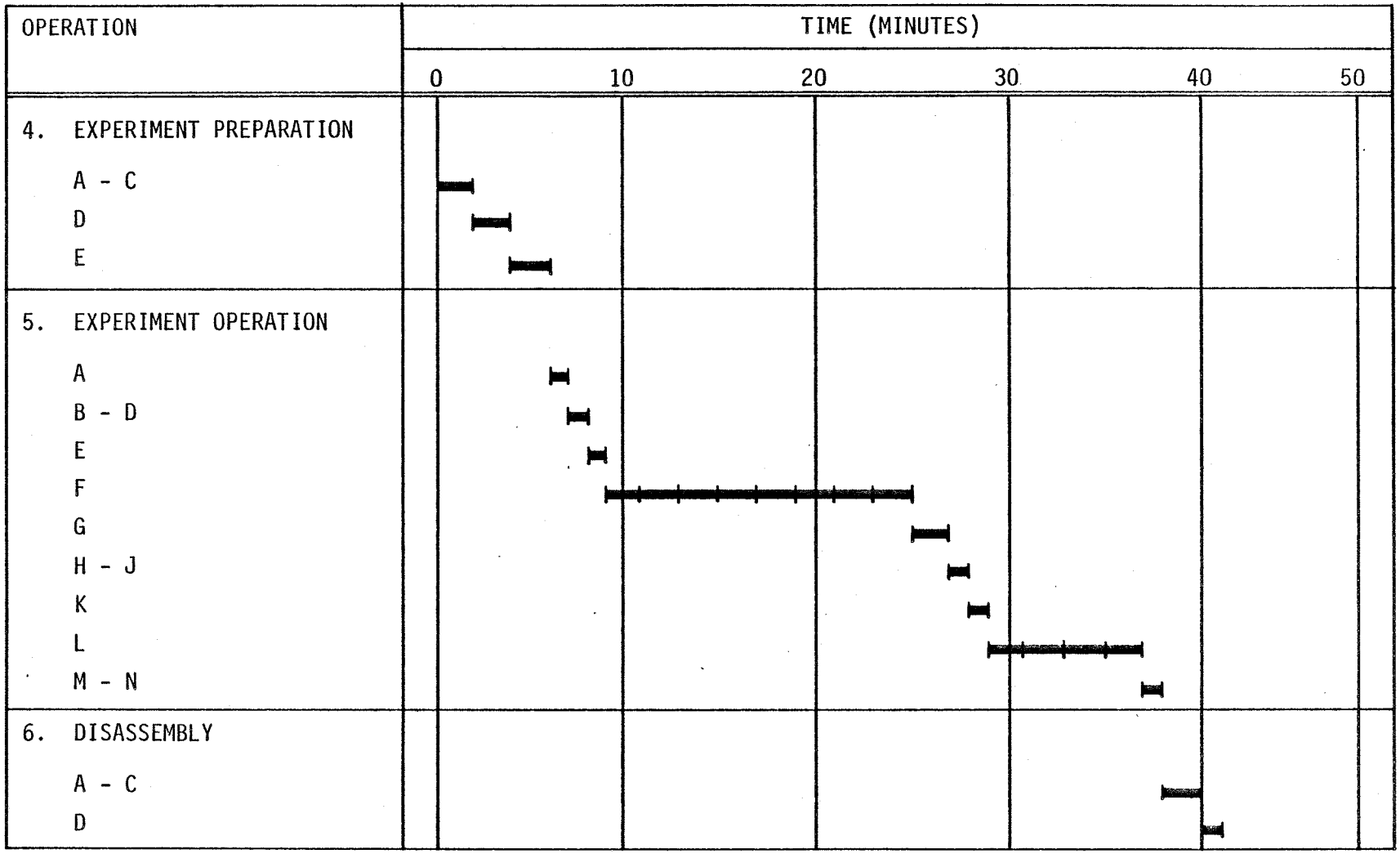

Figure 67 PRELIMINARY MISSION TIMELINE, FLOW BOILING EXPERIMENT

TABLE LIII EXPERIMENT OPERATING PROCEDURES - FLOW BOILING

Mission Phase	
1. Pre-flight Handling:	A. Final checkout of pumps, heaters and test section. B. Evacuate Freon loop and fill with Freon 11; evacuate and fill water loop. C. Verify system integrity D. Package all equipment. E. Mount flow module on middeck adapter plate; stow DACS and miscellaneous experiment hardware in support locker.
2. Launch:	A. Rely on packaging to withstand launch loads and contain potential leakage, fragments, etc.
3. On-orbit Stowage:	A. Rely on packaging to withstand launch loads and contain potential leakage, fragments, etc.
4. On-orbit Experiment Preparation:	A. Visually inspect flow module for leakage; remove protective covers. B. Connect Orbiter water cooling interface. C. Connect DACS to flow module. D. Run diagnostics to verify system operation. E. Prepare camera--load, position and install.
5. On-orbit Experiment Operation:	A. Activate water cooling loop, camera in strobe mode. B. Set Freon flowrate for data point (DACS input). C. Adjust regulator for desired inlet conditions (astronaut input). D. Activate heater. E. Fire RCS +X thrusters for 60 seconds; initiate DACS data taking mode. F. Repeat operations B through E for all high gravity data points; null out Orbiter motion after each burn. G. Establish Orbiter in drag -g mode. H. Set Freon flow rate for data point (DACS input). I. Adjust regulator for desired inlet conditions (astronaut input). J. Activate heater. K. Initiate DACS data taking mode. L. Repeat operations H through K for all drag -g data points. M. Shutdown Freon loop. N. Shutdown water loop.
6. On-orbit Experiment Disassembly:	A. Disconnect DACS from fluid module. B. Stow camera and miscellaneous hardware in DACS locker. C. Disconnect Orbiter water cooling interface. D. Stow all gear and replace protective covers on fluid module.
7. Re-entry and Landing:	A. Rely on packaging to withstand landing loads and contain leakage, fragments, etc.
8. Post-flight:	A. Remove data storage memory boards. B. Remove flight hardware.

TABLE LIV FLOW BOILING EXPERIMENT DEVELOPMENT TESTS

Component	Test	Description
Functional		
Test Section	Heater Calibration Check	Check resistance versus temperature calibration of heaters following boiling tests.
Environmental		
Test Section	Shock/Vibration	Subject test section, filled with Freon 11, to handling, prelaunch, launch, re-entry, and post-landing shock and vibration loads.
Condenser	Shock/Vibration	Subject condenser, filled with Freon 11, to handling, prelaunch, launch, re-entry, and post-landing shock and vibration loads.
Performance		
Test Section Quality Meter, Condenser, Pumps, DACS	Boiling	Assemble flow boiling and coolant loop and perform boiling heat transfer tests on test section and on DACS control logic.
Condenser	Low-gravity Condensation	Use parabolic aircraft flights to determine the effects of low-gravity on condenser performance.

TABLE LV FLOW BOILING EXPERIMENT
COMPONENT ACCEPTANCE TESTS

Component	Test	Description
Functional		
Test Section	Heater Calibration	Develop resistance versus temperature curve for each heater of test section.
	Dielectric Strength	Check dielectric strength of heaters on test section.
	Proof Pressure	Subject test section to a pressure of at least two times the operating pressure as per Reference 14.
	Leak Check	Determine if test section leaks.
Quality Meter	Electrical	Perform an electrical check on quality meter.
Condenser	Proof Pressure	Subject condenser to a pressure of at least two times the operating pressure as per Reference 14.
	Leak Check	Determine if the condenser leaks.
Pumps	Proof Pressure	Subject pump to a pressure of at least two times the operating pressure as per Reference 14.
	Leak Check	Determine if pump leaks while operating and when stopped.
	Flow	Check flow rate versus head pressure characteristics of pump.
Preheater	Electrical	Perform an electrical check on the preheater.
Accumulators	Proof Pressure	Subject accumulators to two times their maximum operating pressure as per Reference 14.
	Leak Check	Determine if accumulators leak.
Flow, Temperature, and Pressure Switches	Electrical	Perform an electrical check on the switches.
Temperature Sensors	Calibration	Check calibration of temperature sensors at ice bath, ambient and boiling conditions.

TABLE LV FLOW BOILING EXPERIMENT
COMPONENT ACCEPTANCE TESTS (Concluded)

Component	Test	Description
Functional		
Pressure Transducers	Calibration	Check calibration of pressure transducers at zero and full scale output.
Flow Meter	Calibration	Check flow meter calibration at zero and full scale.
Programmable Power Supply	Electrical	Perform an electrical check on the programmable power supply.
DACS	Electrical	Perform an electrical check on the DACS.
Camera	Operational	Check operation of camers, including lens, film, advance, etc.
Batteries	Electrical	Check output of batteries and temperature rise during planned discharge cycle.
Accelerometer	Operational	Check output of accelerometer in each axis and temperature readout.

TABLE LVI FLOW BOILING EXPERIMENT QUALIFICATION TESTS

Component	Test	Description
Functional		
Experiment Package	Proof Pressure	Pressurize package to two times maximum operating pressure as per Reference 14.
	Leak Check	Determine if experiment package leaks.
Test Section	Heater Calibration Check	Check resistance versus temperature calibration of heaters following mission simulation tests.
Environmental		
Experiment Packages	Shock/Vibration	Subject assembled experiment package, filled with Freon 11, to handling, prelaunch, launch, re-entry, and post-landing shock and vibration loads.
	Acceleration	Subject assembled experiment package, filled with Freon 11, to anticipated acceleration loads.
	Pack and Ship	Pack and ship simulated experiment package load in instrumented container to buyer.
Performance		
Experiment Package	Mission Simulation	Perform mission simulation test on the experiment package, including evacuation, fill, setup of experiment test runs, all tests and shutdown and safing of experiment.

TABLE LVII FLOW BOILING EXPERIMENT -
END ITEM ACCEPTANCE TESTS

Component	Test	Description
Functional		
Experiment Package	Proof Pressure	Pressurize package to 1.5 times the maximum operating pressure.
	Leak Check	Determine if package leaks.
	Flow	Conduct flow test on package.
	Electrical	Perform check on package electrical systems.

5.0 DEVELOPMENT PLAN

A development schedule was prepared for each individual experiment. September 1983 was the assumed starting date for the development. The schedules for each experiment were divided into the following tasks:

- Experiment Design. This task consists of preparation of detailed design drawings of the flight hardware. Also included in this task are the required structural, thermal and system analyses of the experiment, preparation of a preliminary and detailed design report, and engineering support of manufacturing and test.

- Safety. This task includes detailed reliability and fault hazard analyses of the experiment as well as the preparation safety matrix data for all safety reviews.

- Ground Support Equipment (GSE). This task consists of defining the GSE for the experiment. In the subsequent procurement, fabrication, assembly and testing tasks, GSE was not included, since a preliminary design of the GSE was beyond the scope of this study. GSE development should have a small effect on the overall development program, since very little GSE is required for any of the experiments.

- Integration. This task runs the length of the development program and consists of the engineering necessary to integrate the experiment into the Orbiter middeck. Preparation of the required Interface Control Documentation (ICD) is included.

- Procurement. This task defines the length of procurement activity for the experiment.

- Fabrication and Assembly. Fabrication of the experiment components and assembly of the experiment packages are included in this task.

- Component Acceptance Testing. As previously described in Section 4.0, component acceptance tests verify that a component meets its specification requirements.

- Development Testing. This task included those tests necessary to evaluate new designs, verify analytical assumptions and fill in data voids.

- Qualification Testing. The tests required to qualify the final experiment assembly and its subassemblies for use are included in this task.

- End Item Acceptance Tests. EIATs are made on the final flight article prior to shipment. The EIAT task is not necessary if the qualification unit also serves as the flight article.

- Delivery. This includes packing and shipment of the experiment assembly to NASA.

- Installation. This task shows the estimated time required to install the experiment in the Orbiter middeck.

- Flight. The estimated flight duration is shown in this task.

- Quality Assurance. This task runs the length of the fabrication, assembly and testing tasks, and defines the length of time required for quality assurance.

The development schedules for the liquid reorientation, pool boiling and flow boiling experiments are shown in Figures 68, 69 and 70. As shown in the figures, the development program times through hardware delivery were estimated to be:

Liquid Reorientation - 14½ months
Pool Boiling - 18½ months
Flow Boiling - 18 months

Long Lead Time/High Cost Items. The only long lead time and high cost item identified for the two-phase experiment is the accelerometer. Accurate measurement of low-level acceleration is essential for all of the experiments. The accelerometer selected for these

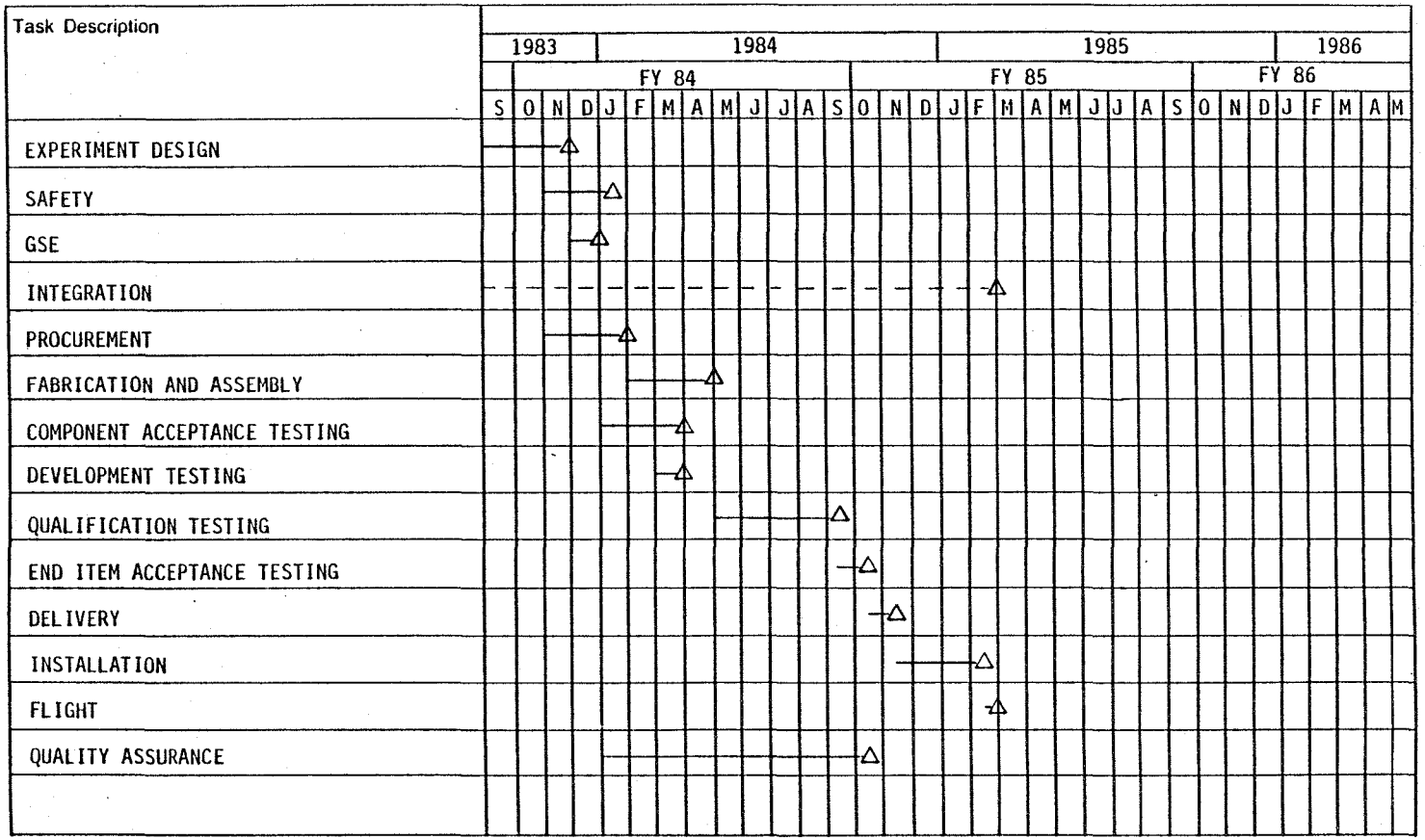

Figure 68 LIQUID REORIENTATION EXPERIMENT DEVELOPMENT SCHEDULE

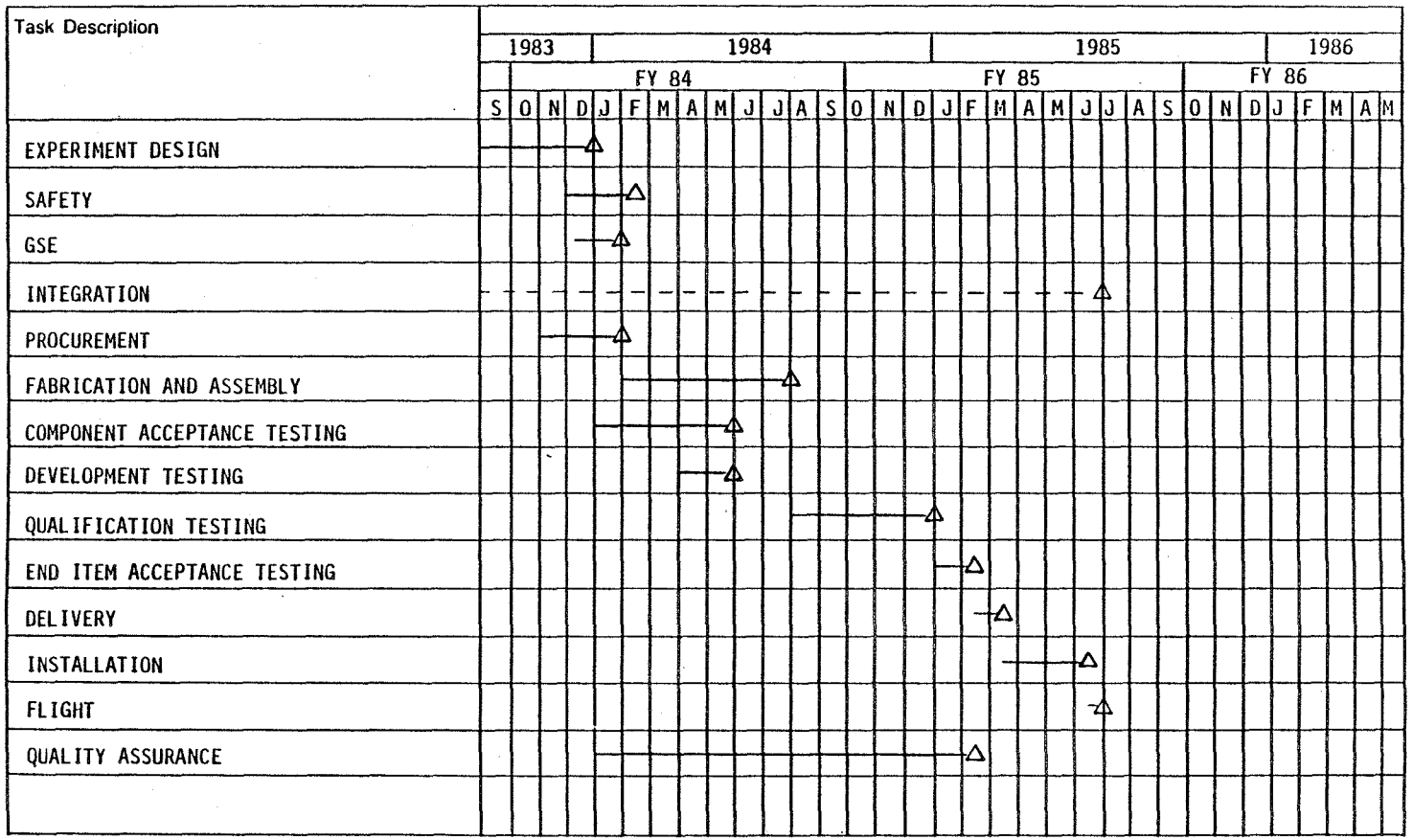

Figure 69 POOL BOILING EXPERIMENT DEVELOPMENT SCHEDULE

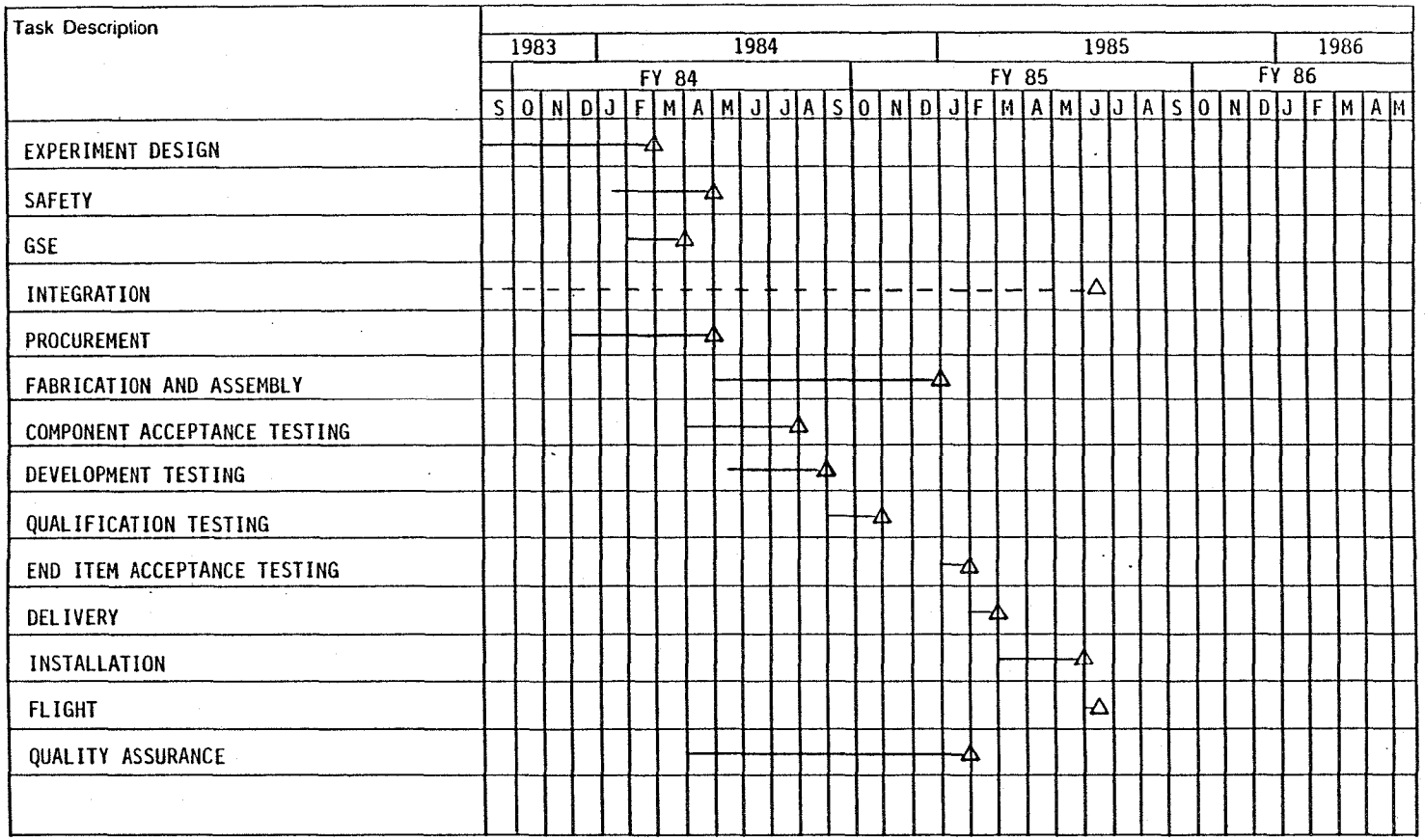

Figure 70 FLOW BOILING EXPERIMENT DEVELOPMENT SCHEDULE

experiments is capable of measuring accelerations down to $10^{-6}g_o$, and would be built by the same supplier who is currently providing the Orbiter High Resolution Triaxial Linear Accelerometer Package (HIRAP) and Aero Coefficient Instrumentation Package (ACIP) accelerometer packages. The lead time on delivery of the first unit is one year.

Subsequent units would be delivered at one month intervals. The cost of the first unit is $390,000 and subsequent units are $230,000 (1982 dollars).

5.1 Cost Estimate. Rough order of magnitude cost estimates (in 1981 dollars) were prepared for each experiment. The elements included in the cost estimates were detailed design (primarily engineering effort in the production of drawings, analyses, specifications reports and test plans), fabrication (manufacturing, quality control, and material costs for all experiment hardware) and testing (test engineering, manufacturing and material costs involved in development, component acceptance, qualification and end item acceptance tests). Also included was a prime contractor fee of ten percent based upon a cost plus fixed fee type contract. Specifically excluded from the estimate were flight costs, flight support engineering, experiment data analyses and ground support equipment.

The estimates given are based on assumptions about the level of documentation and NASA review required during the actual hardware program. For the purposes of this estimate it was assumed that the program would be operated to essentially the same standards as current Shuttle hardware programs (e.g., PRSA, FCSS, etc.). Engineering and testing estimates are based on Beech experience with other NASA programs. Fabrication material costs include vendor quotes for many of the standard items. For development items such as the pool boiling heaters or flow boiling test section, no vendor data was available. Consequently, these items were estimated based on Beech experience with the PRSA program. Cost for each of the three experiments was estimated as stand alone programs and savings would result if two or more of the experiments were designed in parallel.

Costs were estimated for four different program approaches:

1. Each experiment procured with a high resolution accelerometer and a flight article (versus flying the qualification test article).

2. Each experiment procured with a high resolution accelerometer but without a flight article (the qualification test article is flown) and its associated accelerometer.

3. Each experiment procured without any high resolution accelerometers but with a flight article.

4. Each experiment procured without a high resolution accelerometer or a flight article.

Tables LVIII, LIX and LX show overall program costs by fiscal year for each experiment. These costs show the relative order of cost savings using different combinations of deliverable hardware. More accurate estimation of total program costs (for examle during a detailed design phase) would require a clear definition of hardware documentation, test and quality assurance requirements by NASA. The following tables indicate the funding commitment by year rather than expenditure by year. Commitments differ from expenditures since commitments include the full cost of material when the purchase order is issued rather than when material is received.

TABLE LVIII LIQUID REORIENTATION EXPERIMENT ROM COSTS
BY GOVERNMENT FISCAL YEAR

($1000's) Commitment

Approach	GFY83	GFY84	GFY85	Total
1. With Accelerometer With Flight Article	27	1317	19	1363
2. With Accelerometer Without Flight Article	27	963	10	1000
3. Without Accelerometer With Flight Article	24	482	17	523
4. Without Accelerometer Without Flight Article	24	431	8	463

TABLE LIX POOL BOILING EXPERIMENT ROM COSTS
BY GOVERNMENT FISCAL YEAR

($1000's) Commitment

Approach	GFY83	GFY84	GFY85	Total
1. With Accelerometer With Flight Article	33	1720	295	$2048
3. With Accelerometer Without Flight Article	33	1313	189	1535
3. Without Accelerometer With Flight Article	31	903	273	1207
4. Without Accelerometer Without Flight Article	31	791	176	998

TABLE LX FLOW BOILING EXPERIMENT ROM COSTS
BY GOVERNMENT FISCAL YEAR

($1000's) Commitment

Approach	GFY83	GFY84	GFY85	Total
1. With Accelerometer With Flight Article	18	1708	57	$1783
2. With Accelerometer Without Flight Article	18	1200	41	1259
3. Without Accelerometer With Flight Article	18	977	57	1052
4. Without Accelerometer Without Flight Article	18	744	41	803

As shown in the tables, the minimum costs in 1981 dollars for experiment development were estimated to be:

Liquid Reorientation - $463K
Pool Boiling - $998K
Flow Boiling - $803K

5.2 Vendor Quotes. It was possible to obtain vendor quotes for some of the major but fairly conventional components. These are summarized in Table LXI.

TABLE LXI VENDOR QUOTES
(1982 Dollars)

Item	Vendor	Cost	Delivery
High Resolution Accelerometer	KMS Fusion P.O. Box 1567 Ann Arbor, MI 48106	First Unit: $390K Each Additional Unit: $230K	First Unit: 12 months Additional Units: 1 month
Liquid Reorientation Experiment Tanks	Reynolds & Taylor 2109 S. Wright Santa Ana, CA	Three Reorientation Tanks $3.5K Supply Tank: $0.4K	Reorientation Tanks: 10 weeks Supply Tank: 4 weeks
Pool Boiling Cells	Plastic Technology 3050 Valmont Road Boulder, CO 80302	First Unit: $4.0K (9 cells) Each Additional Unit: $2.9K	4 weeks
Data Acquisition and Control Computer	RCA 6767 S. Spruce St. Englewood, CO 80112	$4.0K	Stock
Camera	Instrumentation Marketing 820 S. Mariposa St. Burbank, CA 91506	16mm-1VN Camera - $4.0K Film Magazine - $2.5K	Stock
Pressure Transducers P305-A	Validyne Engineering 8626 Wilbur Avenue Northridge, CA 91324	$0.5K each	4 weeks
Titanium Foil (0.025 mm)	Teledyne-Rodney Metals 7305 Paramount Blvd. Pico Rivera, CA 90660	$0.2K per 40 sq. ft.	Stock

6.0 CONCLUSIONS AND RECOMMENDATIONS

This study has defined the preliminary designs for three two-phase fluid research experiments for the middeck of the Space Shuttle Orbiter:

- Liquid reorientation--to study the motion of liquid in tanks subjected to small accelerations. Applicable to fuel settling problems in orbital vehicles.
- Pool boiling--to study low-gravity boiling from heated horizontal cylinders.
- Flow boiling--to study low-gravity flow patterns and boiling in a heated horizontal tube.

For each experiment, the design definition includes fluid system schematics, electrical schematics, and assembly drawings sufficiently detailed for realistic estimates of development costs and schedules.

Safety analyses were carried out for each experiment and consist of a fault hazard analysis, a safety matrix (JSC Form 542) and a hazards list (JSC Form 542A). The safety data generated is the basic data required for a Phase-Zero safety review of the experiments.

Development plans for the three experiments were defined. The effort required to develop the experiments includes detailed design, hardware procurement and fabrication, ground testing and payload integration. The development span times for the three experiments are:

- Liquid Reorientation--14½ months
- Pool Boiling--18½ months
- Flow Boiling--18 months

The minimum hardware ROM costs for the detailed design, procurement and fabrication, and ground testing effort estimated in 1981 dollars are:

- Liquid Reorientation--$463,000
- Pool Boiling--$998,000
- Flow Boiling--$803,000

These estimates assume that the qualification test article will be flown in place of a separate flight article and that a high resolution, micro-gravity accelerometer will be procured separately from the three experiments. The estimated cost for the one accelerometer is $390,000 in 1982 dollars.

Conclusions. A major objective of this study was to evaluate the relative merits of conducting the three experiments in a Spacelab facility or as individual carry-on experiments elsewhere in the Orbiter. It was found during this study that the three experiments could be conducted more economically in the Orbiter middeck than in Spacelab. Total costs for the three experiments in a Spacelab facility were found to be roughly four times the costs for the three experiments as middeck carry-ons. Further, it was found tht all three experiments could be designed to be compatible with all known middeck payload requirements. The most restrictive of these requirements are that middeck experiments cannot vent (either to space or to the cabin atmosphere), that external power for the experiments is not available (internal battery power required) and that the maximum heat that can be rejected to the middeck is 10 watt-hours per locker. The power dissipated by the flow of boiling experiment requires the use of a water cooling loop installed on the 099 and 102 Orbiters.

During the course of this study a number of long-lead time or high-risk development items were identified:

- All experiments--A high-resolution, micro-gravity accelerometer is required to monitor the acceleration environment in the middeck during experiment operation. Based on vendor estimates, the cost for the accelerometer is $390,000 with a 12 month delivery time.

- Pool boiling experiment--The heaters with their associated instrumentation require development. The instrumentation inside the heaters, in particular, requires proof-of-concept testing and development testing to determine accuracy and time response.

- Flow boiling experiment--The heated test section requires development testing to evaluate fabrication techniques and verify thermal performance.

- Flow boiling experiment--The condenser requires low-gravity development testing to verify the unit's thermal performance. Aircraft testing will probably be sufficient to measure the condenser's performance.

Recommendations. During the course of this study it became apparent that specific action by NASA is required to support detailed design and development of the two-phase fluid research experiments.

1. NASA should first pursue the development of the pool boiling experiment. Of the three experiments considered, the data obtained from the pool boiling experiment would be the most immediately useful. Most correlations of flow boiling heat transfer are combinations of pool boiling and forced convection, consequently data obtained from a low-gravity pool boiling experiment could probably be applied to low-gravity flow boiling. Data from the liquid reorientation experiment may not be generally applicable to on-orbit liquid settling applications. The momentum associated with experiment fluid will have virtually no effect on the test tank acceleration. In most on-orbit liquid settling applications however, propellant momentum will have significant effects on the propellant tank acceleration.

2. Much of the needed engineering design data for the middeck are undefined. A clear middeck user policy defining the availability and price of the following is needed:

   - Orbiter primary RCS firings
   - Middeck utility power
   - Middeck water cooling
   - Experiment mounting/attachment outside of the middeck lockers
   - Experiment venting

   Finally, definition is needed to determine whether middeck qualification articles can be used for flight, or whether separate flight articles must be fabricated.

3. NASA should measure the Orbiter middeck on-orbit acceleration during long duration RCS firings. Measurements of random noise, the magnitude of "jitter" level should also be made.

4. Consideration should be given to developing the accelerometer as a separate package and subsequently providing it as a middeck payload service. Similarly camera and lighting equipment could be provided as an optional service.

5. NASA should consider developing a standard middeck recommended equipment list which would include batteries, computers, and other components of general use to middeck experiments.

In addition to these general recommendations, there are specific recommendations which apply to each individual experiment if they are to be developed.

Liquid Reorientation Experiment Recommendations. There are no hardware or design uncertainties that need to be answered before the development of the liquid reorientation experiment. However, NASA should consider a variant of this experiment in which the momentum associated with the liquid motion significantly affects tank acceleration. This would require an independent unrestrained package which would probably be flown outside the Orbiter.

Pool Boiling Experiment Recommendations. The heater and heater temperature instrumentation to be used on the pool boiling experiment should be ground tested. In addition, the test cell surface temperature during heater operation should be determined. This latter test may require low-gravity aircraft flights to adequately determine the maximum temperatures.

Flow Boiling Experiment Recommendations. There are two development items which need to be addressed before development of the flow boiling experiment can proceed: (1) the test section and (2) the condenser. The experiment test section is a hardware development item; the particular method of providing uniform heating and simultaneously allow viewing of the boiling should be further defined.

The condenser for the flow boiling experiment is not a hardware development problem. However, the effects of low-gravity on condenser performance are not known and need to be answered by low-gravity aircraft flight testing.

The quality meter shown in the flow boiling experiment should be eliminated. It is the largest pressure drop component in the experiment flow loop and does not provide any data required to meet the primary experiment objectives. Development testing of the quality meter should first be completed on the ground before attempting flight tests.

APPENDIX A

LIQUID REORIENTATION EXPERIMENT SAFETY DATA

PAYLOAD SAFETY MATRIX

PAYLOAD: Liquid Reorientation Experiment	PAYLOAD ORGANIZATION: NASA Lewis Research Center	DATE	PAGE

HAZARD GROUP / SUBSYSTEM	COLLISION	CONTAMINATION (TOXICITY, ETC)	CORROSION	ELECTRICAL SHOCK	EXPLOSION	FIRE	INJURY AND ILLNESS	LOSS OF ENTRY CAPABILITY	RADIATION	TEMPERATURE EXTREMES									
Biomedical																			
Hazard Detection and Safing																			
Cryogenics																			
Electrical		X	X		X	X	X		X										
Environmental Control																			
Human Factors																			
Hydraulics																			
Materials		X				X	X												
Mechanical	X	X					X												
Optical																			
Pressure Systems		X			X		X												
Propulsion																			
Pyrotechnics																			
Radiation																			
Structures	X						X												

JSC Form 542 (Feb 78) NASA-JSC

HAZARD LIST

PAYLOAD	SUBSYSTEM	DATE
Liquid Reorientation Experiment	Electrical	

HAZARD GROUP		HAZARD TITLE	APPLICABLE SAFETY REQUIREMENT
Contamination	1.001	Battery failure or rupture could release battery fluids.	201* 209
Corrosion	1.002	Rupture of batteries could result in corrosive attack of structural members.	209
Explosion	1.003	Excessive battery discharge could result in explosive gas mixture.	201 209
Fire	1.004	Battery explosion or internal heating could result in cabin fire.	201 209
Illness/injury	1.005	Crew contact with battery electrolytes or hot batteries could result in injury.	209 201
Radiation	1.006	EM interference	212

*Paragraph numbers refer to NHB 1700.7A.

HAZARD LIST

PAYLOAD	SUBSYSTEM	DATE
Liquid Reorientation Experiment	Materials	

HAZARD GROUP		HAZARD TITLE	APPLICABLE SAFETY REQUIREMENT
Contamination	2.001	Orbiter cabin material.	209(2)
Contamination	2.002	Offgassing of all experiment materials in habitable environment.	209(4)
Fire	2.003	Use of flammable materials in orbiter cabin.	209(2)
Illness/injury	2.004	Use of shatterable material.	201

JSC Form 542A (Feb 78) NASA-JSC

HAZARD LIST

PAYLOAD	SUBSYSTEM	DATE
Liquid Reorientation Experiment	Mechanical	

HAZARD GROUP	HAZARD TITLE	APPLICABLE SAFETY REQUIREMENT
Contamination	3.001 System valves fail and release. FC-77	201, 209
Collision	3.002 Failure of test stand anchors-uncontrolled motion of experiment.	201, 209
Illness/injury	3.003 Impact of rotating experiment package.	201

JSC Form 542A (Feb 78) NASA-JSC

HAZARD LIST

PAYLOAD	SUBSYSTEM	DATE
Liquid Reorientation Experiment	Pressure Systems	

HAZARD GROUP		HAZARD TITLE	APPLICABLE SAFETY REQUIREMENT
Contamination/ Toxicity	4.001	Supply tank rupture could contaminate middeck with FC-77.	SP&R 208.7 209.2 213
Explosion	4.002	Explosion of supply tank could result from thermal expansion of liquid.	208.7 208.4 213
Explosion	4.003	Implosion of reorientation or supply tanks could result from external pressurization.	208.4 213
Injury	4.004	Implosion or rupture of tanks could result in fragments.	201 213

JSC Form 542A (Feb 78) NASA-JSC

HAZARD LIST

PAYLOAD	SUBSYSTEM	DATE
Liquid Reorientation Experiment	Structures	

HAZARD GROUP	HAZARD TITLE	APPLICABLE SAFETY REQUIREMENT
Collision	5.001 Handling shocks.	208
Collision	5.002 Failure of Test Stand.	201
Collision	5.003 Experiment hardware failure during crash loads.	208

JSC Form 542A (Feb 78) NASA-JSC

FAULT HAZARD ANALYSIS - LIQUID REORIENTATION

Component	Component Failure Mode	Component Failure Rate	System Operational Mode	Effect Of Primary Component Failure On Subsystem	Factors That May Cause Secondary Component Failure	Upstream Components Or Inputs That May Cause Sequential Failures	Further Analysis Required	Remarks	Liquid Reor.
Manual Valve MV-1	Fails closed	.000093	Normally closed (opened only to add liquid to RT1)	RT1 cannot be filled				Loss of data for RT1	
	Fails open		Opened to add liquid to RT1	RT1 will be filled with liquid	Stem opened excessive number of turns Loss of Handwheel	Leak in RT1 may cause loss of vacuum in system		Loss of data from RT1	1394 cu^3 left for RT2, RT3 1729 reg.
	Leaks externally		Normally closed	Loss of vacuum in RT1 or piping leak to cabin	Vibration corrosion			Unable to fill any tanks Loss of experiment	
Manual Valve MV-2	Fails closed	.000093	Normally closed	RT2 cannot be filled	Loss of Handwheel			Loss of data for RT2	
	Fails open		Opened to add liquid to RT2	RT2 will be filled	Stem opened excessive number of turns Loss of Handwheel	Leak in RT2 may cause loss of vacuum in system		Loss of data for RT2	3869 cu^3 left 3462 cu^3 reg.
	Leaks externally		Normally closed	Loss of vacuum in RT2 or piping leak to cabin	Vibration corrosion			Unable to fill any tank Loss of experiment	
Manual Valve MV-3	Fails closed	.000093	Normally closed	RT3 cannot be filled				Loss of data for RT3	
	Fails open		Opened to fill RT3	RT3 will be filled	Stem opened excessive number of turns Loss of Handwheel	Leak in RT3 may cause loss of vacuum in system		Loss of data from RT3	
	Leaks externally		Normally closed	Loss of vacuum in RT3 or piping	Vibration corrosion			Unable to fill any tank Loss of experiment	

FAULT HAZARD ANALYSIS - LIQUID REORIENTATION (continued)

Component	Component Failure Mode	Component Failure Rate	System Operational Mode	Effect Of Primary Component Failure On Subsystem	Factors That May Cause Secondary Component Failure	Upstream Components Or Inputs That May Cause Sequential Failures	Further Analysis Required	Remarks	Liquid Reor.
Air Vent V-1	Fails Closed	.00005	Normally closed	Unable to fill any tank	Excessive Torque			Experiment fails	
	Fails open		Open during fill	Potential leak path to cabin		Piston leakage could allow liquid to leak to cabin		No effect on exp. op.	
Supply Tank	Piston does not move		Storage, fill	Liquid thermal expansion could be restrained - Loss of expulsion capability		Tank rupture if relief valve fails closed	Determine modes of piston lock up - O ring failure, cylinder distortion, cocking	Experiment fails - Potential for leakage	
	Piston leaks		Fill	Inaccurate fill potential for leakage to cabin	Thermal expansion of cylinder	Air vent fails open. May permit leakage	Evaluate failure modes, reliability		
	Tank collapses from external pressure		Fill	Leakage of liquid into cabin	Excessive external pressure, temp. impact			Middeck contamination - Loss of experiment	
	Tank rupture		Storage - Thermal expansion of liquid	Liquid discharged into RT1	Temperature extremes Improper air volume for expansion	Relief valve fails closed - Tank rupture		Unknown liquid quantity in RT1	
Test Stand	Connection to middeck fails		Rotating package	Impact of package, personnel injury, fracture of tanks	Excessive rotational speed. Incorrect connection to floor		Evaluate reliability	Use lanyard restraints	
	Package restraint fails		Rotating package	"	Incorrect connection. Structural failure			Use lanyard restraints	

FAULT HAZARD ANALYSIS - LIQUID REORIENTATION (concluded)

Component	Component Failure Mode	Component Failure Rate	System Operational Mode	Effect Of Primary Component Failure On Subsystem	Factors That May Cause Secondary Component Failure	Upstream Components Or Inputs That May Cause Sequential Failures	Further Analysis Required	Remarks	Liquid Reor.
Reorientation Tanks	Fitting leak		Partially filled with FC-77. Internal pressure ∿ 1 psia	Tank cannot be filled. Temperature increase of leaking gas may weaken plastic.	Shock, vibration	Manual valve leak	Evaluate reliability	Loss of data - Leak is fail safe since tank is at reduced pressure.	$m_i C_p T_1 = m_2 C_v T_2$ $T_2 = \frac{C_p}{C_v} T_1$
	Tank fractures		Partially filled with FC-77. Internal pressure ∿ 1 psia	Leak FC-77	Over pressure, shock, impact			Leak of FC-77 into middeck - Design is conservative.	
Relief Valve RV-1	Fails closed	.00005	Manual valves closed	Rupture supply tank	Temperature vibration	Piston jams in supply tank and thermal expansion occurs.		Two failures required for leak or rupture.	
	Fails open		Manual valves closed	RT1 filled; fill of RT2 & RT3 may be possible.				Loss of data	
Accelerometer Package	Inoperative		Reorientation experiment in progress	Loss of g-data. Use backup data from Shuttle accelerometer.	Shock, battery failure		Evaluate reliability	Loss of data	
	Battery failure		Any	Leak corrosive battery contents	Temperature, discharge			Loss of data - contamination of middeck	

APPENDIX B

POOL BOILING EXPERIMENT SAFETY DATA

PAYLOAD SAFETY MATRIX

PAYLOAD: POOL BOILING EXPERIMENT	PAYLOAD ORGANIZATION	DATE	PAGE

HAZARD GROUP / SUBSYSTEM	COLLISION	CONTAMINATION (TOXICITY, ETC)	CORROSION	ELECTRICAL SHOCK	EXPLOSION	FIRE	INJURY AND ILLNESS	LOSS OF ENTRY CAPABILITY	RADIATION	TEMPERATURE EXTREMES								
Biomedical																		
Hazard Detection and Safing																		
Cryogenics																		
Electrical		X		X		X			X	X								
Environmental Control							X			X								
Human Factors		X					X											
Hydraulics																		
Materials		X				X	X											
Mechanical																		
Optical																		
Pressure Systems		X			X	X	X											
Propulsion																		
Pyrotechnics																		
Radiation																		
Structures	X		X															

JSC Form 542 (Feb 78)

NASA-JSC

HAZARD LIST

PAYLOAD	SUBSYSTEM	DATE
Pool Boiling Experiment	Electrical	

HAZARD GROUP		HAZARD TITLE	APPLICABLE SAFETY REQUIREMENT
Contamination	1.001	Battery leakage.	201*
Electrical Shock	1.002	Crew exposure to shock during cable connection & experiment operation.	201, 209
Fire	1.003	Fire caused by excessive battery or component temperatures.	213, 209
Radiation	1.004	Electromagnetic interference generation.	212.2
Temperature Extremes	1.005	Excessive temperatures at test cell surface.	201

*Paragraph numbers refer to NHB 1700.7A.

JSC Form 542A (Feb 78) NASA-JSC

HAZARD LIST

PAYLOAD	SUBSYSTEM	DATE
Pool Boiling Experiment	Environmental Control	

HAZARD GROUP	HAZARD TITLE	APPLICABLE SAFETY REQUIREMENT
Injury	2.001 Crew exposure to high temperature surfaces during experiment operation.	201
Temperature Extremes	2.002 Surface temperatures in excess of 113^{o}F.	201

JSC Form 542A (Feb 78) NASA-JSC

HAZARD LIST

PAYLOAD	SUBSYSTEM	DATE
Pool Boiling Experiment	Human Factors	

HAZARD GROUP	HAZARD TITLE		APPLICABLE SAFETY REQUIREMENT
Contamination	3.001	Failure to open vacuum space valve prior to experiment operation.	201
Injury	3.002	Excessive test cell surface temperatures - in excess of 113^{o}F.	201

JSC Form 542A (Feb 78) NASA-JSC

HAZARD LIST

PAYLOAD	SUBSYSTEM	DATE
Pool Boiling Experiment	Materials	

HAZARD GROUP		HAZARD TITLE	APPLICABLE SAFETY REQUIREMENT
Contamination	4.001	Hazardous/toxic fluids in middeck.	209
Fire	4.002	Fuels in middeck.	209
Contamination	4.003	Offgassing from all experiment materials.	209
Illness/injury	4.004	Use of shatterable material.	201

JSC Form 542A (Feb 78) NASA-JSC

HAZARD LIST

PAYLOAD	SUBSYSTEM	DATE
Pool Boiling Experiment	Pressure Systems	

HAZARD GROUP		HAZARD TITLE	APPLICABLE SAFETY REQUIREMENT
Contamination	5.001	Leakage of test fluids into middeck.	201 209
Contamination/illness /injury	5.002	Rupture of test cell or vacuum space.	208.7
Explosion	5.003	Ignition of explosive mixture in test cell.	201 209
Contamination/injury/ illness	5.004	Failure of fittings or lines.	208 209

JSC Form 542A (Feb 78) NASA-JSC

HAZARD LIST

PAYLOAD	SUBSYSTEM	DATE
Pool Boiling Experiment	Structures	

HAZARD GROUP	HAZARD TITLE	APPLICABLE SAFETY REQUIREMENT
Collision	6.001 Unrestrained motion of test cells.	208
Corrosion	6.002 Degradation of test cell material.	208

JSC Form 542A (Feb 78) NASA-JSC

POOL BOILING EXPERIMENT FAULT HAZARD ANALYSIS

Component	Component Failure Mode	Component Failure Rate	System Operational Mode	Effect Of Primary Component Failure On Subsystem	Factors That May Cause Secondary Component Failure	Upstream Components Or Inputs That May Cause Sequential Failures	Further Analysis Required	Remarks
Heaters	Mechanical joints leak		Boiling test	Loss of vacuum	Vibration Over temp.		Evaluate component reliability	
	Overheating at heater junction		Boiling test	Heater joint failure, exceed touch temp.			Evaluate surface temperature rise	
Relief Valves	Fails closed	.00005	Storage Boiling test	Excessive pressure rise in box	Incorrect. Set pressure -temp effects			Overpressurization not likely - Heater collapse will relieve pressure.
	Fails open		Storage Boiling test	Unwanted vapor in test cell.				Not hazardous
Manual Valves	Fails closed	.000093	Boiling test	Pressure rise during heating	Loss of valve handle	Relief valve fails closed		Protected by pressure switch
	Fails open		Boiling test	Unwanted vapor in test cell				Not hazardous
Vacuum Tanks	Leak		Storage	No boiling - Ambient pressure in test cell	Vibration		Evaluate component reliability	Experiment Loss of data
Pressure Switch	Fails open	.000056	Boiling test	No power to heater	Shock	Leak to ambient		No data from cell
	Fails closed		Boiling test	Pressure increase in test cell	Excessive current - Welded contacts	Manual valve closed		Potential for overpressure - Relief protection + boiling suppression
Temperature Switch	Fails open	.000007	Boiling test	No power to heater				Loss of data
	Fails closed		Boiling test	Excessive surface temp - Struct. failure	Excessive current - Welded contacts			Touch temp exceed Power=100w x 45 sec=4.3 Btu $\Delta T=113-70=43^{o}F$

POOL BOILING EXPERIMENT FAULT HAZARD ANALYSIS (continued)

Component	Component Failure Mode	Component Failure Rate	System Operational Mode	Effect Of Primary Component Failure On Subsystem	Factors That May Cause Secondary Component Failure	Upstream Components Or Inputs That May Cause Sequential Failures	Further Analysis Required	Remarks
Test Cell	Rupture		Boiling test	Leak of liquid into middeck	Closed manual valve. Failed closed relief valve. Pressure switch.	Excessive heater temperature	Reliability, thermal	
	Rupture		Storage - thermal expansion of liquid	Leak of liquid into middeck	Failed closed			
	Excessive surface temperature		Boiling test	Exceed touch temperature	Weaken test cell	Failed temperature switch; misplaced sensor		
Test Stand	Collapse		Boiling test	Uncontrolled motion of test cell	Impact, shock		Reliability, structures	

APPENDIX C

FLOW BOILING EXPERIMENT SAFETY DATA

PAYLOAD SAFETY MATRIX

PAYLOAD	PAYLOAD ORGANIZATION	DATE	PAGE
FLOW BOILING EXPERIMENT	NASA Lewis R. C.		

HAZARD GROUP / SUBSYSTEM	COLLISION	CONTAMINATION (TOXICITY, ETC)	CORROSION	ELECTRICAL SHOCK	EXPLOSION	FIRE	INJURY AND ILLNESS	LOSS OF ENTRY CAPABILITY	RADIATION	TEMPERATURE EXTREMES								
Biomedical																		
Hazard Detection and Safing																		
Cryogenics																		
Electrical		X		X		X			X	X								
Environmental Control		X					X			X								
Human Factors							X			X								
Hydraulics																		
Materials		X				X	X											
Mechanical		X			X		X											
Optical		X					X											
Pressure Systems		X			X		X											
Propulsion																		
Pyrotechnics																		
Radiation																		
Structures	X		X															

JSC Form 542 (Feb 78)

NASA-JSC

HAZARD LIST

PAYLOAD	SUBSYSTEM	DATE
FLOW BOILING EXPERIMENT	ELECTRICAL	

HAZARD GROUP		HAZARD TITLE	APPLICABLE SAFETY REQUIREMENT
Contamination	1.001	Battery Leakage	201, 202
Electrical Shock	1.002	Crew exposure to shock during cable connection or experiment operation.	201, 209, 202
Fire	1.003	Fire caused by excessive component (e.g., battery) temperature.	213, 209
Radiation	1.004	EMI	212.2
Temperature Extremes	1.005	Excessive surface temperature of heaters.	201

JSC Form 542A (Feb 78) NASA-JSC

HAZARD LIST

PAYLOAD	SUBSYSTEM	DATE
FLOW BOILING EXPERIMENT	ENVIRONMENTAL CONTROL	

HAZARD GROUP		HAZARD TITLE	APPLICABLE SAFETY REQUIREMENT
Contamination	2.001	Leakage if water or freon into middeck.	201, 202
Injury/Illness	2.002	Crew exposure to excessive surface temperatures.	201, 202
	2.003	Offgassing from heaters.	201, 202
Temperature Extremes	2.004	Heater and motor surface temperatures.	201, 202

JSC Form 542A (Feb 78) NASA-JSC

HAZARD LIST

PAYLOAD	SUBSYSTEM	DATE
FLOW BOILING EXPERIMENT	HUMAN FACTORS	

HAZARD GROUP	HAZARD TITLE		APPLICABLE SAFETY REQUIREMENT
Injury	3.001	Overpressurization of flow loop due to misoperation of experiment controls.	201, 202
Temperature Extremes	3.002	Excessive heater temperatures.	201, 202

JSC Form 542A (Feb 78) NASA-JSC

HAZARD LIST

PAYLOAD	SUBSYSTEM	DATE
FLOW BOILING EXPERIMENT	MATERIALS	

HAZARD GROUP		HAZARD TITLE	APPLICABLE SAFETY REQUIREMENT
Contamination	4.001	Hazardous/toxic materials in middeck.	209
	4.002	Offgassing from motors or heaters.	209
Fire	4.003	Flammable materials near heated surfaces.	201, 202, 209
Illness/injury	4.004	Use of shatterable material in middeck.	201, 202

JSC Form 542A (Feb 78) NASA-JSC

HAZARD LIST

PAYLOAD	SUBSYSTEM	DATE
FLOW BOILING EXPERIMENT	MECHANICAL	

HAZARD GROUP	HAZARD TITLE	APPLICABLE SAFETY REQUIREMENT
Contamination	5.001 Leakage of Freon or water from pumps.	201, 202
Explosion	5.002 Failure of rotating equipment.	201, 208
Injury/illness	5.003 Crew exposure to Freon.	201, 202

JSC Form 542A (Feb 78) NASA-JSC

HAZARD LIST

PAYLOAD	SUBSYSTEM	DATE
FLOW BOILING EXPERIMENT	OPTICAL	

HAZARD GROUP	HAZARD TITLE	APPLICABLE SAFETY REQUIREMENT
Contamination	6.001 Shatterable optical material in middeck.	201, 202
Injury	6.002 Crew injury from fragments of optical material.	201, 202

JSC Form 542A (Feb 78) NASA-JSC

HAZARD LIST

PAYLOAD	SUBSYSTEM	DATE
FLOW BOILING EXPERIMENT	PRESSURE SYSTEMS	

HAZARD GROUP	HAZARD TITLE	APPLICABLE SAFETY REQUIREMENT
Contamination	7.001 Leakage of freon or water into middeck.	201, 202, 209
Explosion	7.002 Rupture of test section or lines.	201, 208
Injury/Illness	7.003 Failure of pressure boundary.	201, 208, 209

JSC Form 542A (Feb 78) NASA-JSC

HAZARD LIST

PAYLOAD	SUBSYSTEM	DATE
FLOW BOILING EXPERIMENT	STRUCTURES	

HAZARD GROUP	HAZARD TITLE	APPLICABLE SAFETY REQUIREMENT
Collision	8.001 Unrestrained motion of test package.	201, 202, 208
Corrosion	8.002 Degradation of structural support members.	208

JSC Form 542A (Feb 78) NASA-JSC

FLOW BOILING EXPERIMENT FAULT HAZARD ANALYSIS

Component	Component Failure Mode	Component Failure Rate	System Operational Mode	Effect Of Primary Component Failure On Subsystem	Factors That May Cause Secondary Component Failure	Upstream Components Or Inputs That May Cause Sequential Failures	Further Analysis Required	Remarks
Regulator RV-1	Fail Shut	.00081	Freon Flowing	No Freon Flow Pressure/Temp Rise in Flow Loop	- Misadjustment - Vibration - Contamination			Loss of Experiment
	Fail Open		Freon Flowing	Loss of Inlet Quality Control	- Misadjustment - Vibration - Contamination			
Flow Meter FM-1	Fails to Send Signal to DACS	.00015	Freon Flowing	Loss of Data; Loss of Flow Control	- Contamination - Electrical Failure			Loss of Flow Rate Data and Exp. Control
	Sends Erroneous Flow Signal to DACS			Improper Control Output From DACS	- Electrical Failure			
Temperature Detector TD-1	Sends False High Signal	.00005	Freon Flowing	Excessively Subcooled Liquid - Heater Shut Down				Variation of Inlet Conditions
	Sends False Low Signal			Maximum Heater Power - Possible Super Heating of Test Section Outlet Flow				
Temperature Switch TS-1	Fails Open	.000007	Heaters On	Heaters Inoperable	- Vibration - Contamination			Loss of Data
	Fails Shut		Heaters On	Excessive Loop Temperature				No Redundancy
Preheater	No Heat Input	.000014	Freon Flowing	Loss of Inlet Temperature Control	- Electrical			- Minor Effect on Experiment Data

FLOW BOILING EXPERIMENT FAULT HAZARD ANALYSIS

Component	Component Failure Mode	Component Failure Rate	System Operational Mode	Effect Of Primary Component Failure On Subsystem	Factors That May Cause Secondary Component Failure	Upstream Components Or Inputs That May Cause Sequential Failures	Further Analysis Required	Remarks
Pressure Detectors	False or no signal	.00045	Flow-heaters on	Loss of pressure drop and fluid condition data	- Electrical - Vibration			Loss of data - No safety hazard
Condenser	Fails to completely condense or sub-cool Freon		Flow-heaters on	- Cavitation in pump - Loss of inlet fluid condition control	- Unknown design problems - Low-G condensation	- Loss of water cooling	Verify condenser performance in low-G	Loss of experiment
Programmable Power Supply	Improper control of heat input to test section		Flow-heaters on	- Quality in tube unknown - Loss of boiling data	- Electrical failure	- DACS		Loss of data
Test Section	Fracture		Flow-heaters on	- Loss of containment	- Vibration - Thermal or mechanical shock			Possible safety hazard
	One or more heater elements inoperable		Flow-heaters on	Unknown temperature distribution in test section	- Vibration - Electrical			Loss of data

FLOW BOILING EXPERIMENT FAULT HAZARD ANALYSIS

Component	Component Failure Mode	Component Failure Rate	System Operational Mode	Effect Of Primary Component Failure On Subsystem	Factors That May Cause Secondary Component Failure	Upstream Components Or Inputs That May Cause Sequential Failures	Further Analysis Required	Remarks
Flow Switch FS-1	False flow signal	.000035	No flow	Heaters energized with no flow - Excessive temperatures	- Vibration - Contamination			
	False no-flow signal		Flow	Heaters cannot be energized				Loss of experiment
Pressure Switch PS-1	False high signal	.000056	Any	Heaters and pump inoperable	- Vibration - Contamination - Electrical overload			Loss of experiment
	False low signal		Flow with heaters on	Excessive loop pressure		Failure of Freon accumulator		Potential safety hazard
Freon Pump	Failure during operation	.000134	Heaters on	No flow-excessive temperature rise in test section	- Mechanical failure - Electrical failure	Flow switch or pressure switch fail closed		Loss of experiment
Freon Accumulator	Liquid unable to enter	.000118	Flow-heaters on	Pressure rise	- Contamination - Mechanical failure - System overfilled	Pressure, temperature switch failed closed		Loss of experiment
Vacuum and Fill Connection	Leaks	.0000005	Flow-heaters on	Loss of liquid containment	- Vibration			Potential safety hazard
Quality Meter	Faulty signal - high or low		Flow-heaters on	Loss of quality meter performance data			Reliability unknown	No effect on primary experiment data

FLOW BOILING EXPERIMENT FAULT HAZARD ANALYSIS

Component	Component Failure Mode	Component Failure Rate	System Operational Mode	Effect Of Primary Component Failure On Subsystem	Factors That May Cause Secondary Component Failure	Upstream Components Or Inputs That May Cause Sequential Failures	Further Analysis Required	Remarks
Flow Switch	False flow signal	.000035	Freon system operational - Water pump off	- Excessive temperature/ pressures in Freon loop	- Vibration - Contamination			Loss of experiment
	False no-flow signal		Freon system operational - Water system operational	- Freon system shut down				Loss of experiment
Temperature Switch	Fails closed	.000007	Freon system on - Water system on	- Excessive water temperature - Vapor uncondensed in Freon loop	- Orbiter - Electrical overload			Loss of experiment
	Fails open		Any	- Experiment inoperable	- Vibration			Loss of experiment
Pressure Switch	Fails open	.000056	Any	- Experiment inoperable	- Vibration			Loss of experiment
	Fails closed		Water pump on	- Excessive system pressure	- Electrical overload			Potential safety hazard
Water Accumulator	Liquid unable to enter	.000118	Water pump off - Cooling interface disconnected	- Excessive system pressure	- Contamination - Mechanical failure			Potential safety hazard
Water Pump	Failure during operation	.000134	Freon loop heaters on	- Condenser inoperative - Excessive Freon temperature and pressure	- Mechanical - Electrical	Pressure switch failure open		Experiment shut down

FLOW BOILING EXPERIMENT FAULT HAZARD ANALYSIS

Component	Component Failure Mode	Component Failure Rate	System Operational Mode	Effect Of Primary Component Failure On Subsystem	Factors That May Cause Secondary Component Failure	Upstream Components Or Inputs That May Cause Sequential Failures	Further Analysis Required	Remarks
Temperature Detector	Erroneous signal	.00005	Experiment operational	Loss of condenser performance data	- Electrical			Minimal impact on experiment
Water Interface Connectors	Leak	.000944	Experiment operational	- Contamination of middeck	- Vibration - Pressure -Misalignment	Pressure switch fails closed		Possible hazard to orbiter

APPENDIX D

LIST OF SYMBOLS

SYMBOLS

A	Area (m^2)
a	Acceleration (m/s^2)
Bo	Bond number
C	Specific heat of heater material (J/kg-^oC)
C	Head configuration constant, Equation 23
C_p	Fluid specific heat (J/kg-^oC)
C_{pf}	Saturated liquid specific heat (J/kg-^oC)
D	Diameter (m)
D_i	Inner diameter (m)
D_j	Vapor jet diameter (m)
D_o	Outer diameter (m)
D_s	Sheath diameter (m)
D_w	Wire diameter (m)
E	Modulus of elasticity (Pa)
E	Joint efficiency, Equations 23, 27
E	Voltage, Equation 112 (v)
E_R	Modulus of elasticity of reference material, Equation 81 (Pa)
e	Error
e_v	Error in volume
F_D	Pressure force on piston (N)
F_F	Friction force on piston (N)
f	Friction Factor
f_{RS}	Static friction force per unit length, Equation 20
G	Mass velocity (kg/m^2-s)
G_g	Superficial vapor mass velocity = Gx (kg/m^2-s)

g	Gravitational acceleration ($m/s^{2)}$
g_c	Dimensional conversion factor ($kg\text{-}m/N\text{-}s^2$)
g_o	Normal earth gravity (m/s^2)
h	Film heat transfer coefficient($W/m^2\text{-}^oC$)
h_b	Boiling film coefficient($W/m^2\text{-}^oC$)
h_c	Forced convection film coefficient ($W/m^2\text{-}^oC$)
h_{fg}	Latent heat of condensation or evaporation (J/kg)
h^*_{fg}	Heat of vaporization plus 34 percent of the sensible heat of vapor at heater wall, Equations 53, 96 (J/kg)
h_r	Radiation heat transfer coefficient ($W/m^2\text{-}^oC$)
h_{TP}	Two-phase heat transfer coefficient ($W/m^2\text{-}^oC$)
$h_{1\phi}$	Single-phase heat transfer coefficient ($W/m^2\text{-}^oC$)
h_w	Water side heat transfer coefficient ($W/m^2\text{-}^oC$)
I	Moment of inertia (m^4)
j	Electrical resistivity (Ω -m)
k	Thermal conductivity ($W/m\text{-}^oC$)
k_t	Tube conductivity ($W/m\text{-}^oC$)
L	Length (m)
L	Load, Equation 38 (Pa)
M	Bending moment (N-m)
m^2	$\frac{h_{TP}}{K\,\delta(1+\delta/D_i)}$ $1/m^2)$
m^2	$\frac{hP}{KS}$ Equations 72, 73, 74 ($1/m^2$)
N	Axial tear out load (Pa)
N	Number of data poiints, Equation 67
Nu	Nusselt Number

P	Pressure (Pa)
P	Buckling load, Equations 26, 29, 44 (Pa)
P	Load, Equations 23, 24, 25, 27 (Pa)
P	Perimeter, Equation 71 (m)
P_{max}	Maximum heater power, Equations 63, 64 (W)
Pr	Liquid Prandtl number (Pa)
P_{SAT}	Saturation pressure (Pa)
ΔP	Pressure differential (Pa)
Q	Heater power (W)
Q_{fluid}	Heat flow into fluid (W)
Q_{leak}	Heat loss from heater (W)
q	Heater input power per unit length or unit area (W/m, W/m^2)
q_{max}	Peak heat flux (W/m^2)
$q_{max\ F}$	Flat plate peak heat flux from Zuber-Kutateladze (W/m^2)
R	Radius (m)
R	Distance from axis of rotation to fluid interface, Equation 32 (m)
R	Reliability, Equations 41, 51
R	Electrical resistance, Equation 70 (Ω)
R_a	Air space thermal resistance (conduction) Equation 103 ($^oC/W$)
Ra*	Modified Rayleigh number, Defined in Equation 53
Re_f	Saturated liquid Reynolds number
Re_g	Saturated vapor Reynolds number
Re_L	Liquid Reynolds number
R_o	Tank radius, Equation 31 (m)
S	Allowable stress, Equations 23, 25, 27 (Pa)
S	Strength distribution, Equation 38 (Pa)
S	Heater cross-sectional area, Equation 71 (m^2)

T	Temperature (^{o}C, ^{o}K)
T	Change in surface temperature from initial surface temperature, Equations 60-74, 97 (^{o}C)
T_a	Ambient temperature (^{o}C)
T_{eq}	Heater equilibrium temperature (^{o}C)
T_f	Fluid temperature (^{o}C)
T_{max}	Maximum temperature (^{o}C)
T_o	Sheath temperature (^{o}C)
t	Time (s)
t_R	Ramp time (s)
t_{RH}	Total ramp and hold time(s)
T	Temperature excess (^{o}C)
$U_{1\emptyset}$	Overall single-phase conductance ($W/^{o}C$)
U_{TP}	Overall two-phase conductance ($W/^{o}C$)
V	Volume (m^3)
V_a	Air volume, Equation 6 (m^3)
V_L	Liquid volume, Equation 6 (m^3)
ΔV_L	Liquid volume expansion (m^3)
v	Specific volume (m^3/kg)
W	Mass (kg)
W	Cell width (m)
w	Width of O-ring, Equation 20 (m)
w	Load per unit length, Equation 85 (kg/m)
w	Heater band width, Equation 114 (m)
X, X_{tt}	Lockhart-Martinelli parameter
x	Axial coordinate along heater, Equation 71 (m)
x	Fluid quality
x	Piston positioning error (m)
Y	Difference between strength and load (Pa)

Greek

α	Coefficient of thermal expansion
α	Void Fraction, Equations 122-130
β	Specific surface tension σ/ρ ($m^3 s^2$)
Δ	Dimensionless vapor blanket thickness, defined in Equation 77
δ	Thickness δ_n = head thickness, δ_w = wall thickness, δ_p = piston thickness (m)
ε	Error in volume increment, Equations 12, 14
ε_t	Tube emissivity
η	Heater efficiency
η_f	Fin efficiency
μ	Viscosity (kg/m-s)
μ_L	Mean load, Equation 42 (Pa)
μ_s	Mean strength, Equation 42 (Pa)
ν	Poisson's ratio
ρ	Density (kg/m^3)
$\vec{\rho}$	Experiment location relative to Orbiter center of gravity, Equations 2, 3 (m)
σ	Surface tension ($\frac{N}{m}$)
σ	Stress, Equations 20, 55-88 (Pa)
σ	Stefan-Boltzmann constant, Equation 104 ($W/m^2\text{-}^oK^4$)
σ	Standard deviation, Equations 39-50
τ	Heater time constant (s)
ω	Angular velocity (rad/s)

Subscripts

a	Air
b	Boiling
cent	Centripetal
cor	Coriolis
dR	Design limit for reference material
eq	Equilibrium
f	Saturated liquid
fg	Vaporization
g	Saturated vapor
H	Hold
i	Inner
L	Liquid
L	Load
max	Maximum
o	Outer
R	Reference
R	Ramp
S	Strength
SAT	Saturation
y	Yield

REFERENCES

1. North, B. F., and Hill, M. E., Conceptual Design of Two-Phase Fluid Mechanics and Heat Transfer Facility for Spacelab General Dynamics, NASA CR-159810, July 1980.

2. Bakhru, N., and Lienhard, J. H., "Boiling From Small Cylinders, International Journal Heat and Mass Transfer, Volume 15, 1972, pages 2011-2025.

3. Lienhard, J. H., "Interacting Effects of Geometry and Gravity Upon the Extreme Boiling Heat Fluxes," Journal of Heat Transfer, ASME, Series C, Volume 90, No. 1, 1968, pages 180-2.

4. Sun, Kawo-Hwa and Lienhard, J. H., The Peak Pool Boiling Heat Flux of Horizontal Cylinders, Bulletin 88, College of Engineering, University of Kentucky, May 1969.

5. Dukler, A. E., and Taitel, Y., "A Model for Predicting Flow Regime Transitions in Horizontal and Near-Horizontal Gas-Liquid Flow," AIChe Journal, Volume 22, No. 1, January 1976.

6. Salzman, J. A., Masica, W. J., Experimental Investigation of Liquid Propellant Reorientation, NASA TN D-3789, 1967.

7. Draft version of middeck payload pricing policy; telephone conversations with Mr. Robert Haltermann, NASA Headquarters.

8. ICD-A-14066 for the Continuous Flow Electrophoresis System (CFES) designed by McDonnell Douglas Astronautics Corporation.

9. Code of Federal Regulations 14 CFR, Part 1214.

10. Orbiter Middeck Payload Provisions Handbook, JSC-16536, Revision A, September 1980.

11. Orbiter middeck payload limitations; telephone conversations with Mr. Robert Haltermann, NASA Headquarters.

12. Safety Policy and Requirements for Payloads Using the Space Transportation System (STS), NASA Handbook NHB 1700.7A, December 1980.

13. ASME BPV-VIII.

14. MIL-STD-1522.

15. Flammability, Odor and Offgassing Requirements, NASA Handbook NHB 8060.1B, September 1981.

16. Rockwell International Corporation MF-0004-014, "Environment Requirements and Test Criteria for the Orbiter Vehicle."

17. Implementation Procedure for STS Payloads System Safety Requirements, NASA/ Lyndon B. Johnson Space Center, JSC-13830, May 1979.

18. System Safety, NASA Handbook NHB 1700.1, Volume 3, March 1970.

19. Roark, R. J., and Young, W. C., Formulas for Stress and Strain, McGraw-Hill Book Company, Fifth Edition, 1975.

20. Masica, W. J., Derdul, J. D., and Petrash, D. A., Hydrostatic Stability of the Liquid-Vapor Interface in a Low-Acceleration Field, NASA TND-2444, August 1964.

21. Cottrell, D. F., et al., Revision of RADC Nonelectronic Reliability Notebook, Martin Marietta Aerospace, Contract F30602-73-C-0135, RADC-TR-69-458, June 1974.

22. Kapur, K. C., and Lamberson, L. R., Reliability in Engineering Design, John Wiley and Sons, New York, 1977.

23. Schenck, H., Theories of Engineering Experimentation, McGraw-Hill Book Company, New York, 1979.

24. Lienhard J. H., and Peck, R. E., Conceptual Design for Spacelab Pool Boiling Experiment, NASA CR 135378, March 1978.

25. Telephone conversation with Charles Chassay, NASA/JSC.

26. Collier, J. G., Convective Boiling and Condensation, McGraw-Hill International Book Company, Second Edition, 1981.

27. ASHRAE Handbook of 1977 Fundamentals, American Society of Heating, Refrigerating and Air Conditioning Engineers, Inc., New York, 1977.

28. Holman, J. P., Heat Transfer, McGraw-Hill, Third Edition, 1972.

DISTRIBUTION LIST
CONTRACT NAS3-23160

	No. of Copies
National Aeronautics and Space Administration Lewis Research Center 21000 Brookpark Road Cleveland, OH 44135	
Attn: Contracting Officer, MS 500-306	1
E. A. Bourke, MS 501-5	2
Technical Utilization Office, MS 7-3	1
Technical Report Control Office, MS 60-2	1
AFSC Liaison Office, MS 501-3	2
Library, MS 60-3	2
Office of Reliability & Quality Assurance, MS 500-211	1
E. P. Symons, MS 501-6	1
T. H. Cochran, MS 501-7	1
Patent Counsel, MS 500-318	1
L. P. Sarsfield, Project Mgr., MS 501-7	20
T. L. Labus, MS 501-7	1
National Aeronautics and Space Administration Headquarters Washington, DC 20546	
Attn: J. Mullin, RTS-6	1
W. Hudson, RTS-6	1
E. Gabris, RST-5	1
M. Cuviello, RST-5	1
National Aeronautics and Space Administration Goddard Space Flight Center Greenbelt, MD 20771	
Attn: Library	1
S. Ollendorf	1
National Aeronautics and Space Administration John F. Kennedy Space Center Kennedy Space Center, FL 32899	
Attn: Library	1
DD-MED-41/F. S. Howard	1
DE-A/W. H. Boggs	1

National Aeronautics and Space Administration
Ames Research Center
Moffett Field, CA 94035
Attn: Library 1
J. Vorreiter, MS 244-7 1

National Aeronautics and Space Administration
Langley Research Center
Hampton, VA 23365
Attn: Library 1

National Aeronautics and Space Administration
Johnson Space Center
Houston, TX 77001
Attn: Library 1
EP2/Z. D. Kirkland 1
EP5/W. Chandler 1
EP4/Dale Connelly 1
PD13/James Thompson 1

National Aeronautics and Space Administration
George C. Marshall Space Flight Center
Huntsville, AL 35812
Attn: Library 1
EP43/L. Hastings 1
EP43/A. L. Worlund 1
EP45/Dr. Wayne Littles 1
EP24/G. M. Chandler 1
ES63/E. W. Urban 1

Jet Propulsion Laboratory
4800 Oak Grove Drive
Pasadena, CA 91103
Attn: Library 1
Don Young, MS 125-224 1

NASA Scientific & Technical Information Facility
P. O. Box 8757
Baltimore/Washington International Airport, MD 21240
Attn: Accessioning Department 10

Defense Documentation Center
Cameron Station - Bldg. 5
5010 Duke Street
Alexandria, VA 22314
Attn: TISLA 1

National Aeronautics and Space Administration
Flight Research Center
P. O. Box 273
Edwards, CA 93523
Attn: Library 1

Air Force Rocket Propulsion Laboratory
Edwards, CA 93523
Attn: LKCC/J. E. Brannigan 1
LKDS/R. L. Wiswell 1

Aeronautical Systems Division
Air Force Systems Command
Wright Patterson Air Force Base
Dayton, OH 45433
Attn: Library 1

Air Force Office of Scientific Research
Washington, DC 20333
Attn: Library 1

Aerospace Corporation
2400 East El Segundo Boulevard
Los Angles, CA 90045
Attn: Library - Documents 1

Beech Aircraft Corporation
Boulder Facility
Box 9631
Boulder, CO 80301
Attn: Library 1
R. A. Mohling 1

Bell Aerosystems, Inc.
Box 1
Buffalo, NY 14240
Attn: Library 1
J. Colt 1

Boeing Company
P. O. Box 3999
Seattle, WA 98124
Attn: Library 1
C. L. Wilkensen, MS 8K/31 1

Chrysler Corporation
Space Division
P. O. Box 29200
New Orleans, LA 70129
Attn: Library 1

McDonnell Douglas Astronautics Company
5301 Balsa Avenue
Huntington Beach, CA 92647
Attn: Library 1
E. C. Cady 1

Missiles and Space Systems Center
General Electric Company
Valley Forge Space Technology Center
P. O. Box 8555
Philadelphia, PA 19101
Attn: Library 1

ITT Research Institute
Technology Center
Chicago, IL 60616
Attn: Library 1

Lockheed Missiles and Space Company
P. O. Box 504
Sunnyvale, CA 94086
Attn: Library 1
G. D. Bizzell 1
S. G. DeBrock 1

Martin-Marietta Corporation
Denver Division
P. O. Box 179
Denver, CO 80201
Attn: Library 1
D. Fester 1
J. Tegart 1
R. Eberhardt 1
R. Dergance 1

Rockwell International Corporation
Space Division
12214 Lakewood Boulevard
Downey, CA 90241
Attn: Library 1
A. Jones 1

Northrop Research and Technology Center
One Research Park
Palos Verdes Peninsula, CA 90274
Attn: Library 1

TRW Systems, Inc.
One Space Park
Redondo Beach, CA 90278
Attn: Tech. Lib. Doc. Acquisitions 1

National Science Foundation, Engr. Div.
1800 G. Street, NW
Washington, DC 20540
Attn: Library 1

RCA/AED
P. O. Box 800
Princeton, NJ 08540
Attn: Mr. Daniel Balzer 1

Southwest Research Institute
Department of Mechanical Sciences
P. O. Drawer 28510
San Antonio, TX 78284
Attn: H. Norman Abramson 1
Franklin Dodge 1

McDonnell Douglas Astronautics Co. - East
P. O. Box 516
St. Louis, MO 63166
Attn: G. Orgon 1
W. Regnier 1

Science Applications, Inc.
1200 Prospect Street
P. O. Box 2351
LaJolla, CA 92037
Attn: M. H. Blatt 1

The University of Houston
Mechanical Engineering Department
Houston, TX 77008
Attn: Dr. John H. Lienhard 2
Dr. A. Dukler 1

University of Michigan
Heat Transfer Laboratory
Department of Mechanical Engineering
Ann Arbor, MI 48109
Attn: Dr. H. Merte 1

Mr. William Haskin
AF Wright Aeronautical Lab
AFWAL/FIEE
Wright-Patterson AFB, OH 45433

End of Document